



**DEPARTMENT OF DEFENSE**  
DEFENSE OFFICE OF PREPUBLICATION AND SECURITY REVIEW  
1155 DEFENSE PENTAGON  
WASHINGTON, DC 20301-1155

October 24, 2018  
Ref: 19-S-0112

Ms. Monica Gruber  
Raytheon Missile Systems  
PO Box 11337  
TU M10 1<sup>st</sup> Floor MS#6  
Tucson, AZ 85734-1337

Dear Ms. Gruber:

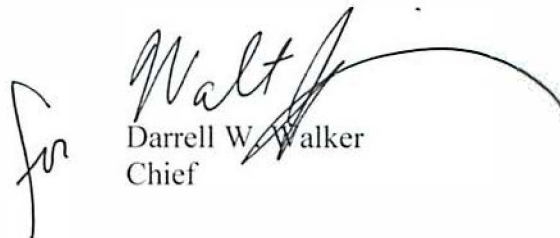
This is in response to the enclosed October 15, 2018, correspondence requesting public release approval of the enclosed paper titled:

- "2018-204 Investigation of the Electrical Resistivity of a Perchlorate Oxidizer Based Electric Propellant Formulation"

The paper is **APPROVED** for public release. However, this approval does not include any photograph, picture, exhibit, caption, or other supplemental material not specifically approved by this office. Our concurrence for release does not imply DoD endorsement or factual accuracy of the material.

Please direct any questions regarding this case to Mr. Donald Kluzik at 703-614-4931, email: [donald.e.kluzik.civ@mail.mil](mailto:donald.e.kluzik.civ@mail.mil).

Sincerely,

A handwritten signature in black ink, appearing to read "Walt", with a large flourish extending to the right. To the left of the signature is a large, stylized handwritten "for".  
Darrell W. Walker  
Chief

Enclosures:  
As stated

2018-204 Pending Public Release Approval

Investigation of the Electrical Resistivity of a Perchlorate Oxidizer Based  
Electric Propellant Formulation

by

Lauren Brunacini

A Thesis Presented in Partial Fulfillment  
of the Requirements for the Degree  
Master of Science

CLEARED  
For Open Publication

OCT 24 2018 2

Department of Defense  
OFFICE OF PREPUBLICATION AND SECURITY REVIEW

Approved [Month of thesis defense] 2018 by the  
Graduate Supervisory Committee:

Dr. James Middleton, Chair  
To be determined  
Dr. Mark T. Langhenry

ARIZONA STATE UNIVERSITY

December 2018

19-5-012

15 October 2018

Department of Defense  
Office of Prepublication and Security Review  
1155 Defense Pentagon  
Washington, DC 20301-1155  
Attn: Action Officer

SUBJECT: Request for Public Release approval of the enclosed 2018-204 Investigation of the Electrical Resistivity of a Perchlorate Oxidizer Based Electric Propellant Formulation Thesis

Dear Sir or Madam,

Raytheon is submitting the enclosed 2018-204 Investigation of the Electrical Resistivity of a Perchlorate Oxidizer Based Electric Propellant Formulation Thesis, for security and policy review and public release approval. The material is intended for general marketing and public relations purposes and for distribution to customers, suppliers, and individuals in the business and defense industry trade press as appropriate. To the best of our knowledge, it does not contain classified or sensitive information.

Raytheon is requesting approval by 15 November 2018.

Raytheon reference eTPCR request RMS-15175

Thank you for your attention to this request. Please contact me via email or phone if you have any questions or concerns.

Sincerely,



Monica Gruber  
Public Release  
Communications and External Affairs  
Raytheon Missile Systems

520-746-2277 office  
520-260-3121 mobile  
[Monica K Gruber@raytheon.com](mailto:Monica_K_Gruber@raytheon.com)

Enclosure(s): Enclosures for review have been uploaded via AMRDEC  
2018-204 Investigation of the Electrical Resistivity of a Perchlorate Ox.pdf  
2018-204 Investigation of the Electrical Resistivity\_Request Letter.pdf



SAFE is designed to provide AMRDEC and its customers an alternative way to send files other than email. SAFE supports file sizes up to 2GB.

[Click here for Getting Started Guide](#)

## Package Status

Package ID:	15596510
Sender's Name:	Monica Gruber
Sender's Email:	Monica_K_Gruber@raytheon.com
Date Uploaded:	10/15/2018 7:06:06 PM
Delete Date:	10/25/2018
Encrypt Email:	True
Notification when Download Starts:	False
Notification when Download Ends:	True
Require CAC:	False

[Cancel Package](#)

Description
Raytheon is submitting the referenced 2018-204 Investigation of the Electrical Resistivity of a Perchlorate Oxidizer Based Electric Propellant Formulation Thesis, for security and policy review and public release approval. The material is intended for general marketing and public relations purposes and for distribution to customers, suppliers, and individuals in the business and defense industry trade press as appropriate. To the best of our knowledge, it does not contain classified or sensitive information. Raytheon is requesting approval by 15 November 2018. Raytheon reference eTPCR request RMS-15175 V/R Monica Gruber

## File Information

File(s)	Privacy Act Data	Date Uploaded	
2018-204 Investigation of the Electrical Resistivity of a Perchlorate Ox....pdf (4 MB)	No	10/15/2018 7:06:06 PM	<a href="#">View File Hash</a>
2018-204 Investigation of the Electrical Resistivity_Request Letter.pdf (28 KB)	No	10/15/2018 7:06:06 PM	<a href="#">View File Hash</a>

[Upload more files to Package](#)

## Recipients List

Resend Notice	Recipients	User Status
<a href="#">Resend Notice</a>	whs.pentagon.esd.mbx.secrev@mail.mil	Not Downloaded

**Resend to:** [All Recipients](#) [All Not Downloaded](#)

<b>Add New Recipient:</b>
<input type="text"/>
<a href="#">Add Recipient</a>

---

## What is AMRDEC

The U. S. Army Aviation and Missile Research Development and Engineering Center, a subordinate laboratory to the Research, Development and Engineering Command, is the Army's focal point for providing research, development, and engineering technology and services for aviation and missile platforms across the lifecycle.

[Learn More](#)

## Quick Links

[Home](#)

[About](#)

[Getting Started Guide](#)

## Resources

[Security Notice](#)

[Accessibility Notice](#)

[ISalute](#)

## Support

[Knowledge Base](#)

[Version History](#)

Approved for Public Release DOPSR 19-S-0112  
Placed in the Public Domain Per E18-9TPV

Investigation of the Electrical Resistivity of a Perchlorate Oxidizer Based  
Electric Propellant Formulation

by

Lauren Brunacini

A Thesis Presented in Partial Fulfillment  
of the Requirements for the Degree  
Master of Science

Approved November 2018 by the  
Graduate Supervisory Committee:

James Middleton, Chair  
Lenore Dai  
Mark T. Langhenry

ARIZONA STATE UNIVERSITY

May 2019

Approved for Public Release DOPSR 19-S-0112  
Placed in the Public Domain Per E18-9TPV

© 2018 Raytheon Company

All Rights Reserved

## ABSTRACT

In recent years, a new type of ionic salt based solid propellant, considered inert until the application of an electric current induces an electro-chemical reaction, has been under investigation due to its broad range of possible uses. However, while many electric propellant formulations and applications have been explored over the years, a fundamental understanding of the operational mechanisms of this propellant is necessary in order to move forward with development and implementation of this technology. It has been suggested that the metallic additive included in the formulation studied during this investigation may be playing an additional, currently unknown role in the operation and performance of the propellant. This study was designed to examine variations of an electric propellant formulation with the purpose of investigating propellant bulk volume electrical resistivity in order to attempt to determine information regarding the fundamental science behind the operation of this material. Within a set of fractional factorial experiments, variations of the propellant material made with tungsten, copper, carbon black, and no additive were manufactured using three different particle size ranges and three different volume percentage particle loadings. Each of these formulations (a total of 21 samples and 189 specimens) were tested for quantitative electrical resistivity values at three different pulse generator input voltage values. The data gathered from these experiments suggests that this electric propellant formulation's resistivity value does change based upon the included additive. The resulting data has also revealed a parabolic response behavior noticeable in the 2D and 3D additive loading percentage versus additive particle size visualizations, the lowest point of which, occurring at an approximately 2.3% additive loading percentage value, could be indicative of the effects of the percolation phenomena on this material. Finally, the investigation results have been loosely correlated to power consumption testing results from previous work that may indicate that it is possible to relate propellant electrical resistivity and operating requirements. Throughout this study, however, it is obvious based on the data gathered that more information is required to be certain of these conclusions and in order to fully understand how this technology can be controlled for future use.



#### ACKNOWLEDGMENTS

I gratefully acknowledge the support that I have received from both the Arizona State University faculty and staff and the Raytheon Missile Systems employees that I have worked with while completing this thesis. This would not have been possible without their continued guidance and encouragement.

TABLE OF CONTENTS

	Page
LIST OF TABLES .....	vii
LIST OF FIGURES .....	viii
LIST OF ACRONYMS .....	xiv
NOMENCLATURE .....	xv
CHAPTER	
1 INVESTIGATION INTRODUCTION .....	1
Introduction .....	1
Background.....	3
Problem Statement.....	8
Purpose of the Study.....	9
Experimental Hypothesis and Research Questions.....	10
Theoretical Foundation and Experimental Framework Review .....	11
Nature of the Study.....	13
Significant Term Definitions .....	14
Scope and Delimitations .....	16
Limitations.....	17
Assumptions .....	18
Significance.....	20
2 LITERATURE REVIEW .....	22
Introduction .....	22
Literature Search Strategy .....	22
Theoretical Foundation.....	22
Experimental Framework of the Study .....	27
Literature Review Related to Key Variables and/or Concepts.....	28
Baseline Propellant Chemical Ingredients and Their Role in the Formulation....	28
Metallic (or Otherwise) Additive, Size, and Amount.....	31

CHAPTER	Page
	Electric Propellant Additive Replacement Chemical Ingredients..... 33
	Related Electrochemistry ..... 37
	Related Percolation Theory and Concepts ..... 42
	Related Electrical Conductivity/Resistivity Properties and Concepts..... 46
	Related Previous RMS Work ..... 49
	Related Solid Polymer Electrolyte and Doped PVA Research..... 52
	Summary and Predictions ..... 55
3	METHODOLOGY ..... 58
	Introduction ..... 58
	Research Design and Rationale ..... 60
	Methodology ..... 60
	Sample Population ..... 60
	Manufacturing Pilot Studies and Sample Manufacturing..... 66
	Sampling and Sampling Procedures ..... 69
	Testing Apparatus and Instrumentation ..... 71
	Procedures for Calibration and Data Collection ..... 75
	Procedure for Data Calibration Correction ..... 79
	Response Surface Methodology ..... 81
	Error Analysis ..... 82
	Summarry ..... 84
4	RESULTS ..... 86
	Introduction ..... 86
	Sample Results and Test Preparation..... 86
	Pre-Mixing Sample Manufacturing ..... 86
	Pilot Study Results ..... 88
	Sample Manufacturing and Preparation..... 90
	Pre-Response Surface Results and Analysis..... 96

CHAPTER	Page
	Data Collection and Initial Raw Data Visualization ..... 96
	Outlier Identification, Re-Testing, and Visualization ..... 103
	Additional Observations ..... 109
	Calibration Corrections and Visualization..... 110
	Regression and Response Surface Results..... 122
	Introduction and a Note on the Normality of the Data..... 122
	Initial Regression and Response Surface Results..... 124
	Updated Regression and Response Surface Results ..... 138
	Error Analysis ..... 146
	Summary..... 148
5	INTERPRETATION AND DISCUSSION OF RESULTS ..... 151
	Introduction ..... 151
	Interpretation of the Findings ..... 152
	Pilot Study and Sample Flat Manufacturing and Preparation Results ..... 152
	Data Collection, Correction, and Visualization Results..... 154
	Normality of the Resultant Data ..... 158
	Initial and Updated Regression and Response Surface Results ..... 159
	Error Analysis Results ..... 163
	Additional Observations ..... 165
	Revised Limitations ..... 167
	Threats to Validity ..... 168
	Implications ..... 169
	Recommendations ..... 171
	Pilot Study and Sample Flat Mnuufacturing Results..... 171
	Data Collection, Correction, and Visualization Results..... 172
	Response Surface Model Results and Revised Limitations ..... 173
	Threats to Validity..... 176

CHAPTER	Page
Conclusions .....	177
REFERENCES .....	179
APPENDIX	
A    ADDITIVE BILL OF MATERIALS .....	183

LIST OF TABLES

Table	Page
1. A Comparison of Proposed Replacement Additive Properties.....	35
2. Values for Cell Potential of Some of the Ingredients/Additive Suggestions and Possible Reactions That Could Be Occurring During ESP-9 Combustion .....	41
3. Depiction of the Experimental Sample Population.....	61
4. The Error Values Used as the “Prime” Values for Testing Set-up Error Propagation.. ..	83
5. All 24 Raw, Outlier Specimen Bulk Volume Resistivity Values Before and After Retesting .	104
6. All of the Measured Values for Voltage Rejection Taken During Sample Testing Sessions.	111
7. The Median of the Three Measured Bulk Volume Resistivity Values at Each of the Three Test Voltages Measured from Each Sample Flat .....	121
8. The Specimen Serial Numbers Corresponding to the Minitab Identified Unusual Observations .....	132
9. The Median of the Three Measured Values at Each of the Three Test Voltages Measured from Each Sample Flat Presented with the Associated Uncertainty Value Calculated During Error Analysis .....	146

LIST OF FIGURES

Figure	Page
1. (Left) Representative Picture of Carbon Black as Typically Placed on the Market. (Right) Scanning Electron Microscope View of a Carbon Black Aggregate Consisting of Fused Primary Particles (Magnification: x 120,000) [26].	37
2. Image Illustrating the Structural Difference Between Low and High Structure Carbon Black [32]	44
3. Percolation Curve Illustrating the Electrical Properties Verses the Amount of Carbon Black Loading in Plastics [32]	45
4. Plot Illustrating the Percentage Mass Loss of Tested Button Samples Versus Their Measured Resistance Values	50
5. Two-point ESP-9 Effective Resistance Test Results Plotted Across Pulse Generator Input Voltage	51
6. Visual Representation of the Response Surface Space to Be Created Using Experimental Electrical Resistivity Results.	59
7. Formulation for the Electric Propellant Samples with No Included Additives.	63
8. Formulations for the Electric Propellant Samples with Varying Tungsten Additive Particle Sizes and Loadings.	64
9. Formulations for the Electric Propellant Samples with Varying Copper Additive Particle Sizes and Loadings.	65
10. Formulations for the Electric Propellant Samples with Aggregate Carbon Black and Various Particle Loadings.	66
11. (Left) Thinky Mixer Used to Manufacture Test and Final Sample Formulations [41]. (Right) The Semco Extruding Gun Used to Extrude Mixed Propellant Out of the Syringes in Which They Were Mixed	67
12. Testing Samples Stored in the Laboratory Desiccator	70
13. Testing Apparatus Electrode Assembly [42]	72

Figure	Page
14. (Left) Creo Parametric Model of Testing Apparatus, with Specimen. (Right) Image of Testing Apparatus Built for This Investigation, Without Specimen.....	73
15. (Left) The Testing Apparatus Integrated into the Testing Set-up. (Right) The Oscilloscope and Differential Amplifier with Connections from the Testing Set-up .....	75
16. The Calibration Resistor Connected to the Testing Set-up .....	76
17. Screen Capture of the Calibration Correction Portion of the Excel Testing Record Sheet. ....	80
18. The Minitab Worksheet Where Experimental Data Was Entered .....	81
19. An Improvised Coaxial Electrode Thruster Shown After Being Pulsed Several Times.....	89
20. (Left) The Unprepared Non-Additive In-Mold Sample Flat. (Middle) The Unprepared 1.5% Loaded Carbon Black In-Mold Sample Flat. (Right) The Unprepared 2.3% Loaded Carbon Black In-Mold Sample Flat.....	90
21. The Unprepared 1.5% Loaded Tungsten (Left) 1-5 Micron, (Middle) -325 Mesh, and (Right) -100 Mesh In-Mold Sample Flats.....	91
22. The Unprepared 2.3% Loaded Tungsten (Left) 1-5 Micron, (Middle) -325 Mesh, and (Right) -100 Mesh In-Mold Sample Flats.....	91
23. The Unprepared 5% Loaded Tungsten (Left) 1-5 Micron, (Middle) -325 Mesh, and (Right) -100 Mesh In-Mold Sample Flats. ....	92
24. The Unprepared 1.5% Loaded Copper (Left) 1-5 Micron, (Middle) -325 Mesh, and (Right) -100 Mesh In-Mold Sample Flats. ....	93
25. The Unprepared 2.3% Loaded Copper (Left) 1-5 Micron, (Middle) -325 Mesh, and (Right) -100 Mesh In-Mold Sample Flats. ....	93
26. The Unprepared 5% Loaded Copper (Left) 1-5 Micron, (Middle) -325 Mesh, and (Right) -100 Mesh In-Mold Sample Flats.....	94
27. A Prepared Sample Flat and Storage Bag, with a Randomly Chosen Specimen Removed from Flat Mold to Display the Specimen Labeling Technique.....	95
28. Values for Bulk Volume Resistivity of the Non-Additive Specimens Plotted as a Function of Pulse Generator Input Voltage. ....	97



Figure	Page
29. Values for Bulk Volume Resistivity of the Carbon Black Specimens Plotted in Groups of Percent Additive Loading as a Function of Pulse Generator Input Voltage.....	99
30. Values for Bulk Volume Resistivity of the Tungsten Specimens Plotted in Groups of Percent Additive Loading as a Function of Pulse Generator Input Voltage. ....	101
31. Values for Bulk Volume Resistivity of the Copper Specimens Plotted in Groups of Percent Additive Loading as a Function of Pulse Generator Input Voltage. ....	102
32. Two Prepared Sample Flats, Both with at Least Four Specimens Identified as Outliers. ....	103
33. Values for Bulk Volume Resistivity, Including the Two Data Points That Have Been Retested as Outliers, of the Non-Additive Specimens Plotted as a Function of Pulse Generator Input Voltage. ....	106
34. Values for Bulk Volume Resistivity, Including the Two Data Points That Have Been Retested as Outliers, of the Carbon Black Specimens Plotted in Groups of Percent Additive Loading as a Function of Pulse Generator Input Voltage.....	107
35. Values for Bulk Volume Resistivity, Including the 10 Data Points That Have Been Retested as Outliers, of the Tungsten Specimens Plotted in Groups of Percent Additive Loading as a Function of Pulse Generator Input Voltage.....	108
36. Values for Bulk Volume Resistivity, Including the 10 Data Points That Have Been Retested as Outliers, of the Copper Specimens Plotted in Groups of Percent Additive Loading as a Function of Pulse Generator Input Voltage.....	109
37. Calibration Corrected Values for Bulk Volume Resistivity, Including the Two Data Points That Have Been Retested as Outliers, of the Non-Additive Specimens Plotted as a Function of Pulse Generator Input Voltage. ....	112
38. Calibration Corrected Values for Bulk Volume Resistivity, Including the Two Data Points That Have Been Retested as Outliers, of the Carbon Black Specimens Plotted in Groups of Percent Additive Loading as a Function of Pulse Generator Input Voltage.....	113

Figure	Page
39. Calibration Corrected Values for Bulk Volume Resistivity, Including the 10 Data Points That Have Been Retested as Outliers, of the Tungsten Specimens Plotted in Groups of Percent Additive Loading as a Function of Pulse Generator Input Voltage. ....	113
40. Calibration Corrected Values for Bulk Volume Resistivity, Including the 10 Data Points That Have Been Retested as Outliers, of the Copper Specimens Plotted in Groups of Percent Additive Loading as a Function of Pulse Generator Input Voltage. ....	114
41. Calibration Corrected Values for Bulk Volume Resistivity, Including the Two Data Points That Have Been Retested as Outliers, of the Non-Additive Specimens Plotted as a Function of Particle Loading Percentage Value. ....	115
42. Calibration Corrected Values for Bulk Volume Resistivity, Including the Two Data Points That Have Been Retested as Outliers, of the Carbon Black Specimens Plotted in Groups of Percent Additive Loading as a Function of Particle Loading Percentage Value. ....	116
43. Calibration Corrected Values for Bulk Volume Resistivity, Including the 10 Data Points That Have Been Retested as Outliers, of the Tungsten Specimens Plotted in Groups of Percent Additive Loading as a Function of Particle Loading Percentage Value. ....	117
44. Calibration Corrected Values for Bulk Volume Resistivity, Including the 10 Data Points That Have Been Retested as Outliers, of the Copper Specimens Plotted in Groups of Percent Additive Loading as a Function of Particle Loading Percentage Value. ....	117
45. Calibration Corrected Values for Bulk Volume Resistivity, Including the 10 Data Points That Have Been Retested as Outliers, of the Tungsten Specimens Plotted in Groups of Percent Additive Loading as a Function of Additive Particle Size.....	119
46. Calibration Corrected Values for Bulk Volume Resistivity, Including the 10 Data Points That Have Been Retested as Outliers, of the Tungsten Specimens Plotted in Groups of Percent Additive Loading as a Function of Additive Particle Size.....	120

Figure	Page
47. (Left) A Histogram Plot of All of the Values Measured for the Bulk Volume Resistivity Response Shown with a Normal Distribution Curve for Comparison. (Right) A Probability Plot of the Bulk Volume Resistivity Responses Used to Verify the Normality of the Response data .....	123
48. The ANOVA Table That Minitab Generated Using the Data Collected for This Set of Experiments. ....	125
49. A Continuation of the ANOVA Table That Minitab Generated Using the Data Collected for This Set of Experiments.....	130
50. A Continuation of the ANOVA Table That Minitab Generated Using the Data Collected for This Set of Experiments.....	132
51. The Minitab Generated Fitted Means Main Effect Plot for the Bulk Volume Resistivity Response Variable.....	134
52. The Minitab Generated Fitted Means Interactions Plot for the Bulk Volume Resistivity Response Variable.....	135
53. Surface Plots of Bulk Volume Resistivity (z-axis) Versus Additive Resistivity (x-axis) and Particle Loading Percentage (y-axis), with an Additive Particle Size Hold Value Equal to 0.0000745m.. ....	136
54. Surface Plots of Bulk Volume Resistivity (z-axis) Versus Additive Loading Percentage (x-axis) and Additive Particle Size (y-axis), with an Additive Resistivity Hold Value Equal to 0.0000005Ω-m. ....	138
55. Surface Plots of Bulk Volume Resistivity (z-axis) Versus Additive Resistivity (x-axis) and Additive Particle Size (y-axis), with an Additive Loading Percentage Hold Value Equal to 0.025.....	138
56. The ANOVA Table That Minitab Generated Using the Data Collected for This Set of Experiments, with the Additive Resistivity Squared and Additive Resistivity Multiplied by Additive Loading Percentage Terms Removed from the Analysis.....	140

Figure	Page
57. A Continuation of the Updated ANOVA Table That Minitab Generated Using the Data Collected for This Set of Experiments, Detailing Coded Coefficients and the Regression Equation Output by the Analysis. ....	141
58. A Continuation of the ANOVA Table That Minitab Generated Using the Data Collected for This Set of Experiments, Detailing the Data Points That Minitab Has Determined to Be Unusual Observations.....	142
59. The Minitab Generated Fitted Means Main Effect Plot for the Bulk Volume Resistivity Response Variable.....	143
60. The Minitab Generated Fitted Means Interactions Plot for the Bulk Volume Resistivity Response Variable.....	144
61. Updated Surface Plots of Bulk Volume Resistivity (z-axis) Versus Additive Resistivity (x-axis) and Additive Loading Percentage (y-axis), with an Additive Particle Size Hold Value Equal to 0.0000745m. ....	145
62. Updated Surface Plots of Bulk Volume Resistivity (z-axis) Versus Additive Loading Percentage (x-axis) and Additive Particle Size (y-axis), with an Additive Resistivity Hold Value Equal to 0.0000005Ω-m.....	145
63. Updated Surface Plots of Bulk Volume Resistivity (z-axis) Versus Additive Resistivity (x-axis) and Additive Particle Size (y-axis), with an Additive Loading Percentage Hold Value Equal to 0.025.....	146

LIST OF ACRONYMS

Acronym	Phrase
ABS	Acrylonitrile Butadiene Styrene
AC	Alternating Current
AD	Anderson-Darling Normality Test Statistic
ASTM	American Society for Testing and Materials
DC	Direct Current
DIW	Deionized Water
DMM	Digital Multi-Meter
DOE	Design of Experiment
DSSP	Digital Solid State Propulsion, LLC
ESD	Electrostatic Discharge
ESP-9	Electric Solid Propellant Formulation no. 9
HAN	Hydroxyl-Ammonium Nitrate
HTPB	Hydroxyl-Terminated Polybutadiene
IM	Insensitive Munitions
IRAD	Internal Research and Development
PVA	Polyvinyl Alcohol
PVAc	Polyvinyl Acetate
SDS	Safety Data Sheet
SPE	Solid Polymer Electrolyte
SRM	Solid Rocket Motor
TRL	Technology Readiness Level
W	Tungsten
2D	Two Dimensional
3D	Three Dimensional

NOMENCLATURE

Term	Definition
$d$	= Test specimen thickness [in or mm]
$E^0$	= Standard electrode potential, cell [V]
$E^0_{red}(reduction\ process)$	= Standard electrode potential, reduction/cathode [V]
$E^0_{red}(oxidation\ process)$	= Standard electrode potential, oxidation/anode [V]
$G_{CM}$	= Common mode gain [unitless]
$G_{DM}$	= Differential mode gain [unitless]
$G_{diff\ amp}$	= Differential amplifier gain [unitless]
$G_{probes}$	= Voltage probe gain [unitless]
$I$	= Current through the current electrodes [A]
$k$	= Correction factor [in or mm]
$l$	= Distance between apparatus potential electrodes [in or mm]
$R$	= Bulk volume resistivity [ $\Omega$ -m]
$R_{CM}$	= Current measurement resistor resistance value [ $\Omega$ ]
$V$	= Potential different across potential electrodes [V]
$V_{CM}$	= Common mode voltage [V]
$V_{DM}$	= Differential mode voltage [V]
$V_{out}$	= Voltage measurement across the potential electrodes [V]
$V_{pgen}$	= Pulse generator input voltage value [V]
$V(1)$	= Voltage probe #1 measurement [V]
$V(2)$	= Voltage probe #2 measurement [V]
$w$	= Test specimen width [in or mm]
$\partial d$	= Test specimen thickness uncertainty [in or mm]
$\partial G_{diff\ amp}$	= Differential amplifier uncertainty [unitless]
$\partial G_{probes}$	= Voltage probes uncertainty [V]
$\partial I$	= Current through the current electrodes uncertainty [A]

Term	Definition
$\partial R$	= Bulk volume resistivity uncertainty [ $\Omega$ -m]
$\partial R_{CM}$	= Current measurement resistor resistance value uncertainty [ $\Omega$ ]
$\partial V$	= Potential different across potential electrodes uncertainty [V]
$\partial V_{oscope}$	= Oscilloscope voltage reading uncertainty [V]
$\partial V_{pgen}$	= Pulse generator input voltage value uncertainty [V]
$\partial V_{rej}$	= Voltage rejection value uncertainty [V]
$\partial w$	= Test specimen width uncertainty [in or mm]

## CHAPTER 1

### INVESTIGATION INTRODUCTION

#### Introduction

Solid propellants are used in many types of specific applications ranging from rocket motors to various kinds of gas generators. Solid propellants are simpler in operation (compared to other forms of chemical propulsion) and are able to deliver high levels of thrust without significant design compromises. Unfortunately, solid propellants usually cannot change thrust levels in response to a change in operating conditions and cannot be restarted or reused after firing following ignition. It is for these reasons that the ability to control the reaction rate of solid propellants would offer significant benefits to almost all applications in which they are utilized.

In recent years, a new type of solid propellant, in which the propellant's reaction rate has been shown to be dependent upon the application of an electrical signal, has been under investigation by two major stakeholders. The range of applicable uses for this technology is broad and "includes attitude control systems and a safe alternative to higher impulse space satellite thrusters," as electrically operated solid propellant "rocket motor thrusters, with thrusts ranging from milli-pounds to several tens of pounds of thrust" "are capable of sustained thrust profiles or may be pulsed at over 30Hz." These types of propellant, "based on ionic salts, are basically inert until an electric current is passed through them at which point they exhibit an electro-chemical reaction." Additionally, the propellant has the ability to be throttled during a single pulse based on current density, and "being that the propellant is self-extinguishing, it may be turned on and off by the application and removal of a threshold current density." The first of these two investigative stakeholders is Digital Solid State Propulsion, LLC (DSSP). "For more than 10 years, DSSP had demonstrated the safety and controllability of ePropellants in many applications. The DSSP formulations are based on a hydroxylammonium nitrate (HAN) oxidizer and have been subjected to safety and insensitive munitions (IM) testing." The second of these two stakeholders is Raytheon Missile Systems (RMS), who "first became aware of these propellants as a result of an interaction with a small business partner," DSSP, and have been investigating them since approximately 2010.



In an attempt take advantage of the operations benefits that could be provided by this type of electrically operated solid propellant, RMS, “working both independently and with DSSP, investigated existing formulations and pursued” propellant formulations “that could meet a wider range of requirements” than those provided by the DSSP formulation mentioned above [1]. United States patent number US-2014-0174313-A1, written by RMS employees James K. Villarreal and Richard D. Loehr, describes the invention of electrically operated propellants “configured to ignite at an ignition condition and extinguish under an extinguishing condition,” with the ignition condition described as “an electrical input” applied “across the electrodes to ignite” the propellant and the extinguishing condition described as an interruption in the electrical input [2]. This patent was granted on June 26, 2014 as part of an RMS Technology Based Internal Research and Development (IRAD) effort. The purpose of this IRAD “is to investigate the use and performance of a new class of solid propellant generically described as “electric propellant” [3]. This propellant, referred to as “Phoenix™ ePropellant, does not use HAN but alternatively uses a perchlorate based oxidizer.”

The most current version of the RMS electric propellant formulation contains, by mass, a perchlorate oxidizer dissolved in deionized water in an 80% concentrated solution (which is equal to 48% perchlorate oxidizer and 12% deionized water), 20% polyvinyl alcohol (PVA) acting as the propellant binder, and 20% powdered tungsten, acting as the metallic additive. The chemical constituents of this formula, and related information, are further discussed in Chapter 2. Based on pressurized environment testing, and when compared to the HAN based propellants, the RMS “electric propellant formulation will not sustain combustion without an electrical input at operationally relevant pressures,” whereas the “HAN formulations will self-sustain burning above threshold pressures of approximately 200 psi.” Additionally, the “Phoenix™ ePropellant can be turned off/restarted at high motor pressures,” a characteristic which “widens the potential applications for which these safe, solid propellants may be utilized and promises the potential of true on/off operation at all pressure levels” [1].

In the eight years in which the use of this electric solid propellant has been investigated, RMS has increased research efforts dedicated to this new technology in scope each year based

on the increase in fundamental science and understanding of this propellant, and on the successful outcomes of the development and application experiments conducted. While many electric propellant uses and applications have been explored over the years, a fundamental understanding of the operational mechanism of this propellant is necessary to move forward with development and implementation of this technology.

Based on a 2015 investigation regarding the chemical and physical combustion mechanisms of electric propellant, written by Jason Wickham in support of the 2015 electric propellant fundamental science research goals, it was suggested that the formulation's current metallic additive, powdered tungsten, is not only acting as an added fuel source, but may also be playing an additional, currently unknown, role in the operation and performance of the RMS electric propellant formulation.

This study investigates several samples of electric propellant, all of which are variations of the propellant formulation given above. This study is an attempt to quantify the role a metallic or non-metallic additive has on the propellant, with the purpose of investigating a chosen response variable, propellant bulk volume electrical resistivity, meant to help reveal any implications regarding the fundamental science behind the operation of this material. The changes made to the electric propellant formula for this study focused on the metallic or non-metallic additive, the additive's particle size, and the relative amount of the additive included in each propellant sample. Ascertaining how the additive contributes to the material properties and operation of the electric propellant, by means of propellant sample electrical resistivity measurements, will support the overarching industry goal of determining the exact combustion and conduction mechanisms under which this propellant operates. Understanding the mechanisms by which this propellant operates will allow for an increase in its technology readiness level (TRL) and further development of its applications, enabling the implementation of this propellant technology in industry.

#### Background

As detailed above in the Introduction section, RMS has been investigating the use of electric propellant since approximately 2010, and each year RMS's efforts have increased following the

promising results of the last. In 2010, RMS conducted an in depth literature review of the DSSP propellant material and of related background research in industry. The interest in and potential of this material remained high, so a request for continuing funding was made to obtain samples of this material and begin independent testing. In 2011, RMS was able to obtain samples of the propellant material manufactured by DSSP. After performing several tests on the DSSP propellant samples, RMS concluded that while the HAN based electric propellant had many desirable characteristics, including relatively clean exhaust products, it also had “poor stability at high temperatures and would probably not be able to meet the stringent thermal requirements typical of missile systems” [4].

During the later months of 2011, RMS continued to research the specific chemistry of the DSSP propellant and arrived at the conclusion that the electric propellant technology may not be limited to a HAN based propellant material; other ionic salt oxidizers, and subsequent propellant formulations utilizing these oxidizers, could have the same electric propellant behavior, with possible improvements in performance and properties that meet the high temperature requirements of the missile systems for which they could be considered. Following this conclusion, RMS manufactured several variations of a perchlorate oxidizer electric propellant, using the same PVA binder and including several varied amounts of powdered tungsten and aluminum additives ranging from 0-20% of the formulation, by mass. These samples were then tested at different voltage levels for power consumed with the goal of determining which samples consumed the least amount of power over different voltage inputs, determining propellant power demand, and understanding the effects on propellant mechanical properties. The ninth electric solid propellant formulation (ESP-9) sample made, a mixture of 60% perchlorate oxidizer solution, 20% PVA, and 20% tungsten powder additive (all mass percentages), had the lowest power consumption out of the nine RMS and DSSP samples tested, with power consumption to initiate approximately 67% lower than the DSSP HAN samples [5].

In 2012, as research focused on understanding the HAN based electric propellant formulations progressed, it was discovered that the electric propellant was not extinguishable once the control volume in which it was being tested reached a certain pressure. Self-sustaining

reactions at high pressures would result in little or no power required during the reaction itself, however, other applications would benefit from the ability to extinguish at higher operational pressures. Concerns regarding the high temperature stability, the high energy input required at ignition, and about the low modulus and polymer water loss of the DSSP propellant were still present. Alternatively, the RMS ESP-9 formulation was able to alleviate some of these concerns, minus the hygroscopicity and hardness concerns associated with the PVA binder; these alleviations included the improved thermal stability of the alternate oxidizer (which was lifetime limiting in DSSP's case), improved aging properties, and increased oxidizer density, as well as the reduced energy demand provided by the metallic additives, an improved linearity of energy input requirements, and an overall increase in propellant density [6].

In 2013, the objectives of the RMS electric propellant research efforts were “to verify previously discovered performance capabilities” of the RMS ESP-9 formula, to “investigate alternate potential applications for this novel propulsion capability.” Additionally, some RMS Materials, Processes & Producibility Department (MP&P) lab testing was performed in order to improve RMS's understanding of the electric propellant material properties. The measurements resultant from this testing included Shore A hardness, thermal decomposition onset evaluation, glass transition temperature evaluation, and the observation of propellant material modulus changes with temperature [7].

The 2014 research efforts were designed around the intent to bring electric propellant to a high TRL involving improvements to the propellant material properties, electrode configurations, and system integration. In order to investigate electrode configurations, a successful electrode test bed was built and parallel plate electrode testing was performed as a part of the test bed check out, which illustrated to the electric propellant researchers some of the fundamental issues surrounding the use of electric propellant. It was discovered that a minimum current density appeared to be controlling the initiation of propellant burning and that previously recorded measurements, based on a wire electrode set-up, were not resulting in a proper understanding of the necessary electric propellant firing power requirements. The parallel electrode testing also illustrated to the team that the combustion path of the propellant between the electrode plates

was not uniform, but instead followed a certain path through the material. It was theorized from this, that the changes in propellant resistivity, due to non-uniform mixing and curing, were causing the applied current to travel through only a portion of the propellant material. Based on these observed results, it was concluded that controlling the current density at the electric propellant burning surface may be the key to being able to fully utilize this material. Further electrode testing was conducted in an effort to use electrode geometry to control the applied current path and the propellant current density by using the resistance of the propellant [8].

Significant advances in electric propellant use and operation were made during the 2015 research efforts, including the development of a “standard test method for isolating the current density across a sample and developing small thrusters.” Additionally, Jason Wickham, an RMS 2015 summer intern, was “hired to investigate the combustion mechanisms of electric propellants” via their chemical composition [3]. In this report Wickham indirectly details several electric propellant characteristics and operational observations that indicate the possibility of the effects of percolation theory on this material. The resulting report is referenced and further expanded upon throughout this study.

In 2016, electric propellant research efforts were based on three main areas of investigation, including “improving the mixing of the material with the use of a vacuum mixer,” “testing the energy release through gas generator and small thruster testing” contracted out to DSSP, and “testing of the initiation and electrical characteristics while using a thermal imaging camera.” In his Final Report for 2016, Mark Langhenry, the Electric Propellant IRAD Principal Investigator, stated that the focus of the 2016 research efforts “represents a step towards understanding the fundamental characteristics of electric propellant such that future efforts may best apply resources to the areas that are the most promising for significant results that will advance the technology.” Testing performed during this year “illustrated that there is a capacitance build up in the material,” which further complicates that ability to accurately repeat testing results; additionally, “what role this plays, along with the heating due to” current flow is still currently unknown. The sequence of events leading up to and including the initiation of the electric

propellant material is one “effect that is difficult to reproduce” in practice. Keeping track of all of the energy put into and produced by the electric propellant is another challenge [9].

Later in 2016, the electric propellant researchers were able to move a significant amount of the electric propellant manufacturing and testing equipment to the previously contracted R3 Aerospace facility to accelerate the study of this material. A mixing test plan was developed to be conducted at the R3 facility in order to prove in the newly acquired electric propellant mixer, to “provide a framework for the investigation of mixing electric propellant in the Thinky ARV-310 Planetary Vacuum Mixer and to further refine the Electric Propellant Manufacturing Instructions.” The design of experiment (DOE) developed for this mixing investigation allowed for the testing of “varying mix times, mixer speeds, and mixer vacuum pressures in order to determine the electric propellant mixing practices that yield the best cast and baked electric propellant samples for future testing.”

The results of this test plan were positive overall and included several advancements in the mixing and casting procedures used to manufacture electric propellant samples. The first of these advancements included the addition of the Thinky mixer to the mixing process, as the “mixer has shown that it can emulsify an ESP-9 mix better than anything else” [10]. Additional advancements include final product bulk setting properties and the almost total elimination of the propellant’s susceptibility to water absorption and loss, a final agreed upon baseline formulation provided above in the Introduction, an updated set of manufacturing instructions specific to the Thinky mixer, and additional research on the desiccation of samples and extruding capabilities, as well as recommendations for future improvements. The experimental mixing investigation that took place at R3 provided additional advantages to any future electric propellant study, as many of the 2014 and 2015 experiments summarized above reported that results could have been skewed due to non-uniform mixing and curing processes.

The results produced during the 2016 year were, again, successful in illustrating “the challenges associated with this material,” including “both the level of understanding of the underlying physics” governing the material and the “ability to make meaningful measurements of the processes” by which it operates. As of yet, “testing configurations have not been sufficient to

reliably and repeatedly” yield results “that may be used to accurately quantify certain effects.” A “major part of the 2017 effort will be to define the parameters of interest and design test configurations that may be used to capture those parameters” in order to better understand the mechanisms that drive the electric propellant initiation. Any effort, including the optimization of the current electric propellant formulation, “will not be efficient” until “repeatable and accurate measurements can be obtained” due to the amount of “variability from test to test with the same material,” making it difficult to identify differences between materials “without a large number of tests with multiple sample and test configurations” [9]. 2017 advances in electric propellant included a refinement of mixing procedures and equipment used, including the addition of a syringe mixing and extruding process, as well as updated hazard classification safety testing, and the beginning of this investigation.

#### Problem Statement

Current measurement and testing configurations have not been sufficient enough to yield reliable and repeatable results that could be used to quantify certain effects to better understand the mechanisms driving propellant initiation and operation; this is the research problem addressed by this study. As previously discussed, the development and understanding of the fundamental science regarding electric propellant is necessary for the application and use of this technology in industry. Based on the current status of the perchlorate oxidizer based electric propellant formula, summarized in Background, only the suggestion for a study regarding the role of tungsten, or a metallic additive in general, in the electric propellant formula has been made in the paper prepared by Jason Wickham. No significant effort dedicated to the measurement of the electric resistivity of such a wide variation in electric propellant sample formulation and size has been conducted previously.

Previous years of RMS research, and research conducted for the RMS electric propellant research team under contract, have suggested that there exists some mechanism by which the electric propellant operation is driven that is related to the propellant’s resistance and the current density at the time of measurements and/or testing. This mechanism is not currently well understood, and researchers, as described above, have only begun testing in recent years in

which the electric propellant current density acts as a known variable, independent or dependent. Additionally, no significant effort has yet been made to define the electrical conductivity and/or resistivity of the perchlorate oxidizer based electric propellant at various levels of measurement and/or across several methods of testing. Looking outwards from RMS, to DSSP and at other research conducted in the aerospace and propulsion industry, as well as outwards from the aerospace industry as a whole and into other commercial industries, such as the battery industry, no study quantifying the electrical conductivity or characterizing a mixture of similar propellant and/or the electric propellant constituent ingredients has been done previously. The only exceptions include the research performed on the chemical and electrical properties of solid polymer electrolyte materials and doped PVA samples, further discussed in Chapter 2.

#### Purpose of the Study

The intention of this thesis was not to discover new electric propellant formulations or to improve upon the current formulation, although this is an additional benefit of the formulation resistivity investigation. The research for this series of experimental propellant mixtures and measurements was designed to be conducted for the primary purpose of aiding in the search for developing and understanding the fundamental science and the combustion and conduction mechanisms that drive the current perchlorate oxidizer based electric propellant formula to operate and still maintain its on/off firing capabilities. This investigation has attempted to quantify one measurable dependent variable, the electrical resistivity, of the propellant samples produced that might indicate how well certain electric propellant variations will perform compared to others developed for this thesis project and in the future. This intention will be described throughout this document, but is most prominently emphasized in the sections of this document discussing propellant sample manufacturing, wherein the additive replacements and sample formulas are described and shown to not deviate in any other way from the most current version of the patented perchlorate oxidizer based electric propellant formulation at the time during which this research took place.

This study not only addresses a meaningful gap in the knowledge of this perchlorate oxidizer based electric propellant formulation and its additive variants, but also contributes to the



beginning stages of filling an industry wide gap in this area of research. The work done for this investigation and the results produced have provided anyone with an interest in electric propellant research with a set of mixing and testing methods, including a testing apparatus, as well as an initial, resultant data set, that can be used to quantify any later variations in the ESP-9 electric propellant formula, and any other electric propellant formulation developed in the future, and to accurately compare results to previous work.

#### Experimental Hypothesis and Research Questions

The following summarizes the researched hypothesis under which this study has been conducted: There exists certain metallic or non-metallic replacement additives for this particular perchlorate oxidizer based electric propellant formulation, and certain additive particle sizes and added particle amounts of that replacement additive, that will not only preserve the integrity of the electric propellant's on/off and throttling mechanisms, but will also reveal the nature of the electrical resistivity of the altered propellant samples with regard to percolation theory, described in Chapter 2. That is, that some percolation curve exists for each replacement additive used (related to the amount of particles used and the size of those particles), that will reveal some limiting critical threshold percolation value, beyond which no added benefit of particle size or amount can be shown. Additionally, there exists a replacement additive, replacement additive particle size, and replacement additive particle amount, or some combination of, that may negate the "electric properties" of this propellant, which can be determined through measuring electrical resistivity (related to the percolation of and assumed to be non-constant across the samples produced for this study), and by doing so may reveal some useful information that could aid in the determination of the conductivity and combustion mechanisms by which this propellant operates. Finally, based on each experimental propellant formulation and its respective resulting conductivity measurements, preliminary predictions can be made regarding the initiation and firing power requirements of the propellant formulations.

This experiment was designed around three interrelated research questions, listed below:

1. It is likely that the powdered tungsten additive is acting as more than a "conductor, heat sink, densifier, and mechanical aid" in the electric propellant. Therefore, would characterization of the

electric propellant formulation with different metallic, or non-metallic, additives aid in the indication of what role the tungsten additive plays in the electric propellant's conduction and/or combustion mechanisms [4]. And, will the removal or replacement of the tungsten additive, in various sizes and amounts, in the current electric propellant formulation yield a change in the electrical resistivity of the materials being studied?

2. The particle size of the additives is/will be critical to the performance of the propellant, "as it will govern not only the reactivity of the fuels, but also the spacing of the particles dispersed in the propellant, which will have an impact on the conductivity and breakdown strength of the material" [4]. Based on the additive particle size and the amount of the additive included in the propellant (analogous to the spacing between particles), is there a certain point at which there is no benefit in the electric propellant additive particle size or spacing? Will this have an impact on the propellant's electrical on/off mechanism? Can this phenomenon be described and/or characterized by the theory of percolation? And, will this help in establishing the resistivity and/or combustion baseline mechanisms that control this type of propellant, or more specifically, this propellant formulation?

3. Based on the resulting electrical conductivity measurements, can anything be said about the relationship between propellant electrical conductivity and the performance related to initiation and continued firing power requirements?

#### Theoretical Foundation and Experimental Framework Review

Chapter 2 details the current theory of the operational mechanisms of this electric propellant material. This theory was used to outline the Experimental Framework of this study and, in conjunction with the established research questions, design a set of experiments with the purpose of measuring the electrical resistivity of varying sample formulations.

Previous years of research have suggested that some mechanism by which the electric propellant operation is driven is related to the propellant's resistance and current density during use, although the importance of the propellant resistance hasn't been established through testing. While the tungsten additive was originally included in the propellant with the purpose of increasing conductivity and mechanical properties, the propellant's conductivity is also influenced

by the other formulation ingredients. However at some point in the process of attempting to understand the propellants operational mechanisms, it may be revealed that a minimum, unknown concentration of metallic, or otherwise, conductivity additive may be required in the propellant formulation. It is suspected that the flow of current through the propellant gradually increases the conductivity of the material, which, in this case, is most likely due to the proton transfer as part of an electrochemical reduction-oxidation reaction. This model proposes that the tungsten particles within the material are acting as electron acceptance and donation sites due to the ability of tungsten to assume both positive and negative oxidation states. Ultimately, the oxidation of the tungsten particles would allow these electrochemical processes to occur within the propellant samples and would ultimately increase sample conductivity, temperature, and reaction rate.

Based on the current theory of operation and the desire of researchers to understand the fundamental science behind the operation of this propellant, an experimental study was researched, designed, and carried out with the purposes of contributing useful information to the determination of the electric propellant operational mechanisms. This study's experimental framework was based on the research questions established above, as well as on the current theory of the propellant operation, and is further detailed in Chapters 2 and 3. The experiments designed only encompassed an investigation of the conduction mechanism of different electric propellant sample formulations as it is related to their electrical resistivity because it is one of the operational phenomena that can easily be broken down into several different standardized experiments and further expanded upon based on results.

Due to the wide number of this propellant's unknown operational and intrinsic variables/properties, this study was designed to simply investigate only a few factors that could be affecting propellant operation. This includes the determination of at least a partial understanding of the role that tungsten is playing in the propellant, which can be done by simply replacing it with different materials, each of which having only one, or some, of the supposed desired properties of tungsten. Additionally, if this type of electric propellant is governed by some phenomena related to its electrical properties and/or percolation, as suspected, then the amount

of metallic additive, or otherwise, if the additive is still conductive, included in the formulation will also have an impact on the propellant performance, as will the size of the additive particles included.

#### Nature of the Study

Based on the outlined Experimental Framework of this study, detailed in Chapter 2, and in order to generate data that will be used to (partially) answer the experimental research questions written above, a set of fractional factorial experiments were designed to provide insight into the role that an additive is playing in this electric propellant formulation. Within these experiments, the baseline propellant formulation's tungsten additive was investigated, along with copper and conductive carbon black additives, in three different particle size ranges and three different volume percentage particle loadings. Each of these new propellant formulations (a total of 21 samples and 189 specimens) were tested for quantitative electrical resistivity values at three different pulse generator input voltage values. Additional data, including sample dimensions, mass, qualitative observations, and images were recorded during the sample mixing, preparation, and testing events.

The most important variable examined during this investigation was the propellant additive itself. It was the most dramatically changed experimental variable and the results provided a wide range of new insights into propellant operation and have allowed for a new avenue of future investigative work, as necessary or desired. Following the additive itself, loading was expected to have a significant influence on the propellant formulations; particle size, however, was not expected to affect results as significantly as the additives themselves, the effects which may or may not be noticeable in the results of a screening experiment of this nature and with the choices of particle size ranges made for this set of factorial experiments. Finally, based on previous work, no notable change in formulation resistivity was expected with the pulse generator input voltage study variable, however this has not been tested to the degree in which this study was initially proposing. Regardless, resistivity versus testing input voltage would be useful information for the researchers to review and have on hand.

The experimental methodology applied throughout this study was largely derived for this study itself, or was otherwise grounded in previous work. Sample flat pre-mixing and mixing plans were written for this investigation based on the current “state of the art” electric propellant mixing procedures and were updated as needed. Testing procedures, apparatus, and instrumentation were based, as much as possible, on widely approved of statistical reasoning and methods, ASTM standards, and previous testing work, and the detailed electrical resistivity testing set-up and procedures were derived from previous work and specifically tailored to this investigation. All of the methodology used/created for this set of experiments was generalized or standardized as much as possible throughout the process to allow for continued use and improvement by the research team and to allow for future use if confirmation or re-establishment of experimental results is required. Finally, the analysis of the resulting data, used to address the research questions and prove or disprove the research hypothesis, was also based, as much as possible, on widely approved statistical reasoning and methods for design of experiments, fractional factorial experiments, and response surface practices.

#### Significant Term Definitions

Electric propellant is defined as a class of solid propellants that do not begin or sustain chemical reaction without the application of an electrical current ignition input applied across a set of electrodes, and do not cease chemical reaction until an extinguishing condition, known as an interruption in the applied electrical current, is subsequently applied. The electric propellant referred to and discussed within this document is that patented by RMS in 2015, as described in the Introduction. Electric propellant is also referred to by its RMS formula name, ESP-9, and with the following terms: “electric solid propellant,” variations of the term “ePropellant,” and variations of the acronym “EP.”

Electrical conductivity is defined as a measurement that indicates the ability of a material to conduct an electric current. Electrical conductivity is the reciprocal of electrical resistivity. This variable will also be referred to solely as “conductivity.”

Electrical resistance is defined as a measure of the difficulty inherent in passing an electric current through a conductor. This electrical measurement is made in units of Ohms ( $\Omega$ ).

Electrical resistivity is defined as an intrinsic measurement that quantifies how strongly a material will oppose the flow of electric current. Electrical resistivity is the reciprocal of electrical conductivity. This variable will also be referred to solely as “resistivity.” This electrical measurement is made in units of Ohm-meters ( $\Omega$ -m).

Replacement/replacement additive/additive is defined as the powdered chemical additives comprising a portion of the electric propellant baseline and the formulations prepared for this study.

Researched hypothesis (or the alternative hypothesis) is defined as the opposite of the null hypothesis written for this study, stating that there is a relationship between two measured phenomena, and will be either proven or disproven through statistical analysis of the study’s measured results. The null hypothesis prepared for any scientific study states that there is no relationship or association between two measured phenomena, and the disproving of the null hypothesis—by concluding that there are reasons to believe that two measured phenomena are related—is the purpose of that scientific study.

Response variable is defined as the term used to describe the variable of interest in an experiment, also known as the dependent variable. This is the variable that will be tested for, observed, and measured.

Response surface is defined as the surface resulting from the data gathered from this investigation in a three dimensional, graphical representation that aids in the visualization of the shape of the resulting experimental response variable based on the size of the two explanatory factors against which the response is plotted. The response surface variable methodology is meant to explore the relationship between several different independent, or explanatory variables, and one (or more) response variable. The main purpose of this methodology is to use a sequence of designed experiments to obtain an optimal response or underlying process with the intention of discovering property combinations that provide maximum yield with minimal cost.

Sample Flat(s) is defined as the form, or mold shape, in which all of the propellant formulations were cast in following mixing, and prior to curing and being cut and labeled for

testing. This term is also used to refer to the configuration in which all of the samples from the same formulation mixture are stored in the desiccator together and conditioned for testing.

Screening experiment is defined as a set of experiments (a specific type of fractional factorial design of experiment) created with the intention of discovering the main, active experimental factors out of all available experimental factors, most useful in the beginning stages of experimentation. Alternatively, a screening experiment's purpose can be defined as identifying the most significant experimental effects, rather than the interaction effects.

Specimen/Testing Specimen is defined as a testing specimen, or simply, a specimen, describes the electric propellant material that was placed in the testing apparatus designed for this experiment and measured for its electrical resistivity value. Each of the nine specimens tested for each propellant sample formulation were cut from the same sample flat.

#### Scope and Delimitations

The propellant samples designed and manufactured for this study were all based on the current version of this perchlorate oxidizer based electric propellant formula. The scope of this research was limited to measuring the electrical conductivity of the propellant samples based upon the metallic or non-metallic additive included in the propellant, the particle size of the additive, and the amount of additive added to the samples. The propellant oxidizer solution and binder included in the ESP-9 formula were left unchanged, as any investigation into the alteration of either or the interactions between the additional propellant ingredients and the additive would necessitate another, or several more, in-depth investigations.

Based on the level of understanding of the fundamental science behind the combustion and conduction mechanisms of this electric propellant formula, it was decided that this study was to be designed as a set of screening experiments, the results of which could potentially point to specific intrinsic material properties of the propellant additives and/or specific mixture properties that could indicate improved propellant performance. Additionally, this study of metallic or non-metallic additives could be mirrored by another set of screening experiments designed to study the effects of the current electric propellant formulation's oxidizer solution or binder for similar

resulting performance improvement properties and/or to increase the fundamental understanding of the propellant operational mechanisms.

Finally, it was decided during the course of planning the experimental mixing and testing operations, that the aluminum additive chosen to be included in a set of samples for testing should be eliminated due to safety concerns outlined further in Chapter 2. Even though it was eliminated from this study, aluminum as a metallic additive is still of interest to researchers and as such, steps for proceeding with the use of aluminum in future studies following the conclusion of this project are discussed in the Recommendations section of Chapter 5.

#### Limitations

The specific, researcher-imposed constraints relating to the electric propellant additive comprise the main design limitations related to this study. The restricted experimental domain used for this study does not include all possible metallic or non-metallic additives, particle size options, and included additive amount options because they were designed as a set of screening experiments. The term “screening experiments” refers to a set of experiments intended to discover the few significant, active experimental factors out of all of the potentially available factors, typically used in the initial stages of experimentation. A screening experiment’s purpose can alternatively be defined as to identify the main, significant effects, rather than the interaction effects, which are usually assumed to be less important. This study was only designed to measure the changes in electrical conductivity of the propellant samples based on metallic additive properties/amounts; this study was not designed to observe the interactions between changes in the metallic additive properties/amounts and either the oxidizer solution, binder, or both. Further expansion of this study based on the limitations defined here is provided in the Recommendations section of Chapter 5.

The specific nature of the electric propellant chemical formulation imposed limitations relating to this study of fundamental science and performance improvement, including the fact that only the additive portion of the most current perchlorate oxidizer based electric propellant formulation was altered in propellant samples, and it was altered with only three alternative additives, in three particle sizes and three added amounts. A strong focus was placed on the



contributions of an additive on the performance and material properties of the electric propellant. While this was partially addressed with the inclusion of a propellant sample with no additive included, it certainly has not been thoroughly negated. Further impact limitations can be concluded, informed by the fact that only the most current propellant formulation has been chosen for study. This set of experiments cannot be exclusively referred to when considering other electric propellant variations or other existing electric propellant formulations (for example, those formulated with a different oxidizer).

A pilot study for each of the sample formulations prepared for this investigation was conducted to verify that each sample formulation did, in fact, retain its on/off firing abilities. This pilot study was, however, only conducted at ambient pressure for each sample formulation. No pressurized testing was conducted due to the limited amount of time to complete this study and the resources available, therefore the results and conclusions of this study, presented in Chapter 4 and discussed in Chapter 5, are only applicable to the sample formulations at a single, verified pressure until further pressure testing is completed.

Lastly, the data taken for this set of screening experiments and the resulting statistical analysis and interpretation of that data will also impose certain limitations regarding the amount of measurements taken and the quality of the data itself. Measurement techniques and propagation of error can always be further improved upon and more data points can always be taken, but as a set of screening experiments the number of measurements taken, the number of variables explored, and the amount of levels at which to test for each had to be limited for this experiment to be completed.

#### Assumptions

In order to design this study, several assumptions were made resulting from the desire to simplify the screening experiment performed to allow for timely completion. The first two assumptions, inherent in the main design study limitations described above, were that the material properties and behavior of these propellant samples will vary accordingly with additive loading percentage and additive particle size, which was not proven prior to the design of experiment, and that the three additive replacements chosen for tungsten were the best three

options to use for the purpose of interrogating tungsten's role in this electric propellant formulation. To illustrate, prior to beginning the mixing and testing operations outlined in Chapter 3 of this study, it was determined that one of the metallic substances chosen as an additive replacement, aluminum, was not suitable for use in this set of design experiments, as outlined in Chapter 2. The statement of these assumptions is necessary, as there is still much more that can be learned from further expansion of this study with regards to the magnitude of electric propellant formula modifications that can be made. Furthermore, although this study does include the investigation of a sample formulation without any additive, metallic or otherwise, it does not include the investigation of a single or set of sample formulations made with a replacement additive that is not conductive. Chapter 5 details recommendations for a continuation of this study that includes several sample formulation additive suggestions, including non-conductive additives that would make a valued addition to this investigation's resultant data set.

As previously mentioned, this study's focus was on the modification of the propellant additive and does not consider the alteration of the other propellant ingredients, or the interactions between them. This assumption is inherent in the scope and delimitations chosen for this study. While the variation in the other electric propellant ingredients could have a significant impact on material properties and propellant behavior and performance, for the purposes of this study, the effects of the additive have been assumed to be a leading contributor to propellant operation mechanisms and therefore, will have a significant impact on the direction of future studies.

The testing methods, procedures, and apparatus used for measuring propellant sample electrical conductivity for this study were taken directly or derived from specific American Society for Testing and Materials (ASTM) standards related to measuring the volume electrical resistivity of certain materials. It was assumed that these standards have provided sufficient techniques for measuring a material with such a unique combination of chemical constituents. This is further emphasized by the fact that no pilot study for this set of experiments was conducted in order to determine whether or not the testing methods outlined below were the most correct and no preliminary testing apparatus models were created and/or proven prior to designing and implementing the testing apparatus detailed in Chapter 3.

Assumptions also include the fact that this study will be further expanded upon by other researchers at a later date in order to determine exactly how the bulk electrical resistivity of any electric propellant sample formulation tested can be used to predict propellant performance, as this information has not yet been theorized or tested. It is important to note here that this investigation was a screening experiment and that “factor’s effects in screening designs may be missed because they were not included in the screening experiment, because they were not given sufficiently wide factor ranges, because the design was underpowered for those factors, because trial order was not properly randomized or blocked, or because of an inadequate model” [11].

Finally, it was assumed, for data and statistical analysis that the trends observed in the cumulative behavior of the varying propellant samples are more important than any specific data point taken throughout all of the screening experiments, as there exists a certain amount of accepted experimental error inherent in this study.

#### Significance

Until the exact conduction and combustion mechanism for this propellant are understood, any step taken in the direction of increasing the understanding of the fundamental science surrounding the operation of this material can be considered beneficial. Furthermore, any step taken towards the development of a set of mixing and testing methods that yield repeatable and reliable results allowing for the characterization and improving the understanding of this perchlorate oxidizer based electric propellant can also be considered beneficial.

The “Technology Based IRAD Final Report Electric Propellant 2015” document details in its Summary and Conclusions section that one of the priorities for the 2016 year was to try and improve the electric propellant formulation and that the “formulation changes might address material properties tailored to specific applications and minimizing power” requirements [3]. While this is not directly considered to be a formulation study, the results of these screening experiments could indicate the material performance and properties of the propellant additive that are significant contributors to the electric propellant conduction and combustions mechanisms

and as a result, may have a significant impact on future electric propellant formulas and the direction of future studies conducted with this material.

## CHAPTER 2

### LITERATURE REVIEW

#### Introduction

The three research questions driving this set of experiments, established in Chapter 1, attempt to cover a lot of ground with regard to what this study is supposed to accomplish, and there has not been much research focused on electric propellant in recent years outside of what RMS and DSSP have done, nor has a mixture of such peculiarity been studied previously. This literature review was conducted with the intent of gaining insight into this electric propellant formulation and its operation by reviewing anything that could shed light on the propellant's combustion and/or conduction mechanisms. This was done by exploring the specific chemical ingredients used in the perchlorate oxidizer based electric propellant formulation and those suggested as additive replacements, and by researching any concept related to either electric propellant or the topics outlined in the experimental research questions.

#### Literature Search Strategy

The two major legs of this literature review include a search of RMS specific documents and a wider search of information associated with electric propellant and related concepts. RMS research documents include those summarizing the work completed over the years the research has been funded and those documents that included summaries of work contracted by the researchers. Additionally, patents filed by RMS, DSSP, and others have also been searched and reviewed. Due to the fact that this technology is relatively new and limited to RMS and DSSP, an external literature search was limited to the fundamental science associated with each individual ingredient in the electric propellant formula, electrical properties, percolation theory, electrochemistry, and related concepts including solid propellant, solid polymer electrolytes, and doped PVA studies.

#### Theoretical Foundation

In order for the patented, perchlorate oxidizer based electric propellant formula to be fully understood, complete knowledge of the combustion mechanism of the propellant is required. As stated in the 2015 "Technology Based IRAD Final Report Electric Propellant," "if any

improvement to the formulation is to be accomplished, then this understanding can point to the specific chemical types that might offer the highest probability of success" [3]. Furthermore, Wickham, in his internally written document, "Electric Propellant Combustion Mechanism Paper," suggests exploring the possible combustion mechanisms of this electric propellant by "determining mechanistic aspects of the propellant as well as exploring chemical alternatives to each of the" chemical components [4]. While additive chemical alternatives are being explored for the highest probability of success in the experiments described below, again, it should be understood that this study is being conducted for the purpose of answering the research questions established in Chapter 1 regarding the role and electrical resistivity contributions of a metallic additive in the propellant, whether or not the conduction/combustion mechanism may be driven by the percolation theory, and if power requirements can be inferred from resulting response variable data.

Currently, based on chemistry fundamentals and the reactions and behavior of this propellant observed so far, it is believed that the main theory driving this electric propellant's operation and combustion mechanism is summarized by the following: Several internal processes are started within an electric propellant sample with the initial application of its electrical ignition input. Presumably, the ions within the propellant mixture begin to move as a current starts flowing through the sample, and the different chemical species that make up the most current version of the sample formulation are reduced and begin to oxidize with this current flow, "with the highest current density being the path of the majority of the reactions." If the temperature of the sample is increased enough, "due to chemical reactions and" sufficiently high "resistive heating," the propellant sample may begin to combust [4]. It is important to note here that the most current version of the electric propellant formula appears to also have capacitive properties, thus allowing it to charge at lower levels of applied voltage and current.

The main theory of electric propellant combustion "suggests that the application of the current facilitates the" oxidation and reduction of the perchlorate oxidizer based components "which act as charge carriers when solvated in the water within the material." Based on the fact that the propellant burning occurs across the material between electrodes, rather than just at the

material ends, this theory proposes that the tungsten particles within the material are acting as “sites for the acceptance and donation of electrons as tungsten can assume negative and positive oxidation states.” This oxidation of tungsten allows for the electrochemical reactions within the material to occur, ultimately “increasing conductivity, heating the propellant, and accelerating the rate of reaction.” As soon as the electrochemical reactions occurring have produced enough heat and oxygen, and “presumably once the temperature has exceeded the activation energy of the redox reaction allowing the perchlorate to directly oxidize the PVA,” the propellant will begin to combust. Alternatively, the combustion may be due to the ignition of the in situ oxygen within the material, the results of arcing within the propellant, or potentially, a combination of both combustion methods, “with the initiation being primarily the result of perchlorate and PVA redox reactions, but sustained burning being due to supplemental production of oxygen.” While the ignition and further burning of the propellant may depend on the chemical reactions occurring, “the enormous discharge that accompanies dielectric breakdown is probably the actual mechanism for ignition, dumping heat, and greatly increasing the rate of reaction” [4].

Several aspects of the processes described are unknown, including the amount of arcing occurring within propellant samples due to voids created during the mixing and casting process. Additionally, recent testing has suggested that the propellant may slowly become “more conductive before experiencing dielectric breakdown and igniting.” Wickham proposes that “localized breakdowns in the material might progressively form electrically conductive pathways across the material which leads to combustion when it forms a conductive pathway across the material”; he continues to add that these pathways may be pre-existing or formed by the electrochemical reactions within the material and “may be a reflection of the amphoteric nature of tungsten oxide.” The formation of these pathways, either during mixing and casting or during electrochemical reactions, may lead to faster combustion of the material following an initial event due to the “partial pathway formation, or reuse of initially formed pathways that significantly lower the breakdown voltage.” Finally, Wickham adds that the “destructive nature of dielectric breakdown and combustion” may destroy these pathways and impact the operation of the material after initial ignition and combustion [4]. (It is important to note here that this paper was

written prior to the introduction of the Thinky mixer to the propellant manufacturing process for increased mix homogeneity and some of the content may or may not still hold true to a varying degree.)

The dielectric breakdown in solids is normally governed by the gradual formation of conductive pathways within the defects of a material, the exact mechanism for which is not very well understood, however, “the most important aspect is that the flow of current gradually increases the conductivity of the material.” In this case, “this is likely due to the transfer of protons as part of the electrochemical/redox process” and “the formation of more charge carriers allow for greater conductivity throughout the material, leading to dielectric breakdown.” Currently, it is believed that “a minimum current density must be reached for the propellant to ignite,” and the introduction of dielectric breakdown provides a mechanism for how a sufficiently large current might pass through the material,” however, Wickham suggests that “testing should be performed to ensure that the breakdown occurs first, if at all, before the current starts the combustion” [4].

In addition to governing the dielectric breakdown of the material, the propellant’s conduction of electricity is also critically dependent upon the effects of plasma, due to the “relative conductivity of plasma and the use of electricity for ignition and burning of the propellant.” Plasma generation may be playing two roles in the combustion mechanism of this material, in the first of which, the propellant “actually ignites before the enormous discharge of current through the material” and combustion “occurs due to electrochemistry and heat generation from reactions within the material leading to an ignition event and the generation of plasma.” However, in this scenario, “the plasma that has been generated is much more conductive than the propellant and for a few microseconds it is still coupled to the propellant. Consequently, there is a large, almost instantaneous, drop in resistance and some of the current deviates from the propellant to travel through the plasma, forming a short circuit.” This process could be responsible for the drop in resistance and the corresponding jump in current observed during electric propellant testing. In the second of the two scenarios that plasma may be responsible for creating, “if the current discharge occurs simultaneously with combustion, the plasma may play a different, less substantial role,” “assuming that the dielectric breakdown is actually occurring and is responsible



for combustion of the material, the plasma may simply further decrease the resistance of the propellant.” During the dielectric breakdown in this process, “the material has already been forced to become a conductor,” so the contribution of the plasma may be negligible depending on the timescale of the dielectric breakdown. If the plasma in this situation is “coupled significantly longer than when the dielectric breakdown takes place, it could be responsible for the continued draining of the capacitor” [4].

Additionally, the temperature of the electric propellant will also, most likely, play a critical role in how and when the propellant will combust, “as the reaction will only occur when the necessary activation energy has been provided.” Any additional heat provided to the system during the combustion process “will increase the solubility of the perchlorate as well as the rate of reaction, but may also drive off residual water within the material.” If propellant combustion “proceeds almost instantaneously at higher temperatures, combustion may be more a result of electrochemistry and heat production rather than something more exotic such as a dielectric breakdown.” In either case, “the temperature at which combustion occurs and the time to a combustion event may be quite revelatory” [4].

In addition to the summary of the main electric propellant combustion theory provided by Wickham, Langhenry has also provided a basic summary for the propellant’s combustion mechanism processes in his 2015 research review presentation, comparable to Wickham’s lengthy analysis. Langhenry theorizes that there are four different processes occurring during the burning of the electric solid propellant. The first of these processes is the initiation of burning “with an electro-chemical reaction that generates a fuel and oxidizer,” followed by “resistive heating as current passes through” the propellant, then pyroelectric heating from the propellant crystalline structure, and finally, a chemical reaction of the fuel and oxidizer driven by heating [12].

Finally, Wickham states that “the importance of the resistance of the material has not yet been established,” even though the tungsten metallic additive “was originally added to increase the conductivity” and “the mechanical properties” of the propellant, but the propellant’s “conductivity is also dependent upon water content which has also not been properly evaluated.”

It is suggested that it may be necessary at some point to achieve both a “minimum concentration, also unknown, of metal and conductivity” required for propellant operation [4].

#### Experimental Framework of the Study

Grounded in the summarized version of the main theoretical foundations upon which the perchlorate oxidizer based electric propellant is suspected to operate, written above, an experimental study was researched, designed, and carried out with the purposes of contributing to the determination of the electric propellant operational mechanisms. While the main theory provided for the combustion mechanism of electric propellant described above comprises several different interacting phenomena, this study will only include an investigation of the electrical resistivity contributions to the conduction mechanism of different electric propellant sample formulations, as it is one of the operational phenomena that can easily be broken down into several different standardized experiments and further expanded upon based on results.

It has been shown that the role of the tungsten in and the conduction mechanism of the electric propellant are both somewhat undefined, but it is suspected that there exists some mechanism by which the electric propellant operation is driven that is related to the propellant's resistivity and the current density at the time of measurements, testing, or initiation. Based on the science described in Wickham's theory of operation and the propellant ignition theory summarized above by Langhenry, it is possible that the tungsten additive could be aiding in the propellant's operation during the electrochemical reaction resulting in the generation of a fuel and oxidizer during the resistive and pyroelectric heating phases, and could be burning as an additional fuel source in the final chemical reaction phase of the propellant operation.

One of the more modest investigations that can be done in order to determine at least a partial understanding of the role that tungsten is playing in the propellant operation is to simply replace it with different materials, each of which having only one, or some, of the supposed desired properties that tungsten has. If the operation of a propellant formulation with one of these additive substitutes performs similar to or has similar or opposite characteristics to the tungsten based propellant, the properties of the substitute additives can be compared in order to determine additive properties that produce desired propellant properties and/or behavior.

Furthermore, if this type of electric propellant is governed by some phenomena related to its electrical resistivity then the amount of metallic additive, or otherwise, included in the formulation will have an impact on the propellant performance. However, since it has been theorized that the electric propellant operation could be driven somewhat by percolation theory, the amount of additive included in the formulation should have a significant effect on the material and there should exist some point where including more or less of the additive could be more harmful than helpful. Knowing this threshold value for the metallic additive would be valuable to any researcher for future formulation and performance optimization, and determining this threshold value is another, more modest experiment that can be carried out in conjunction with a continuation of this additive replacement investigation. Finally, an understanding of how the resistivity of this material influences an increase or decrease in the electric propellant initiation input signal and affects the power consumption of the material would be valuable knowledge that could contribute to propellant understanding and optimization.

#### Literature Review Related to Key Variables and/or Concepts

Based on the experimental framework outlined above, a literature review was conducted in order to gain a better understanding of not only the current propellant formulation, but of the suggested additive replacements, of the concepts that might be governing propellant operation in order to inform the design of a revelatory experiment, and of the possible outcomes of this study.

#### *Baseline Propellant Chemical Ingredients and Their Role in the Formulation*

Stated previously in Chapter 1, the current electric propellant formula consists of four ingredients each of which are further outlined below. The propellant formula contains, by mass, 60% perchlorate oxidizer dissolved in deionized water (DIW) in an 80% concentrated solution (which is approximately equal to 48% perchlorate oxidizer and 12% deionized water), 20% PVA acting as the propellant binder, and 20% powdered tungsten (W) acting as the metallic additive.

A perchlorate oxidizer is used in this electric propellant formula as the propellant oxidizer and, unfortunately, has not been characterized and/or studied as widely as the rest of the electric propellant constituents. The perchlorate oxidizer is an ionic salt, of which several hydrates exist,

and is hygroscopic (tending to absorb moisture from the air), soluble in water and alcohol, and very deliquescent (having a tendency to become a liquid).

Perchlorates (a perchlorate is an anion that consists of one chlorine atom that is chemically bonded with four oxygen atoms, either naturally occurring or man-made) are a common choice of oxidizers used in rocket propellant due to their high oxidizing potential, “which makes this material suited to high specific impulse propellants.” Ammonium perchlorate is the most widely used crystalline oxidizer in solid propellants, because of its “good characteristics, including compatibility with other propellant materials, good performance, quality, uniformity, and availability... Other solid oxidizers, particularly ammonium nitrate and potassium perchlorate, were used and occasionally are still being used in production rockets but to a large extent have been replaced by more modern propellants containing ammonium perchlorate”. Additionally, “many oxidizer compounds were investigated during the 1970s, but none reached production status” [13].

Deionized water is water that has had almost all of its mineral ions removed; these ions include anions like chloride and sulfate, and cations such as sodium, calcium, copper, and iron, and “for many applications that use water as a rinse or ingredient, these ions are considered impurities and must be removed from the water” with a process involving the use of an ion exchange resin [14]. In the case of this electric propellant formulation, the deionized water is being used to dissolve the perchlorate oxidizer into a solution to which PVA and tungsten powder are then added, and the entire mixture is then mixed and cast or extruded, a process that is further explained in Chapter 3.

Polyvinyl alcohol is a synthetic polymer that is soluble in water, and “is unique among polymers (polymers are chemical compounds made up of large, multiple-unit molecules) in that it is not built up in polymerization reactions from single-unit precursor molecules known as monomers. Instead, PVA is made by dissolving another polymer, polyvinyl acetate (PVAc), in an alcohol such as methanol and treating it with an alkaline catalyst such as sodium hydroxide. The resulting hydrolysis, or “alcoholysis,” reaction removes the acetate groups from the PVAc molecules without disrupting their long-chain structure” [15]. PVA is a “semi-crystalline polymer

and its crystalline index depends on the synthetic process and physical aging" [16]. The PVA (homopolymer) used in the electric propellant manufactured for this study has a very high, 99.65% +/- 0.35, degree of hydrolysis (in mole %), meaning that the PVA used has an increased water (humidity) resistance, tensile strength, block resistance, solvent resistance, and adhesion to hydrophilic surfaces. This increase in tensile strength, and corresponding decrease in flexibility, partially provides for the propellants current desired mechanical properties.

In solid propellants, "the binder provides the structural glue or matrix in which solid granular ingredients are held together in a composite propellant," it also acts as additional fuel for the solid propellant and is oxidized during the combustion process. "The binding ingredient, usually a polymer of one type or another, has a primary effect on motor reliability, mechanical properties, propellant processing complexity, storability, aging, and costs" [13]. Binders are "usually long chain polymers that can keep the propellants powders and crystals in place by forming a continuous matrix through polymerizing and cross-linking," and they hold "the entire formulation in a structurally sound grain which can withstand temperature variations as well as pressure and acceleration loads during flight" [17]. Binders with a low density and energy of combustion are usually desired, and "the best binder materials can provide needed structural integrity using a minimal binder volume. The solids loading in the propellant addresses this desired characteristic by expressing the total mass of fuel and oxidizer as a percentage of the total propellant mass. Composite propellants have solids loadings in the 84-90% range, which implies that only 10-16% of the propellant mass is made up of binder and minor ingredients" [17].

Tungsten has one of the highest melting points, approximately 3422°C or 6192°F, of all pure form metals; tungsten also has one of the lowest vapor pressures, at temperatures above 1650°C or 3000°F, and one of the lowest coefficients of thermal expansion of any pure metal, at approximately 4.5  $\mu\text{m}/(\text{m-K})$  at 25°C [18, 19]. Powdered tungsten was originally added to this electric propellant formula for several reasons, and "by using a large amount of tungsten, the conductivity and mechanical properties of the material were pushed to reasonable levels. The tungsten also acts as a thermal sink which assists in the extinguishment capabilities of the

material. However, given the difficulty of oxidizing tungsten, it is unlikely that it is combusted in any significant amount and so may be a significant source of inert mass” [4].

There are very few cases in which tungsten has been added to conventional solid propellants in industry, however, in one researched case, tungsten was added to a composite modified double-based solid propellant utilizing potassium perchlorate, ethyl centralite, and carbon black, as well as the nitrocellulose and nitroglycerin combined fuel and oxidizer. Patent number US 8.545.646 B1, titled “High-density Rocket Propellant,” presents a rocket propellant that “includes propellant material and tungsten powder mixed with the propellant material at a time of manufacture, wherein the tungsten powder includes a mass percentage relative to the propellant material of about 70%-80%, equivalent to 17%-26% by volume of the propellant material.” The tungsten powder described for use in this patent includes a size range of about 44 microns to about 150 microns in diameter. “The mass percentage of the tungsten powder and the tungsten particle size range are selected to optimize total impulse, sound reduction, and Insensitive Munitions performance” in shoulder launched assault weapons [20]. Also patented is the use of tungsten alloy burst discs employed in solid propellant rocket motors, and more widely documented is the use of tungsten as a solid-propellant rocket nozzle material, with notable issues including tungsten erosion and “thermal shock cracking under rapid heat-up conditions” [21].

*Metallic (or Otherwise) Additive, Size, and Amount*

In conventional solid propellants, the shape, size, and size distribution of the solid particles of ammonium perchlorate, aluminum, or HMX (a powerful, insensitive nitroamine high explosive) “in the propellant can have a major influence on the composite propellant characteristics. The particles are spherical in shape because this allows for easier mixing and a higher percentage of solids in the propellant than shapes of sharp-edged natural crystals.” However, Rocket Propulsion Elements describes that the “influence of particle size of the aluminum fuel on propellant burning rate is much less pronounced than that of oxidizer particle size.” The particle size, range, and particle shape of both the propellant oxidizer and solid fuel “have a significant effect on the solid packing fraction and the rheological properties (associated with the flowing or pouring of viscous

liquids) of uncured composite propellant. By definition, the packing fraction is the volume fraction of all solids when packed to minimum volume (a theoretical condition). High packing fraction makes mixing, casting, and handling during propellant fabrication more difficult." Additionally, "the size range and shape of the solid particles affect the solids loading ratio, which is the mass ratio of solid to total ingredients in the uncured propellants." In composite propellants, the "solids loading can be as high as 90%," however with high solids loading, desired due to its high performance, higher cost and higher complexity are introduced into propellant processing [13].

Currently, this electric propellant mixture utilizes a 12  $\mu\text{m}$  tungsten powder particle size, which is unusually small for typical metallic propellant fuel additives. For the purposes of this investigation, the electric propellant samples have been made with a range of different additive particle sizes both for their intrinsic characteristics and for what the additive at different particle sizes may do to the properties of the material, such as influencing propellant conductivity, reactivity, and the material breakdown strength. The evaluation of electric propellant made with different additive particle sizes may shed some light on the idea of the propellant operation being at least partially driven by the percolation theory, discussed later in this chapter. It may also help determine why the electric propellant formulation made with tungsten performs so well. Wickham has predicted that a "smaller particle size will increase conductivity" of the material, but will also "decrease the breakdown voltage due to the closer spacing of the particles," and suggests that a move to a larger particle size, while desirable for processing ease, may prove harmful to the ignition characteristics of the propellant"[4].

According to the paper written by Wickham, while tungsten is not "normally an easily oxidized metal," and it is unlikely to combust without a significant amount of heating, the voltage supplied to the propellant by the power supply being used "is more than enough to lead to oxidation of the tungsten if oxygen is supplied. Consequently, it is likely that the tungsten is doing more than acting as a conductor, heat sink, densifier, and mechanical aid." Wickham goes on to discuss several electric propellant additive replacement suggestions worthy of investigation, including aluminum, a common fuel included in solid rocket motor formulations for performance enhancement. Copper is also suggested, as it has a lower reactivity than other metals commonly

included in solid propellants, and its resistance to water corrosion and proneness to the formation of a protective layer may be advantageous in a propellant requiring a thermal dump or stabilizer. Finally, carbon black is discussed as a potential additive replacement due to its conductivity and past performance in propellants as a thermal barrier included to prevent early ignition. It is finally suggested by Wickham, that utilizing metals with similar reduction potentials as tungsten, “but choosing metals such that one metal can assume positive and negative oxidation states and the other can only assume positive oxidation states” could help to prove the hypothesis that states an electric propellant sample containing a metal capable of positive and negative oxidation states will burn under the same conditions and following the same trend as the most current patented formulation being used [4]. This is further discussed in the Electrochemistry subsection below.

#### *Electric Propellant Additive Replacement Chemical Ingredients*

The Raytheon Missile Systems Patent entitled “Electrically Operated Propellants,” discussed in the Introduction section of Chapter 1, lists possible metal based additives in quantities of 5-30% by mass for this perchlorate oxidizer based electric propellant formula including, but not limited to, tungsten, magnesium, copper oxide, copper, titanium, and aluminum. “Optionally, the patent also includes a statement describing the electrically operated propellant without an additive, meaning the metal based additives in the formula would be equal to 0%.” Initially, the most diverse trio of additive replacements was desired to be included in this experiment due to the screening-type nature of this study. “Additional additives could have been included in the experiment or could have replaced one of the already chosen materials as desired, but time to complete the mixing and testing experiments did have an impact on the ability to complete this investigation” [22].

Powdered copper was the first of the chosen replacement additives due to its lower reactivity, higher thermal conductivity, and low electrical resistivity when compared to tungsten and some of the other metals suggested above. Copper is a well-known chemical element and copper powder is widely used in industry for self-lubricating bearings, structural components, injection molding, and electrical parts, among other things. In the aerospace industry, copper has been used in liquid rocket engines, but only for specific applications due to material compatibility.



While copper has not widely been used in solid propellant applications like aluminum powder has, its effects as a burn rate catalyst, or modifier acting to change the propellant combustion mechanism, in composite propellants have been previously studied. Additionally, although copper has a lower reactivity and less remarkable combustion, due to its resistance to water corrosion and proneness to the formation of a passive layer, powdered copper could be used as a fuel additive where the electric propellant requirements include thermal dumps or stabilizers.

Powdered aluminum, a common fuel additive in other types of propellant, was the second replacement material chosen, as its electrical and thermal conductivity and resistivity fall midway between those of copper and tungsten, but its melting point is much lower than either, shown in Table 1 below. Powdered spherical aluminum is one of the most common fuel additives in solid rocket motors, consisting of “small spherical particles (5 to 60  $\mu\text{m}$  diameter), and is used in a wide variety of composite and composite-modified double-base propellant formulations, usually constituting 14 to 20% of the propellant by weight.” Adding powdered aluminum to solid propellant “increases the heat of combustion, the propellant density, the combustion temperature, and thus the specific impulse” of the solid rocket motor (SRM) [13]. Other reasons for the addition of aluminum to solid propellants include the suppression of combustion instabilities, for modification of the propellant burning rate, for a reduction of the propellant’s sensitivity to detonation, and the favorable supply of aluminum at reasonable costs.

During 2011 and 2012, in the infancy stages of this perchlorate oxidizer based electric propellant formulation development, a number of alternate formulations to be tested and compared with ESP-9 were manufactured with the “goal of characterizing the power demand and understanding the effects of different mixtures on the mechanical properties of the propellant” [23]. This characterization included 10 electric propellant samples composed of 70% by mass of the concentrated perchlorate oxidizer solution in mixture amounts between 55-80%, polyvinyl alcohol in mass percentage amounts between 20-30%, and either powdered tungsten in mass percentage amounts between 0-25% or powdered aluminum in mass percentage amounts between 0-20% (the tungsten and aluminum were only combined in one of the samples at a mass percentage amounts of 5% each). Each of the 10 samples was then tested at power consumption

levels of 300 Volts, 500 Volts, 700 Volts, and 900 Volts. The samples that showed the lowest mass specific power consumption were those with either little to no metallic additive (5% aluminum and 5% of tungsten and aluminum) or with higher amounts of added powdered tungsten. Following these results, the formula with a higher amount of tungsten additive was chosen for continued study, and formulas containing aluminum have not been investigated since [24]. It is also important to note here that researchers who have previously worked with aluminized electric propellant have stated that the propellant's on/off abilities were not retained and future investigation of aluminized electrical propellant formulations, including electrical resistivity measurements, could provide some insight. This is further discussed below in the Electrochemistry subsection.

**Table 1. A Comparison of Proposed Replacement Additive Properties. (All data below was gathered from chemical SDS/technical information sheets.)**

<b>Additive/ Additive Property</b>	<b>Tungsten (W)</b>	<b>Aluminum (Al)</b>	<b>Copper (Cu)</b>	<b>Carbon black (CB)</b>
<b>Purity [%]</b>	99.9	99.9	99.9	N/A
<b>Electrical resistivity [Ω-m]</b>	$5.6 \cdot 10^{-8}$	$2.655 \cdot 10^{-8}$	$1.69 \cdot 10^{-8}$	N/A
<b>Density [g/cm<sup>3</sup>]</b>	19.3	2.699	8.94	1.79 -1.99
<b>Melting point [°C]</b>	3387	660.1	1083	>3000
<b>(Crystal) Structure</b>	Cubic, body centered	Cubic, face centered	Cubic, face centered	Amorphous

Finally, because of its conductive nature, due to its high surface-to-volume ratio, and the “thermal properties that the fuel additive supposedly imparts on this electric propellant formula, carbon black powder will also be considered as one of the three ingredient replacements. Although powdered carbon black is not a metal, it is being investigated to fill a similar role to that of the tungsten included in the current electric propellant formula, which is, acting as a thermal barrier and potentially introducing its effects on conductivity, while also acting as additional fuel

for the oxidizer in the propellant. Carbon black is often added to other chemical mixtures, including plastics,” because of its ability to add or increase electrical conductivity and material hardness. Carbon black is used in the propellant industry in order to form a thermal barrier between the surface and bulk of the fuel to prevent early ignition, as well as providing increased conductivity in order to prevent a buildup of potentially dangerous static charge. Additionally, “many double-base formulas require a darkening agent” (such as carbon black, also referred to as an “opacifier”) “to make the translucent propellant darker and avoid excessive thermal radiation throughout the propellant itself” [17]. More widely in industry, carbon black is used in the manufacturing of tires and is added to some plastics for increased conductivity and mechanical properties.

The ASTM D3053 standard, “Standard on Terminology Relating to Carbon Black,” defines carbon black as the following: “Carbon black exhibits aciniform morphology composed of spheroidal “primary particles” strongly fused together to form discrete entities called aggregates. The primary particles are conceptual in nature, in that once the aggregate is formed the “primary particle” no longer exists, they are no longer discrete and have no physical boundaries amongst them. The aggregates are loosely held together by weaker forces forming larger entities called agglomerates. The agglomerates will break down into aggregates if adequate force is applied (e.g., shear force)” [25]. These aggregates are considered the smallest dispersible unit of the carbon black, however, carbon black on the market for use is usually in the form of agglomerates, and is typically “shipped/placed on the market in the form of pellets (i.e., compressed agglomerates) to facilitate the ease of handling and to reduce the creation of dust. The size of pellets generally falls between 0.1 and several micrometers” [26].

The smallest carbon black unit, the primary particle, has characteristics including size, shape, crystallinity, and graphite content, and these characteristics influence the color, UV blocking, and electrical conductivity of carbon black. While most manufacturing processes produce nearly spherical particles, some processes produce particles with higher aspect ratios, leading to a higher surface area per unit volume and a more wettable surface area, allowing for an increase in electrical conductivity. Aggregates of carbon black, clusters of the primary

particles, have a given size, shape, structure, and void volume, each of which contribute to the utility and grade of the carbon black. The “size of the aggregate influences the color aspect of the carbon black and its tinting strength. The shape and structure influence dispersability and to some extent electrical conductivity. Void volume influences wettability and is a critical concern in applications where the carbon black will be used in a liquid medium such as a coating, paint, or ink” [26].

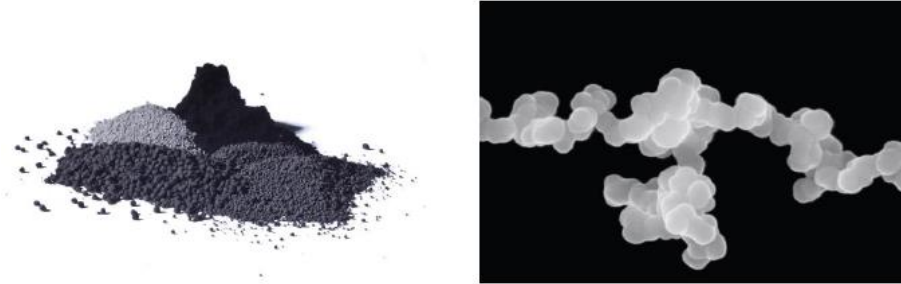


**Figure 1. (Left) Representative Picture of Carbon Black as Typically Placed on the Market. (Right) Scanning Electron Microscope View of a Carbon Black Aggregate Consisting of Fused Primary Particles (Magnification: x 120,000) [26].**

In addition to the three replacement ingredients chosen, propellant samples without any included additive were also included in the sample population for this study, as it has been shown that even the electric propellant samples with no included additive will fire with the application of an electric current and cease firing when it is removed. The final sample formulations, created for this study and informed by this literature review, are presented and further discussed in Chapter 3.

#### *Related Electrochemistry*

In an attempt to analyze the current ESP-9 electric propellant formulation and prospective additive replacements from another perspective, some of the propellant formulation’s electrochemical properties were examined. This new perspective was adopted in order to characterize potential propellant performance impacts, as well as to screen for additional unintended reactions that could create an operational and/or storage safety hazard. Moreover, it was suggested by Wickham that the main theory of electric propellant operation “proposes that the tungsten particles within the material” both accept and donate electrons during operations due to the fact that tungsten can assume both positive and negative oxidation states [4]. Therefore,

understanding how the suggested replacement additives compare electrochemically to tungsten could inform this investigation in terms of defining a portion of the propellant's operation mechanism. For example, the ESP-9 formulation currently makes use of an external electrical current to drive chemical reactions in the propellant to produce gases that can be harnessed for propulsion applications. However, spontaneous transfer of electrons within the propellant, depending on any formulation changes that could be made, may defeat the designed intrinsic safety aspects of ESP-9, resulting in spontaneous, rapid reactions that may create an explosion hazard or consume much of the metal particle matrix and oxidizer in non-gas producing reactions that would affect propellant functionality.

Electrochemistry, simply stated, is the study of the chemical processes that encompass chemical change and electrical energy. The main chemical interaction believed to be involved in the operation of ESP-9 propellant is the reduction-oxidation reaction, commonly referred to as a "redox" reaction, of molecules or ions through electron transfer. The reacting chemical species in a redox reaction will undergo a change in the formal oxidation state(s) of certain elements participating in the reaction. These redox reactions typically fall into two categories, the first of which are Galvanic, or Voltaic, processes, which are spontaneous chemical reactions. The movement of electrons in these reactions can be harnessed to produce electricity. The second category of redox reactions are electrolytic processes in which chemical reactions are driven by the passage of an electrical current through the system. The electrolytic mode of operation for ESP-9 is currently thought to be a driving force in propellant operation, as discussed above in the Theoretical Foundation and Experimental Framework of the Study sections of this chapter. It is the prospect of a runaway galvanic reaction that presents a potential safety issue, the causes of which were thoroughly reviewed prior to conducting experimental operations.

In a redox reaction, when a substance loses an electron, its oxidation state increases and it has been oxidized; when a substance gains an electron, its oxidation state decreases and it has been reduced. In a typical redox reaction, both of these processes occur simultaneously and determining which of the molecules, ions, elements, and electrons that are changing or reacting can become complex. In order to simplify the system and keep track of the reactions, the redox

reaction can be modeled as an electrochemical cell, such as a battery. In a battery, the electrochemical cell is a device that produces an electric current from the energy released by a spontaneous redox reaction. These cells have two conductive electrodes, an anode where oxidation occurs, and a cathode where reduction occurs. Typically, these electrodes can be made from any material that sufficiently conducts electricity, and in between them sits the electrolyte in a bridge, containing ions free to move around in order to transport electrons. The anode and cathode are separated in such a way that electricity flows when an external circuit is completed. These cells can be broken down into the reduction reaction and the oxidation reaction. When presented in this broken down form, these reactions are called half reactions, or half cells, and can be recombined for the complete reaction, or cell. The equations for the half cells will include electrons within and will be both chemically and charge balanced, and the half reactions can be recombined to form the full cell chemical equations. The use of half cells allows for the formation of new, theoretical electrochemical cells to be able to predict behavior of chemical systems. Standard tables, usually organized by reduction potential, providing known chemical half cells are widely available from chemical engineering handbooks, as well as online.

Reduction potential is the tendency for a reduction reaction to occur, or the tendency for substances to gain electrons; the more positive the reduction potential of a substance is, the greater the tendency of the substance to be reduced, and the lower the reduction potential is, the greater the tendency of the substance to be oxidized. In the standardized tables, the reduction potentials are reported and organized by the electrical potential (voltage) associated with the chemical half reaction. In order to obtain the oxidation reaction from the standardized reduction potential table, the equation is simply reversed and the sign on the reduction potential is reversed to obtain the oxidation potential. These reactions can occur under the conditions of either the release of chemical energy or under the application of an external voltage. The term "half-reaction" describes either of the two redox reactions, and is determined by examining the change in oxidation states of the substances involved in the reaction; this is often the method used for balancing redox reactions and obtaining an electrical potential (voltage) for the cell. In some cases, such as magnesium being dissolved in hydrochloric acid to produce aqueous magnesium

chloride plus hydrogen gas, there are no separate physical “anodes,” “cathodes,” or bridges. However, the electron transfer occurs in the solution as soon as the metal touches the acid. The half-cell method of looking at the reaction is still applicable and is a useful tool for evaluating the possibility of spontaneous electrochemical reactions occurring in a mixture.

The “difference in potential energy between the anode and the cathode dictates the direction of electronic movement. Electrons move from areas of higher potential energy to areas of lower potential energy” and “the potential difference between these two electrodes is measured in units of volts.” In a voltaic cell, this potential difference is called the “cell potential”, and for a reaction that is spontaneous, the cell potential is positive and the Gibb’s free energy (used to determine if a reaction occurs spontaneously) is negative. Cell potential is different for each voltaic cell and its value is dependent upon several things including “the concentrations of specific reactants and products, as well as temperature of the reaction” [27].

A “positive voltage that forms across the electrodes of a voltaic cell indicates that the oxidation-reduction reaction is a spontaneous reaction for reduction at the cathode and oxidation at the anode.” Conversely, a negative voltage “indicates that the reverse reaction,” reduction at the anode and oxidation at the cathode, is spontaneous. Based on the actual reduction and oxidation processes that occur in a redox reaction, “the general description of the standard reduction potential for any redox reaction” is given by Equation 1.

$$E^0 = E^0_{red}(reduction\ process) - E^0_{red}(oxidation\ process) \quad (1)$$

According to Equation 1,  $E^0$  will be positive when the redox reaction is spontaneous, negative when the reaction is spontaneous in the reverse direction, and zero for a redox reaction at equilibrium [28]. The voltage of an electrochemical cell is an indication that the system is out of equilibrium and any redox reaction occurring is meant to spontaneously allow electrons to flow within the cell in order to bring the cell to equilibrium.

The electrochemical concepts described above were simply applied to the ESP-9 formula and the chemical additive replacements proposed to determine cell potential and the degree of spontaneity of the possible reactions. A tungsten and water reaction was examined for cell potential, which was slightly positive, but very close to zero. Copper was also analyzed for its cell

potential with water or perchlorate, both of which were shown to be close to zero as well, but had slightly negative values compared to tungsten's positive values. Since both tungsten and copper have been shown to have potentials close to zero (meaning close to equilibrium), both of these metals have been determined to be fairly safe to handle, to include in sample formulations, and to conduct operations with for the purposes of this study.

**Table 2. Values for Cell Potential of Some of the Ingredients/Additive Suggestions and Possible Reactions That Could Be Occurring During ESP-9 Combustion.**

Reaction	Ingredient/Additive	Half Cell Potential [V]	Cell Potential [V]
$\text{ClO}_4^- + \text{H}_2\text{O} + 2\text{e}^- \rightleftharpoons \text{ClO}_3^- + 2\text{OH}^-$	Chlorine	+0.17	N/A
$\text{W(s)} + 2\text{H}_2\text{O(l)} \rightleftharpoons \text{WO}_2 + 4\text{H}^+ + 4\text{e}^-$	Tungsten, Deionized water	+0.12	+0.29
$\text{W(s)} + 3\text{H}_2\text{O(l)} \rightleftharpoons \text{WO}_3\text{(s)} + 6\text{H}^+ + 6\text{e}^-$	Tungsten, Deionized water	+0.09	+0.21
$\text{Al} \rightleftharpoons \text{Al}^{3+} + 3\text{e}^-$	Aluminum	+1.66	+1.83
$\text{Cu} \rightleftharpoons \text{Cu}^{2+} + 2\text{e}^-$	Copper	-0.34	-0.17

Some metals, however, have been known to be more active, meaning they can displace a less active metal from a solution of its salt; a more active metal will more readily donate electrons to the cation of a less active metal, and can be considered more reactive than other metals. Aluminum, known to be a more active metal, was analyzed and was found to have a highly positive cell potential in a water or perchlorate mixture, indicating that its inclusion as a metallic additive replacement for tungsten in the current electric propellant formulation, and in altered versions, may permit a more spontaneous redox reaction in the positive direction, resulting in the potential for uncontrolled chemical reactions that could lead to explosions or other safety concerns. For these reasons, in addition to warnings in the aluminum safety data sheets (SDS) regarding its undesirable reactions with water, it was decided that aluminum would be removed from this study as an additive replacement option. However, the understanding and ability to apply this electrochemical information to the ESP-9 formula, may be advantageous for future investigation into aluminum, as it has been discovered previously that at certain particle sizes,



when aluminum is added to the electric propellant instead of tungsten, the propellant mixture loses its on/off firing abilities; this electrochemical insight could help explain this phenomenon.

Additionally, it may be of interest at a later date to perform the same study described in this document not only with aluminum, but with an electrochemically neutral metal additive such as platinum, silver, or gold. Again, in his white paper Wickham suggests investigating metallic additives with reduction potentials similar to that of tungsten, but choosing metals with different oxidation states for the purposes of determining if a metal capable of both a positive and a negative oxidation state will burn under the same conditions as the tungsten does in the current formulation. This possible expansion of the investigation of metallic materials that could replace tungsten, and that could possibly improve upon the current electric propellant formula, is further discussed in the Recommendations section of Chapter 5.

#### *Related Percolation Theory and Concepts*

If, as Wickham has stated, it becomes necessary at some point to achieve both a “minimum concentration, also unknown, of metal and conductivity” required for propellant operation, then an understanding of the effects of percolation on electric propellant will aid in the process of finding and the achievement of that minimum metallic concentration. The “percolation theory refers to a class of models that describe the properties of a system given the” random “networking among its constituents,” in which the disorder, or networking, “is defined by a random variation in the degree of connectivity” [29, 30]. Two basic percolation models exist; in the first, referred to as the “site percolation model,” “points are defined on an underlying lattice in such a way that, in every lattice site there is a probability  $p$  to exist there.” In the second model, called the “bond percolation model,” “bonds are defined between two neighboring sites on a lattice. Each bond has a probability  $p$  to exist.” In both cases, structures of connected points can be defined (clusters), in a way that it is possible to create a path between any two points of the cluster. As the probability,  $p$ , is increased, large clusters will be formed. Eventually, a cluster that has a path that spans the whole system will be formed... The value of  $p$  that creates this cluster is called the critical probability, denoted by  $p_c$ .” “In the case of periodic or infinite lattices, the existence of a diverging quantity, namely the (average) cluster size, at a specific, finite value, or a parameter, and the

qualitative change in the behavior of the system after crossing this value tells us that one should look for critical behavior. In fact, near  $p_c$ , several quantities exhibit power-law behavior, and there are scaling laws relating the different critical exponents" [29].

The percolation threshold, described using this critical probability value,  $p_c$ , is the defining concept of the percolation theory. Using the definition provided above for  $p$ , it is the "average degree of connectivity between various sub-units" of a system. When the value of  $p$  is equal to zero, all of the sub-units within the system are completely isolated from each other, and when the value of  $p$  is equal to one, all of the system's sub-units have the maximum number of connections possible with neighboring sub-units, at which point the system connects from one side to the other via the newly clustered sub-units. In order to determine the value of  $p_c$ , the sub-unit connections, starting at  $p$  equal to one, are randomly broken so the connectivity across the system is decreased. The value of  $p_c$  is defined as the point at which there is no longer an unbroken connection from one side of the system to the other. Following this logic, for any  $p$  larger than  $p_c$ , there is always a cluster of sub-units that will span the system from end to end, and for any  $p$  smaller than  $p_c$ , only isolated clusters will exist within the system [30].

The size and amount of additive replacement particles included in the electric propellant sample mixtures should have an effect on the propellant, if it is experiencing the percolation phenomenon, in which the level of additive particles included in a mixture between a dielectric and a metallic component, is sufficient to cause a significant and abrupt increase in electrical conductivity. (A dielectric is an insulating material, or a very poor conductor of electrical current.) Further increases in additive particle amount, past the percolation threshold, would result in little added benefit. (For statistical analysis purposes it is important to note that this phenomenon may also be influenced by additive particle size if the particle size was large enough and there was a sufficient amount added to the electric propellant samples.) Knowing this additive value, not only for each of the experimental additive replacement materials, but especially for the chosen additive in future electric propellant formulations, would be of value for the purposes of increasing propellant performance.

Carbon black, one of the tungsten additive replacement options considered for this investigation, provides an excellent example of the percolation theory at work in electrically conductive plastic compounds that can be applied to the particle loading portion of this experiment for all of the suggested tungsten replacement additives. The most important features that affect carbon black's electrical performance are its aggregate and agglomerate structures, discussed above in the Electric Propellant Additive Replacement Chemical Ingredients subsection. However, carbon black's particle size and porosity will also have an impact on its electrical performance. Carbon black with a high structure, shown in Figure 2 on the left and compared to low structure carbon black on the right, indicates that the carbon black agglomerates have formed long, branched chains that are considered ideal for compounds that are supposed to be conductive. The smaller the carbon black primary particle size, the higher the corresponding electrical conductivity based on the particle surface area, and the higher the carbon black particle porosity, the better the electrical conductivity [31]. Using high structure carbon black, desired conductivity levels can be achieved with lower carbon black loading levels.

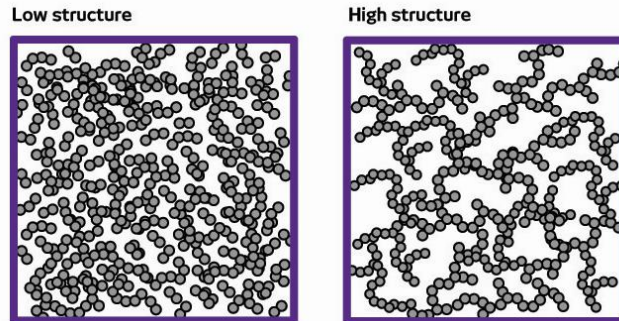


**Figure 2. Image Illustrating the Structural Difference Between Low and High Structure Carbon Black [31].**

It is important to find the correct loading level of carbon black used to achieve the desired electrical properties, as past a certain loading level, “carbon black changes the electrically insulating base polymer into electrically conductive plastic.” However, too high of a carbon black loading will have “a negative impact on the compound's mechanical properties” and “also increases viscosity, causing problems in the injection molding process” [26].

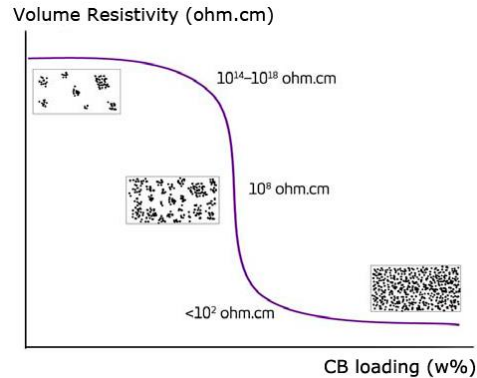


**Figure 3. Percolation Curve Illustrating the Electrical Properties Verses the Amount of Carbon Black Loading in Plastics [31].**

This “decrease in electrical volume resistivity due to the increased amount of carbon black can be described using a percolation model. The percolation behavior of carbon black depends on the qualities mentioned” above including particle size, structure, and porosity. The percolation curve above “illustrates the relationship between the quantity of added carbon black (CB loading (w%)) and the achieved electrical resistivity. Note the narrow threshold in which the electrical resistivity dramatically drops,” after which, increasing the amount of added carbon black will no longer improve electrical properties [31].

To date, most percolation problems studied involve a regular lattice from which sites or bonds are removed according to some random process. Researchers “Scher and Zallen found that the critical thresholds for many lattice percolation problems, when expressed as area or volume fractions (in 2D or 3D), were approximately the same.” “For percolation problems where a structure was being randomly built-up of non-overlapping particles,” Scher and Zallen defined the critical area or volume fraction as the phase fraction at which a cluster spanning the system end to end first appears, and they discovered that the critical volume fraction for percolation for 3D “systems was approximately 0.16, and was 0.45 for” two dimensional (2D) systems. These roughly defined, unchanging values were first quantified for simply modeled lattice problems, but have however, emerged out of more complex simulations, “leading Scher and Zallen to hypothesize that these thresholds have more general or “universal” validity,” with exceptions, including the case “when the particles that are being used to randomly build up the spanning cluster are allowed to overlap” [30].

Stated otherwise, “a noteworthy exception” to the results produced by Scher and Zallen “is the percolation problem for overlapping circles of spheres with randomly located centers, an intensively studied problem which is equivalent to a percolation problem on an irregular lattice, or network, whose sites are the circle or sphere centers.” “A variety of methods have been employed to compute the percolation thresholds and the critical exponents for the two-dimensional and three-dimensional versions of this problem”, including the method used by Alan Kerstein in his work entitled “Equivalence of the void percolation problem for overlapping spheres and a network problem.” Here, Kerstein analyzes “a percolation problem for which no underlying network, regular or irregular, is defined a priori, namely the percolation problem for the region of space which is the complement of the union of randomly located spheres,” or, in other words, the matrix in which the randomly located spheres are suspended. Kerstein states that the results of a “Monte Carlo calculation of the percolation threshold for this problem” (for which the critical exponents were not considered) have “provided an estimate of 0.966 for the critical volume fraction” [32]. This means that the critical volume fraction for the spheres randomly located in a matrix is estimated to be equal to 0.034.

Having an idea of the critical volume fraction, or the value of  $p_c$ , for this investigation was necessary in order to prevent a sample loading value equal to or in the vicinity of the percolation threshold of the electric propellant material. As shown by the volume resistivity versus carbon black loading sloping “S” curve in Figure 3, if any of the sample sets have an additive loading near their (currently unknown) percolation threshold, the measured values of electrical resistivity are likely to yield inconclusive results regarding the electrical resistivity values of a particular sample set. This could be due to small changes in additive characteristics from mixing inconsistencies or variations resulting in large changes in conductivity across a set of finished samples.

#### *Related Electrical Conductivity/Resistivity Properties and Concepts*

Previously defined in the Definitions section of Chapter 1, electrical conductivity is the value of a material’s ability to conduct an electric current, and is calculated as the ratio of the current density within the material to the electric field that is causing the flow of current. (Electrical

resistivity is the reciprocal of electrical conductivity.) Stated in other words, electrical conductivity is a measurement of a material's intrinsic ability to allow for the transport of an electric charge. A higher electrical conductivity, or a lower electrical resistivity, corresponds to a material that will readily allow the flow of an electric current. For the purposes of this investigation, it is important to note that even if the resistance of an individual material is known, calculating the resistivity of something made from several different materials may be much more complicated, especially in this case, as the material is not homogeneous, nor is it perfectly mixed, and the exact path(s) of the current flow through the material are not known. Additionally, resistivity is, among other things, often temperature dependent, but it is possible to predict this dependence using resistance temperature coefficients if they are known (they are not in the case of this study).

Direct current (DC) is defined as the unidirectional flow of electric charge; alternating current (AC) is an electric current that periodically reverses its direction. AC resistance can also be referred to as impedance, which extends the concept of resistance to AC circuits. Impedance has both a magnitude and a phase, unlike resistance, which has only a magnitude. The idea of impedance in an AC circuit is justified by the fact that there are two additional impeding mechanisms that must be taken into account besides the normal resistance in DC circuits. These are: the induction of voltages in conductors self-induced by the magnetic fields of currents, called inductance, and the electrostatic storage of charge induced by voltages between conductors, called capacitance. The "impedance" created by the inductance and capacitance combined is referred to as the reactance, which forms the imaginary part of complex impedance, and resistance forms the real part of complex impedance. The measured and/or observed differences between AC and DC conductivity/resistance measurements are discussed below in the Solid Polymer Electrolytes and Doped PVA Research subsection.

The more accurate devices employed to measure resistance use "four terminal sensing," otherwise known as the "four point technique," as it is more accurate than using an ohmmeter or employing "two terminal sensing." Four terminal sensing is a technique that is used to measure electrical resistivity with separate current carrying and voltage sensing electrodes; and is considered more accurate because of the elimination of leads and contact resistance from

measurements due to the separation of electrodes. The four point sensing operating principle is based on Ohm's law, which states that resistance is equal to voltage divided by current. In a four terminal sensing set-up, current is supplied to a sample via a pair of current carrying electrodes connected to the sample. A pair of potential electrodes, also connected to the sample, indicate the voltage drop across the sample and within the bounds of the current carrying electrodes. Using the known and measured values for current and voltage, respectively, and the dimensions of the measured sample, a value for resistivity can be calculated.

Written in his 2015 white paper and stated previously, Wickham believes that "the importance of the resistance of the material has not yet been established," even though tungsten was originally added to the propellant formula with the intention of increasing conductivity [4]. The importance of the resistivity of this electric propellant, in terms of both performance and what operational mechanisms it affects, is still unknown. However, electrical "resistivity or conductivity may be used to predict, indirectly, the low-frequency dielectric breakdown and dissipation factor properties of some materials" and, often is "used as an indirect measure of: moisture content, degree of cure, mechanical continuity, or deterioration of various types." How useful these indirect measurements are depends upon the "degree of correlation" between resistivity measurements and the desired information, and is normally "established by supporting theoretical or experimental investigations" [33].

In solid rocket motors, "the major determinants for" electrostatic discharge (ESD) "sensitivity are volume resistivity, dielectric constant, and dielectric strength. Covino and Hudson measured these parameters for HTPB binder, inert HTPB propellants, and live propellants. The volume resistivities were measured as a function of temperature, voltage, time of voltage application, relative humidity, and sample thickness." The results of Covino and Hudson's work, "applied using the percolation calculations advocated by Kent and Rat," show that "the overall electrical properties of the propellant were most influenced by the HTPB binder and to a lesser extent by the concentration and particle size of aluminum powder. The contribution of the oxidizer particles was primarily in determining the spacing of the aluminum particles and the thickness of the binder layer between particles" [34].

ASTM standards D257-07 Standard Test Methods for DC Resistance or Conductance of Insulating Materials, D4496-87 Standard Test Method for DC Resistance or Conductance of Moderately Conductive Materials, and D991-89 Standard Test Method for Rubber Property—Volume Resistivity of Electrically Conductive and Antistatic Products detail several different versions of an electrical resistivity testing apparatus and a variety of sample conditioning and testing procedures that can be used to measure conductivity. The testing apparatus and procedures used to determine the electrical conductivity of the samples formulated for this study were provided or derived from the standards listed above and are described in detail in Chapter 3.

#### *Related Previous RMS Work*

A review of the previous electric propellant research conducted at RMS is included in several sections of Chapter 1. However, some additional information regarding RMS work specifically related to this electric propellant resistivity investigation is detailed below.

In 2015, a series of tests, referred to as moisture controlled “button tests,” were completed in order to “determine the ignition parameters of the propellant (i.e., energy required for ignition per unit mass, minimum current, minimum voltage).” After manufacturing the button propellant specimens, “each button underwent a secondary cure above and beyond its initial cure.” The power supply used for these tests “attempted to maintain a potential different of 600V across the electrodes for every test, and allowed current to change at will.” Several data parameters were recorded before, during, and after testing including: button specimen mass, resistance, time to ignite specimen, and energy to ignite the specimen.

During testing and after results analysis, “it was observed that a decreasing amount of water caused the variance of the data to decrease and the average [button specimen] resistance to decrease,” as shown in the Figure below, in which propellant resistance values ranged from 0- $1200 \times 10^3 \Omega$ .



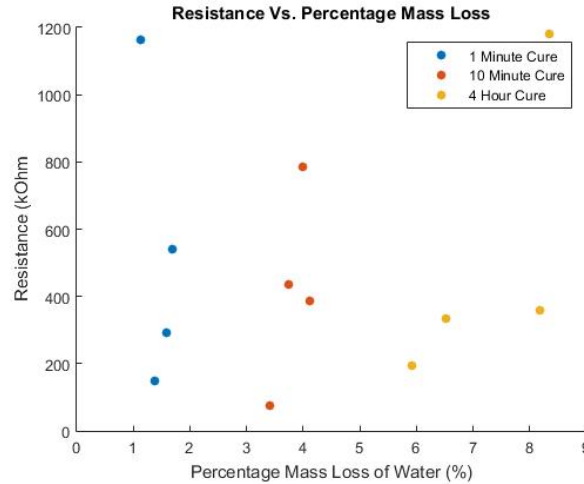


**Figure 4. Plot Illustrating the Percentage Mass Loss of Tested Button Samples Versus Their Measured Resistance Values.**

In addition to decreasing resistance, as the water content of the button specimens decreased, it was also observed that the time to ignite specimens increased and the energy consumed during the first pulse of ignition decreased; one of the experimenters, concluded in a final write up, given the collected data, that “it is easier to maintain combustion when the amount of water present in the material is lower.”

Also completed during the summer of 2015 were a series of “wedge tests,” conducted in order to “demonstrate control of the burn surface of the propellant by forcing an electric field concentration favorable to igniting one part of the grain over another.” Notably, it was observed during the straight wedge configuration testing that “the resistance of propellant samples decreases during the charging phase of a test,” and that the “resistance is initially very high, then steadily decreases to a certain point, at which time another spike is seen, igniting the propellant.” Experimenters detailed that this was an interesting test result, “since decreasing the resistance of a material will also decrease its dielectric strength,” which means that it is “entirely possible that, aside from merely charging the propellant, the initial electric field is decreasing the dielectric strength of the propellant until a dielectric breakdown” occurs [36].

Wickham noted in his 2015 summation of theory and research guide that “it appears that the resistance of the material decreases leading up to combustion and then dielectric breakdown occurs which is responsible for the burning of the propellant... therefore the dielectric strength of

the binder mix, conductivity, and distance between metal particles will be very important” [4]. Several other related RMS electric propellant experiments were carried out in parallel with the 2015 button testing, however, these tests and their results are not directly related to the electric propellant formulation additive or resistivity and are not discussed here.

Most recently, during 2017, a member of the RMS research team, successfully made several measurements on a thick dog-bone shaped ESP-9 specimen using the same or similar equipment utilized for this investigation in a testing set-up configured for a two point resistivity measurement. Calculations for effective resistivity were made by dividing the set pulse generator input voltage value by the oscilloscope measured mean value for current.

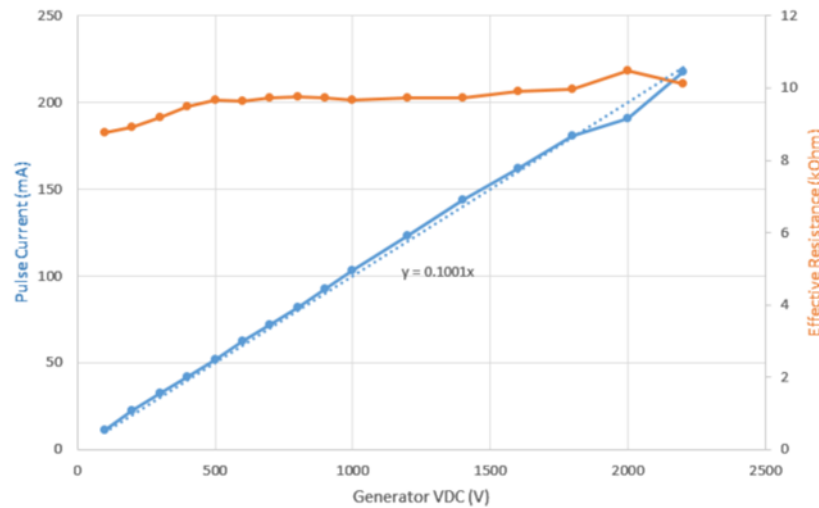


**Figure 5. Two-point ESP-9 Effective Resistance Test Results Plotted Across Pulse Generator Input Voltage.**

Test results show that as the pulse generator input voltage value was increased in increments of 100 V, the effective resistance of the propellant specimen tested remained conclusively constant at a value of approximately  $10 \times 10^3 \Omega$  (the same specimen was used for all of the results shown). This means that as applied voltage increases or decreases, in this case, the resistance of the electric propellant specimen tested remained the same (see Figure 5). A slight positive increase in resistance values exists at voltages lower than 500 V, however for the high voltage application in which this propellant would be normally operated, the overall trend

remains as described. The testing set-up used for the study described above informed the testing set-up utilized for this investigation, and is detailed below in Chapter 3.

#### *Related Solid Polymer Electrolyte and Doped PVA Research*

While solid polymer electrolyte (SPE) materials are an area of research in the battery industry and not widely associated with the propulsion industry, the basic formula for a solid polymer electrolyte is comparable to that of the current RMS electric propellant formula both in its similarity of ingredients and in the overall peculiarity of its mixture. For these reasons, and for the fact that various solid polymer electrolyte formulation's AC and DC conductivity information is publically available, this topic has been included in this literature review.

A solid polymer electrolyte is defined as an electrically conducting solution of a salt in a polymer, and although described as a solid, the material may also occur in a liquid form. Also defined in conjunction with a solid polymer electrolyte is a conducting polymer composite, which is an electrically-conducting composite comprising a non-conducting polymer matrix and an electrically-conducting material, such as metal particles or carbon black [16]. Additionally, the term "polymer electrolyte" has also been "used for compositions which are essentially liquids absorbed into a polymer," similar to that of the current electric propellant formula's PVA dissolved into a perchlorate oxidizer and deionized water solution [37]. Solid polymer electrolyte "compositions which exhibit a conductivity of at least approximately  $10^{-3}$  -  $10^{-4}$  S/cm at 25°C comprise a base polymer or polymer blend containing an electrically conductive polymer, a metal salt, a finely divided inorganic filler material, and a finely divided ion conductor" [38]. Many of these polymer electrolytes "will exhibit to a greater or lesser extent the following properties: adequate ionic conductivity for practical purposes; low electronic conductivity; good mechanical properties; chemical, electrochemical and photochemical stability; ease of processing." "The ionic conductivity of polymer electrolytes is typically 100 to 1000 times less than exhibited by a liquid- or ceramic-based electrolyte... and a great deal of effort has gone into improving the bulk conductivity of polymer electrolytes over the years" because these materials offer many advantages in several areas of industry including large, high energy density batteries for electric

propulsion, different fuel cell applications, and for smaller electronic devices in which the battery takes up a significant portion of the device.

Solid polymer electrolytes are typically found within a wide range of “solid-like character” due to that fact that the solid character of polymers is, in general, related to the molecular weight of the polymer. Polymers of lower molecular weight are often liquid, meaning the solid polymer electrolytes can range from “liquids to very hard and rigid materials” and include crystalline, dry, plasticized, and single- or two-phase solvent doped solid polymer electrolytes. Polymers organized as crystalline at the molecular level have lower conductivity, since “conductivity comes about through molecular motion in the structure, and are usually not considered options for batteries. Dry solid polymer electrolytes are single phase and non-crystalline materials that contain a dissolved salt in which the “ions of that salt are mobile.” Plasticized polymer electrolytes are single-phase and usually contain organic additives included to soften the polymer, and they have a higher conductivity when compared to dry polymer electrolytes due to the greater freedom of molecular motion. Solvent-doped solid polymer electrolytes can be either single- or two-phase depending mostly on their molecular make up; two-phase polymer electrolyte materials can also be described as gels in which both the “anions and cations are mobile at the molecular level, and ion-selective two-phase solid polymer electrolytes are used in the fuel cell industry, but have not been applied specifically in the area of lithium batteries” [37].

An average value of the electrical conductivity of a solid polymer electrolyte “can be obtained by measuring the AC conductivity of  $P_n:MX$ ” (“where P is the structural repeat unit of the polymer chain and n is the stoichiometric ratio of structural repeat units to formula units of salt MX”) “between two inert electrodes and with an inert gas passing over the sample. Alternatively, four probes can be used and the IR drop is measured between the two inner probes” [37]. When a polymer matrix has dissolved a salt, the conductivity of the polymer increases because of the charge carrier concentration increase, “moreover, as the salt concentration, for example for a polyether, is increased above  $\sim 0.1 \text{ mol dm}^{-3}$  (M:O ratio of  $\sim 1:100$  to  $1:50$ ), the conductivity is found to reach a maximum and then falls.” This conductivity drop is believed to be due to the “introduction of an ever-increasing number of the transient crosslinks in the system, which causes

a reduction in chain mobility.” Additionally, “ion aggregation can still contribute to the observed decrease in conductivity as, if aggregates do exist, they are likely to have retarded diffusion rates,” causing a further drop in the conductivity [37].

Many factors control the magnitude of polymer electrolyte conductivity, the most important include: the nature of the salt and polymer, salt concentration, and the degree of crystallinity. Additionally, temperature and pressure may also play a role in the conductivities of polymer electrolytes and “have been used in a great number of studies as variables in investigations of these conductivity” factors. The total DC conductivity of SPEs “has routinely been used to characterize polymer electrolytes and a threshold of approximately  $10^{-5}$  S  $\text{cm}^{-1}$  has been used as the criterion for possible application purposes,” with a “large number of the measured materials reaching such conductivity values between “room temperature and 100°C.” However, with the use of either blocking or non-blocking electrodes for measurement purposes, DC conditions do “give rise to polarization problems” in polymer electrolyte conductivity measurements [37]. These problems can usually, largely be avoided if AC is used instead of DC for testing and measurement purposes [37].

With the intent of addressing the broader topic of this investigation, regarding the conduction and operational mechanisms of electric propellant, additional investigation into the possible conduction mechanisms, AC conductivity, and dielectric constants of SPEs and doped PVA samples was also performed.

Research conducted by Gurusiddappa, et al, and summarized in the publication titled “Conductivity and Dielectric Behavior of Polyethylene Oxide-Lithium Perchlorate Solid Polymer Electrolyte Films,” has concluded that “the conduction mechanism in polymer electrolytes can be understood by knowing the dielectric relaxation phenomena” and showed that the “electric modulus spectra is a powerful tool” that can be used “to understand the conductivity relaxation process, ion hopping mechanism, transport process, and type of charge carrier present in an ionic conducting solid electrolyte” [40].

Additionally, a study done by Taha Hanafy titled “Dielectric relaxation and alternating current conductivity of lanthanum, gadolinium, and erbium-polyvinyl alcohol doped films” has proven that

the amount of a PVA additive, or “filler,” does influence the conductivity values of the material. This study was conducted with the purpose of carrying out” research on the “Fourier transform infrared spectrum dielectric constant,  $\epsilon'$ , loss tangent,  $\tan(\delta)$ , electric Modulus,  $M^*$ , and ac conductivity,  $\sigma_{ac}$ , of pure polyvinyl alcohol (PVA) as well as La-, Gd-, and Er-PVA doped samples.” Based on the first wave of results produced and depicted in this paper, “it is clear that the [dielectric constant] of pure PVA increases smoothly with increasing temperature due to the increase of the mobility of the dipoles within the polymeric sample.” Additionally, Hanafy deduces that, “in polymers and composite polymeric materials, interfacial polarization is almost always present. This refers to the existence of the additives, filler or even impurities that make these materials heterogeneous,” therefore, it can be suggested “that there is a role of electrode polarization for all these samples. In other words, the concentration of the filler influences polarization as well as the DC and AC conductivity values.” Final results of this study conclude that AC “conductivity increases with increasing frequency and temperature,” which “indicates that the hopping conduction mechanism is predominant for all PVA samples” [36].

#### Summary and Predictions

Based on the insights gained from the literature review information presented above, meant to inform an examination of the RMS electric propellant formula and operation that could help answer the research questions established in Chapter 1, and to help fill out the experimental framework discussed earlier in this chapter, several assumptions can be made regarding the set up and conclusions of this investigation.

Previously conducted SRM research results detail that the primary propellant chemical component contributing to electrical resistivity was the propellant binder, followed by the solid aluminum fuel additive, with the solid oxidizer only contributing to particle spacing, contrary to the nature of the additive and oxidizer contributions in SPEs. However, it was believed that sample resistivity values would be altered enough, with only a change in additive, to capture valuable data. This electrical properties research also led to methods and ASTM standards detailing best practice for determining DC electrical conductivity measurements of materials, further discussed in Chapter 3.

Research regarding the response variable chosen for this investigation has shown that electrical conductivity measurements have the potential to provide important information about materials and, if correlated correctly, could lead to important propellant operating or performance predictions. This was discussed above in the Previous Related RMS Work subsection, which detailed 2015 experimental results showing that resistivity could be used as an indirect measurement of at least propellant moisture content.

Finally, research done on solid polymer electrolytes and similar chemical mixture advancements has shed light on the fact that results of this research should indicate that metallic, or otherwise, additives do play a part in electric propellant conduction and that DC conductivity measurement conditions could give rise to polarization problems, among others, in tested specimens. Based on the conclusions of this research, discussed in the subsection above and on the results of this study, presented and discussed in Chapters 4 and 5, suggestions for experimental improvement and further investigation can be made.

Research conducted on additive chemicals, particle sizes, and loading amounts helped contribute to the decision that copper and conductive carbon black were to be the chosen replacement additive chemicals for this investigation, in addition to tungsten and samples with no additives, and that aluminum was eliminated from this study due to safety reasons. However, taking a deeper look at the baseline perchlorate oxidizer based electric propellant formulation through an electrochemistry lens could provide some further clues regarding propellant operation. Additionally, several replacement additive particle sizes and loading amounts should be investigated, but, based on speculation by Wickham in his white paper, smaller particle sizes should increase the resistance of the electric propellant samples. In this case, however, particle size may not have as drastic of an effect on the electric propellant burning rate as particle size does in solid propellants. Lastly, in order to avoid the negative the effects of percolation on the measured values of conductivity, if it does in fact influence electric propellant properties, sample loading values were chosen with the intention of avoiding the best guess particle loading percolation threshold value and are further discussed in Chapter 3.

Predictions of the possible results of this study include the following: as Wickham has suggested, it is predicted that smaller particle sizes will increase the resistivity of the propellant samples, but will not have as significant of an effect on overall resistivity given the nature of this investigation. Additionally, since tungsten was originally added to the formulation in order to increase conductivity, it is predicted that as the metallic additive loading percentage increases, so will the propellant conductivity (meaning lower electrical resistivity). This effect is also expected to occur with the copper additive, but to a lesser extent given the material properties difference, and based on the information gathered regarding the addition of carbon black to plastics, it is also expected to occur with the carbon black additive. Lastly, it is expected that the critical volume fraction for the additive loading percentage included in the formulations developed for this investigation will be equal to approximately 0.034, or 3.4%, as suggested by Kerstein based on his analysis described above.

As detailed in the Experimental Framework of the Study section of this Chapter, based on this literature review and the above summary and predictions, an experimental study was researched, designed, and carried out with the purposes of contributing to the determination of the electric propellant operational mechanisms. The methodology used to design and carry out this study is detailed below in Chapter 3.



## CHAPTER 3

### METHODOLOGY

#### Introduction

As discussed in Chapters 1 and 2, this experiment was designed to investigate and potentially answer several research questions surrounding the role of the additive in this perchlorate oxidizer based electric propellant formula and the effects of the additive's particle size and loading percentage on the propellant's electrical resistivity properties.

Traditionally, a screening experiment, meant to determine important controllable or uncontrollable experimental factors, is the first step in an experimental design, followed by response surface methodology, to define the optimal space and factors for the experiment, and then model validation, to confirm experimental predictions. Full-factorial experimental designs (experiments whose results feed the response surfaces created) "include all combinations of factor levels and provide a predictive model that includes main effects and all possible interactions," while a fractional factorial experimental design includes "fewer trials and may be more efficient than the corresponding full factorial design" [11]. This investigation has been designed as a set of fractional factorial experiments, the results of which were used to fill out a response surface plot template like the one shown below for three different pulse generator input voltage values. "In statistics, the response surface methodology explores the relationships between several explanatory variables, or independent variables that may not be statistically independent, and one or more response variable. The main purpose of this methodology is to use a sequence of designed experiments to obtain an optimal response or underlying process with the intention of discovering property combinations that provide maximum yield with minimal cost" [39].

The response surface template presented in Figure 6 illustrates a three axis plot (two explanatory factors and one response factor), where the maximum (or minimum, or range of values, depending on what is desired) of the response surface plot indicates the optimum response based on the explanatory factors being investigated. Stated in other words, the primary objective of the response surface method is finding the optimum set of factor levels to achieve

some goal. In this case, this goal outcome would be some optimal or local extrema value of bulk volume resistivity response, based on additive type, additive loading percentage, and additive particle size included in a specific propellant formulation.

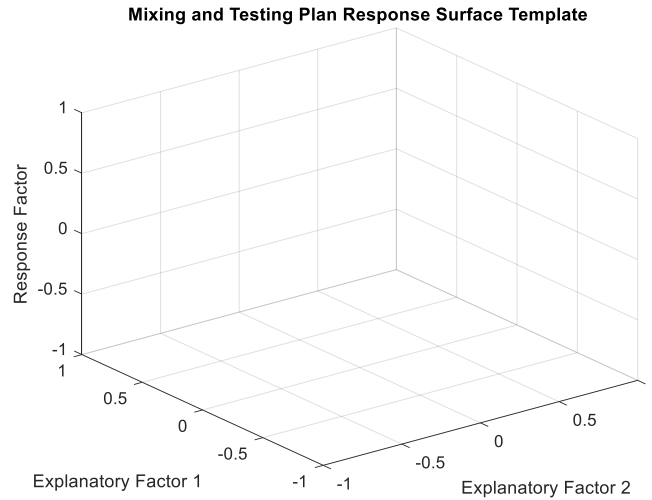


**Figure 6. Visual Representation of the Response Surface Space to be Created Using Experimental Electrical Resistivity Results.**

For this thesis project, the purpose of the screening-type experiment and response surface interpretation was to identify any of the electric propellant formula additive variables that could have significant effects on propellant properties or performance for further, future investigation, and to further specify a potential range of values for future exploration that might help to “round out” the results of this investigation or to allow researchers to “hone in” on desired outcome responses. The response surface template plot shown above in Figure 6 has been set up to aid in the visualization of the experimental design outlined in the sections below.

Based on the ASTM standards and research collected and summarized in the literature review in Chapter 2 of this document, as well as on all of the electric propellant work done prior to this study, and with the intention of filling out the response surface template above for each combination of this investigation’s dependent variables, the sample formulations, pre-manufacturing pilot study, sample manufacturing instructions, testing apparatus, and testing methods described below were developed and used during this investigation.

## Research Design and Rationale

In the case of this investigation, based on the established research questions, the determination of whether or not the various replacement additives chosen for this experiment influence the overall electric propellant resistivity and if the overall additive amount and particle size further influences that resistivity value are of the highest interest. As the time required to complete this set of experiments was limited, only two replacement additives (due to the elimination of aluminum from the study), three particle sizes, and three particle loadings have been considered for this set of experiments. Due to the wide range of limited factors chosen to bound the experimental space of this investigation, these experiments were defined as a set of fractional factorial experimental designs, as outlined in Table 3 below.

Since such a wide study of sample formulation additive, particle size, and loading has never previously been conducted, this experiment, regardless of how limited it may be, has contributed to the advancement of electric propellant knowledge. Additionally, the mixing and testing methods and apparatus designed for this set of screening experiments, and preserved in this document, have added to the ability of researchers to gain electric propellant manufacturing and electrical conductivity knowledge related to any further formulation study efforts put forth in the future.

## Methodology

### *Sample Population*

In Table 3, there are four different groups of sample particle loading amounts: no loading, light loading, medium loading, and heavy loading; within each loading group the replacement additives and the range of particle sizes are shown. Due to the screening type nature of these experiments and the lack of knowledge regarding electric propellant additive particle size effects, particle sizes were chosen based on increasing factor of order 10 and include the following sizes: aggregate for all carbon black samples, and 1-5 micron, -325 mesh (44 micron and below), and -100 mesh (149 micron and below) for all samples formulated with a metallic additive. (Mesh is a measurement of particle size used to describe particle size distribution based on the sorting screen opening size and is not necessarily a precise measurement of particle size because of the possible error in the size of the wires in a mesh screen.) The largest two particle size options,

-325 and -100 mesh, limit the investigation in terms of their wide range of particle size, but were chosen due to the difficulty and increased cost of finding powdered copper and powdered tungsten in the same particle size ranges and shapes.

Each numbered cell of the particle loading sets shown in Table 3 corresponds to the number of samples tested for that particular propellant formulation, either nine samples or none. If a particular cell shows a "9," three of the sample specimens were measured at each of the three pulse generator input voltage values chosen for this study for that particular sample formulation. Again, the number of voltage settings chosen for this study were limited due to time constraints, equipment capability, and because this experiment is classified as a fractional factorial experiment and, as such, does not require a wide spectrum of power settings. The number of specimens to be tested across the experimental design totals 198, not including any additional samples that were manufactured and used while proving in the testing apparatus and testing methods, or in the case of any problems encountered during the testing/measuring process.

**Table 3. Depiction of the Experimental Sample Population.**

<b>Additive/ Particle Size</b>	<b>Non-additive</b>	<b>Tungsten</b>	<b>Copper</b>	<b>Carbon black</b>
	<b>Zero Loading</b>			
<b>No Applicable Particle Size</b>	9	-	-	-
	<b>Light Loading (1.5%)</b>			
<b>Order 10<sup>0</sup>, 1-5 micron</b>	-	9	9	-
<b>Order 10<sup>1</sup>, -325 mesh</b>	-	9	9	-
<b>Order 10<sup>2</sup>, -100 mesh</b>	-	9	9	-
<b>Aggregate</b>	-	-	-	9
	<b>Medium Loading (2.3%)</b>			
<b>Order 10<sup>0</sup>, 1-5 micron</b>	-	9	9	-
<b>Order 10<sup>1</sup>, -325 mesh</b>	-	9	9	-

<b>Additive/ Particle Size</b>	<b>Non-additive</b>	<b>Tungsten</b>	<b>Copper</b>	<b>Carbon black</b>
<b>Order 10<sup>2</sup>, -100 mesh</b>		9	9	-
<b>Aggregate</b>	-	-	-	9
	<b>Heavy Loading (5.0%)</b>			
<b>Order 10<sup>0</sup>, 1-5 micron</b>	-	9	9	-
<b>Order 10<sup>1</sup>, -325 mesh</b>	-	9	9	-
<b>Order 10<sup>2</sup>, -100 mesh</b>	-	9	9	-
<b>Aggregate</b>	-	-	-	9

Particle loading values of approximately 1.5%, 2.3%, and 5%, by volume, have been chosen for the light, medium, and heavy particle loading groups, respectively. As discussed in the Percolation Theory and Concepts subsection of Chapter 2, particle loadings above and below the assumed percolation threshold of approximately 3.4%, by volume, were desired for investigation. The medium particle loading value of approximately 2.3% was chosen because it is approximately the tungsten particle loading value in the current electric propellant baseline formula, and comparison of the baseline formula tungsten loading to the copper and carbon black loading was desired.

A lighter particle loading value of 1.5% was chosen because, based on the literature review, more useful information can be gathered by focusing on several points below the volume fraction percolation threshold rather than above. However, the value of the volume fraction percolation threshold for this material and its variants has not yet been established, so the third value of particle loading of 5% was selected above the assumed threshold in order to increase the chances of ascertaining a possible threshold location.

If this investigation shows that electric propellant sample electrical resistivity values are a function of replacement additive, additive particle size, and particle loading, and are driven by percolation, then the scaling of the average additive particle cluster size within samples, in

addition to the value of the volume fraction percolation threshold, will become important. Testing enough propellant formulation loading variations and overall sample sizes to determine scaling exponents, length scaling factors, and “s” curve slope change would then be required.

Each of the propellant samples tested were prepared following the method outlined in the most updated previously written version of the “ESP-9 Electric Propellant Manufacturing Instructions” as closely as possible, and following the guidelines outlined in the “ePropellant Pre-Mixing Test Plan” and the “ePropellant Mixing and Testing Plan” developed for this thesis project. The 10 baseline propellant sample formulations designed for the experiment are given below in Figures 7, 8, 9, and 10.

<b>Non-additive Propellant Formulation</b>		
<b>Chemical</b>	<b>Mass %</b>	<b>Volume %</b>
Perchlorate Oxidizer Solution	75	65.9
Polyvinyl Alcohol	25	34.1
Total	100	100

**Figure 7. Formulation for the Electric Propellant Samples with No Included Additives.**

<b>Propellant Formulation at 1.5% W Volume Fraction</b>		
<b>Chemical</b>	<b>Mass %</b>	<b>Volume %</b>
Perchlorate Oxidizer Solution	65	65.7
Powdered Tungsten	14	1.5
Polyvinyl Alcohol	21	32.9
Total	100	100

<b>Propellant Formulation at 2.3% W Volume Fraction</b>		
<b>Chemical</b>	<b>Mass %</b>	<b>Volume %</b>
Perchlorate Oxidizer Solution	60	64.5
Powdered Tungsten	20	2.2
Polyvinyl Alcohol	20	33.3
Total	100	100

<b>Propellant Formulation at 5.0% W Volume Fraction</b>		
<b>Chemical</b>	<b>Mass %</b>	<b>Volume %</b>
Perchlorate Oxidizer Solution	48	62.7
Powdered Tungsten	36	4.9
Polyvinyl Alcohol	16	32.4
Total	100	100

Figure 8. Formulations for the Electric Propellant Samples with Varying Tungsten Additive Particle Sizes and Loadings.

<b>Propellant Formulation at 1.5% Cu Volume Fraction</b>		
<b>Chemical</b>	<b>Mass %</b>	<b>Volume %</b>
Perchlorate Oxidizer Solution	70	65.3
Powdered Copper	7	1.5
Polyvinyl Alcohol	23	33.3
Total	100	100

<b>Propellant Formulation at 2.3% Cu Volume Fraction</b>		
<b>Chemical</b>	<b>Mass %</b>	<b>Volume %</b>
Perchlorate Oxidizer Solution	67	64.7
Powdered Copper	11	2.4
Polyvinyl Alcohol	22	32.9
Total	100	100

<b>Propellant Formulation at 5.0% Cu Volume Fraction</b>		
<b>Chemical</b>	<b>Mass %</b>	<b>Volume %</b>
Perchlorate Oxidizer Solution	59.5	63.0
Powdered Copper	21	5.0
Polyvinyl Alcohol	19.5	32.0
Total	100	100

**Figure 9. Formulations for the Electric Propellant Samples with Varying Copper Additive Particle Sizes and Loadings.**



<b>Propellant Formulation at 1.5% CB Volume Fraction</b>		
<b>Chemical</b>	<b>Mass %</b>	<b>Volume %</b>
Perchlorate Oxidizer Solution	73.75	64.9
Aggregate Carbon Black Powder	1.5	1.4
Polyvinyl Alcohol	24.75	33.7
Total	100	100

<b>Propellant Formulation at 2.3% CB Volume Fraction</b>		
<b>Chemical</b>	<b>Mass %</b>	<b>Volume %</b>
Perchlorate Oxidizer Solution	73.25	64.5
Aggregate Carbon Black Powder	2.5	2.3
Polyvinyl Alcohol	24.25	33.1
Total	100	100

<b>Propellant Formulation at 5.0% CB Volume Fraction</b>		
<b>Chemical</b>	<b>Mass %</b>	<b>Volume %</b>
Perchlorate Oxidizer Solution	71.25	62.9
Aggregate Carbon Black Powder	5.25	4.9
Polyvinyl Alcohol	23.5	32.2
Total	100	100

**Figure 10. Formulations for the Electric Propellant Samples with Aggregate Carbon Black and Various Particle Loadings.**

*Manufacturing Pilot Studies and Sample Manufacturing*

Prior to manufacturing the samples used for experimental testing, a document detailing experimental test mixes and procedures was written and a set of pre-mixing test samples were made and examined in order to determine the best set of mixing and curing instructions for each sample formulation. In order to preserve materials and decrease time to complete test mixing, only the -100 mesh tungsten and copper formulations were prepared, in addition to the carbon black samples and the test sample with no included additive. The -100 mesh samples were chosen because they contained the largest additive particle sizes, and it was assumed that if any of the additive particle sizes were to negatively affect the propellant, it would be the largest particle sizes that may settle or sink within the samples after being allowed to set in their molds.

The written documents detailing experimental test mixing and final sample manufacturing called for the use of the most up to date version of the electric propellant mixing instructions at the time. These mixing instructions detailed the chemical ingredients needed for a baseline

propellant formulation mixture, the mixing equipment and expendables required to manufacture the propellant to the current, best practice quality, and the instructions detailing how the ingredients should be mixed. Current best practice for mixing electric propellant at the time during which this investigation was completed included the use of a Thinky ARV-310 planetary mixer.



**Figure 11. (Left) Thinky Mixer Used to Manufacture Test and Final Sample Formulations [41]. (Right) The Semco extruding gun used to extrude mixed propellant out of the syringes in which they were mixed.**

Based on previous work, discussed in the Background section of Chapter 1, one of several advancements made in 2016 included the addition of the Thinky mixer to the mixing process, as the “mixer has shown that it can emulsify an ESP-9 mix better than anything else” [40]. This improved propellant emulsification was probably due to the fact that the Thinky ARV-310 mixer combines “vacuum pressure reduction function with rotation and revolution mixing for general purposes,” enabling the “efficient elimination of submicron-level air bubbles” when compared to the previously standard hand mixing instructions [41].

Also included in the current best practice manufacturing processes was the addition of Semco cartridge syringe mixing and extrusion, added in 2017 in order to ease the time and effort required for propellant casting. Using the Thinky mixer, and mixing in the smaller diameter syringes, adapted to fit into the Thinky mixing chamber, propellant was mixed within a Semco syringe cartridge and then placed right into the Semco extruding gun for casting into the flat molds. The Semco model 250-A sealant gun used for this process is widely considered an aerospace and electronics industry standard and has been designed for the pneumatic application of sealants, adhesives, and other materials that can be filled into Semco disposable cartridges.

Following the completion of the mixing all of the test samples for the pre-mixing plan, it was decided that added dehydration time was absolutely necessary in order for the samples to retain their required shape based on the amount of relaxation observed in the finished samples. Additionally, all sample formulations, with the exception of the tungsten formulation at 2.3% particle loading, were adjusted so their PVA to perchlorate oxidizer solution volume ratio matched that of the baseline formulation at 2.3% tungsten particle loading as closely as possible; these are the sample formulas presented in Figures 7 through 10. This was done to ensure that the desirable mechanical properties of the 2.3% tungsten particle loading formulation (hardness, resistance to relaxation, ease of mixing and extruding) were preserved across the entire sample population.

In addition to improving sample manufacturing techniques, the sample dimensions, in accordance with ASTM standards, and the sample molds were also updated based on the pre-mixing results. Samples made during the pre-mixing study were extruded into 3D printed molds of ASTM standard specified sample shape 6 in by 0.5 in by 0.25 in, however as the testing apparatus designed for this experiment matured, sample dimensions were decreased dramatically, but still kept within the allowable ASTM standards, down to 2.75 in by 0.5 in by 0.125 in, in order to continue to preserve material and allow for quicker testing sample manufacturing. It was also decided that extruding syringe mixed propellant into sheets, referred to as "flats," that could then be cut down would be more time efficient in terms of manufacturing all of the required test samples, and would, again, decrease material waste.

Following the pre-mixing plan, and prior to taking any electrical measurements, the left over material from each sample manufactured for the pre-mixing study described above was set aside and later configured for open atmosphere on/off test firing to verify that each formulation retained the on/off properties of the baseline propellant formulation. However, as discussed in the Limitations section of Chapter 1, no pilot study was done to determine if the on/off mechanism of these various propellant samples has been preserved across different operating pressures, as stated in the original electric propellant patent. This may be desired as a follow up experiment, as the determination of such may provide vital clues to the propellant burning and control

mechanisms, and it is possible that not all formulations being studied retain their on/off mechanism at higher pressures.

The final samples used during the testing process of this investigation were manufactured as closely to the most current version of the “ESP-9 Electric Propellant Manufacturing Instructions” as possible, with notable exceptions including a hand mix time of approximately 90 seconds, and a planetary centrifugal vacuum mixer time of approximately 60 seconds. Additionally, after being extruded into their molds, each flat of propellant was dehydrated (cured) in a digitally timed dehydrator. The countertop five tray dehydrator used was controlled by a 550 Watt heating element and a rear-mounted fan designed for uniform drying, with an adjustable 95-155°F thermostat and a 30 hour digital timer. Each propellant flat was dehydrated for a total of 30 hours at a set temperature of 135 °F in order to remove a portion of the water from the samples and prevent them from relaxing out of their desired shape throughout the testing process. After dehydration, each flat of propellant was then cut down into the required testing specimen size according to the dimensions above.

#### *Sampling and Sampling Procedures*

Unfortunately, the electric propellant material’s ability to absorb water from its surroundings has not yet been fully eliminated and the degree to which this ability has been mitigated by dehydrating the propellant sample flats is currently unknown. While sample conditioning measures were put in place in order to preserve, as closely as possible, the condition of the samples immediately after dehydration time, the samples may still have been able to absorb enough water to affect experimental conductivity measurements and make the researched hypothesis developed for this experimental investigation difficult to prove or disprove. In the interest of understanding how the samples/specimens manufactured for this experiment absorbed water over time, specimens were each weighed at several instances throughout their experimental life including once before being placed in a desiccator for storage, once immediately before being tested, and one final time after all testing had been completed.



**Figure 12. Testing Samples Stored in the Laboratory Desiccator.**

Cut specimens were conditioned, stored, and prepared for testing inside of a laboratory desiccator located near the testing set-up. Figure 12 above shows the prepared samples inside of the desiccator prior to the beginning of testing. Each flat of propellant manufactured allowed for approximately 9-14 specimens to be cut, from which the 9 specimens required for testing were randomly chosen and numbered for recording purposes. Specimens were kept within their propellant flat mold after cutting in order to prevent relaxation and were stored in sealed plastic bags inside of the desiccator when not in use in order to prevent contamination. Tested specimens were only electrified for measurement and data collection once before being placed back in their flat mold, and all results were recorded on a soft copy of the testing record sheet designed to record results for this investigation.

Usually, the order of running and testing experimental trials is “randomized to protect against the presence of unknown lurking variables,” as well as bias of any kind [11]. For this thesis project, and in accordance with ASTM standards, specimen testing (and sample manufacturing) was done at random using a pre-ordered testing record sheet to determine the order in which to test and record specimen measurements. This record sheet was assembled in Excel; all of the specimens to be tested for this investigation were given a serial number and each of those serial numbers were given a number 1 through 198. Each of the serial numbers were then assigned a

random number value between 0 and 1 using Excel's "rand" function, the random numbers were then sorted from smallest to largest using Excel's "small" function, and finally, the sorted random values were matched to their serial specimen number to determine a final testing order for all of the specimen.

#### *Testing Apparatus and Instrumentation*

The testing apparatus electrode system designed for this investigation to employ the "four point technique" in order to determine electrical resistivity was chosen based on ASTM standards, ease of design and construction, and ease of use during testing operations. As described in Chapter 2, in a four terminal sensing set-up, current is supplied to a sample via a pair of current carrying electrodes connected to the sample. A pair of potential electrodes, also connected to the sample, indicate the voltage drop across the sample and within the bounds of the current carrying electrodes. Using the known and measured values for current and voltage, respectively, and the dimensions of the measured sample, a value for resistivity can be calculated. ASTM standard D991-89 dictates that the "electrode assembly shall consist of a rigid base made from an electrically insulating material having a resistivity greater than  $10 \text{ T}\Omega\text{-m}$  ( $10^{12} \Omega\text{-m}$ ) to which "a pair of current electrodes and a pair of potential electrodes are fastened in such a manner that the four electrodes are parallel and their top surfaces are in the same horizontal plane. Another pair of current electrodes identical with the first pair shall be fastened to a second piece of insulating material so that they can be superimposed on the specimen directly above the first pair" [42]. The electrode assembly presented below in Figure 13 shows the position of the current and potential electrodes described with respect to an example testing specimen.

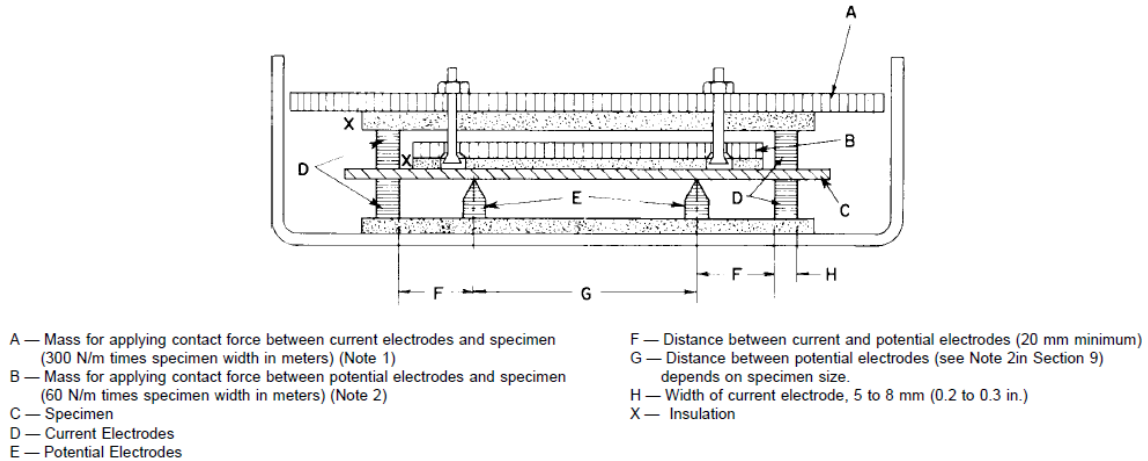


**Figure 13. Testing Apparatus Electrode Assembly [42].**

Per ASTM standard D257-07, the material used to make the testing apparatus electrodes “should be corrosion-resistant under the conditions of the test” and should be made “of a material that is readily applied, allows intimate contact with specimen surface, and introduces no appreciable error because of electrode resistance or contamination of the specimen.” Copper was chosen for this testing apparatus electrode material because it has been used successfully as an electrode material for previous electric propellant efforts and it was readily available for fabrication. ASTM standard D257-07 also suggests choosing a flat metal plate/metal bar electrode shape for “testing flexible and compressible materials, both at room temperature and at elevated temperatures,” however the standard notes that “considerable pressure is usually required” to ensure “intimate contact with the specimen” [33]. Electrode assembly specifications detail the electrode contact masses required to provide constant contact force between the sample and the electrodes; these masses were made out of stainless steel, also due to its availability for fabrication.

The specimen dimensions, decided upon during the examination of pre-mixing plan results, dictated the final dimensions of the testing apparatus, specifically the distance between electrodes and the weight of the contact force masses. All other apparatus design details and dimensions were either provided by one of the three ASTM standards relied upon for this investigation (D257-07, D991-89, and D4496-87) or were chosen based on ease of constructing and/or using the testing apparatus.

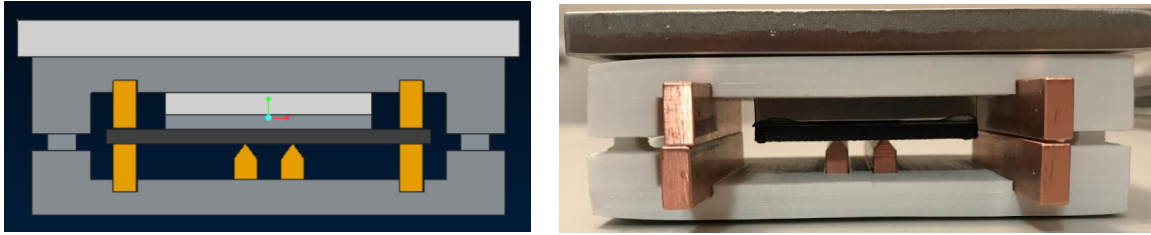


**Figure 14. (Left) Creo Parametric Model of Testing Apparatus, with Specimen. (Right) Image of Testing Apparatus Built for This Investigation, Without Specimen.**

The final apparatus assembly's rigid base and insulation parts were 3D printed out of acrylonitrile butadiene styrene (ABS) due to its volume resistivity values of  $>10^{15} \Omega\text{-m}$ , as well as its material flexural strength and higher temperature resistance. The stainless steel current and potential contact forces machined for this testing apparatus weigh approximately 0.943 and 0.194 lbm, respectively, and apply slightly higher than the amount of force required to the copper current and potential electrodes (the standards require 0.857 and 0.171 lbm of force, respectively).

The desired testing instrumentation output data values required to compute electrical resistivity of the tested propellant samples included values for the current through the testing apparatus current electrodes and the potential difference across the testing apparatus potential electrodes for each specimen. In order to electrify specimen in the testing apparatus assembly, to accurately calibrate the testing set-up, and to collect the desired output data values, several electronic test instruments, along with some additional testing hardware items, were required.

For the purposes of this investigation, a Cober Electronics, Inc. High Power Pulse Generator Model 605P was deemed appropriate for generating the required signals to be delivered to the testing apparatus. The output of this pulse generator was connected to each of the testing apparatus current electrodes and to a LeCroy LC574A 1GHz Oscilloscope to ensure that a pulse of the correct shape, magnitude, length of time, etc. was being delivered to the specimens tested. The Cober 605P is a "versatile, High-Power Pulse Generator that produces a broad range of excellent wave shape pulses at peak powers of up to" 24 kW at 1.5% duty, and the output of which is continuously adjustable from 0 to 2200 V at an output current of 11 A. The 605P "is a precise tool for research and testing" in which "specific applications include "use as a power source for solid-state devices," "for performing destructive or non-destructive testing of electrical



and electronic components and for determining their electrical and life characteristics”, and applications “in the pulse testing of magnetic components, nuclear research, and as an all-purpose source of high power pulses for the laboratory” [43].

A 100  $\Omega$  resistor assembly, referred to as the “current measurement” resistor,” was placed between the testing apparatus current electrodes and the negative end of the pulse generator output, and was connected to the oscilloscope with a coaxial cable. Using the measured value of the voltage drop across the resistor, the current passing through the testing apparatus current electrodes could be computed. A current sensing probe could have been used in place of this resistor, however, it was found during set-up verification that the signal detected by the current probe and output on the oscilloscope was noisier than the sensing precision resistor assembly and was slightly less accurate. Use of the resistor assembly also simplified steps required for taking data points, as there was no longer any need to constantly degauss a current probe.

Finally, a set of voltage probes connected to a differential attenuator were attached to each of the potential electrodes and connected to the oscilloscope through a differential amplifier, included in order to amplify the difference between each voltage probe while suppressing any common voltage between the two probes. The two channel, 100 MHz LeCroy DA1855A PR2 Differential Amplifier was intended to act as a signal conditioning preamplifier for the oscilloscope used, providing a differential measurement capability to instruments (the oscilloscope, in this case) having only single-ended input options. By connecting each of the voltage probes plugged into the differential amplifier, or voltage inputs, to each of the potential electrodes during sample electrification, the resultant output voltage, displayed on the oscilloscope, was proportional to the voltage difference between the two input voltage signals.



**Figure 15. (Left) The Testing Apparatus Integrated into the Testing Set-up. (Right) The Oscilloscope and Differential Amplifier with Connections from the Testing Set-up.**

All three of the recorded testing signals (the pulse generator output, the voltage drop across the “current measurement” resistor, and the voltage drop across the potential electrodes) were captured by the oscilloscope as voltage signals and analyzed for data collection as outlined in the written testing procedures.

#### *Procedures for Calibration and Data Collection*

Due to the large number of data points that were required for experimental analysis, sample testing and data collection for this investigation was broken up into discrete testing sessions conducted over a period of several weeks. Prior to testing any samples during these discrete testing sessions, and in order to ensure that the testing set-up and instrumentation used to collect data were functioning properly, all testing hardware and instrumentation were inventoried and re-calibrated to the specific testing set-up requirements. A 10 k $\Omega$  wire wound resistor, referred to as the “calibration resistor,” in place of the testing specimen and the bottom shell of the 3D printed testing apparatus (including the attached potential and current electrodes), was used during calibration to verify the settings of the oscilloscope, differential amplifier, voltage probe assembly, and pulse generator, as well as to establish the testing day’s required data correction values, to be used later during the data analysis process. It is understood that “wire wound resistors naturally have some capacitance and inductance. Because of this, they influence current flow in an alternating current circuit,” but “with a DC current fewer problems with the winding arise than

with an AC current, because of the parasitic capacity and self induction" [44]. However, wire wound resistors are usually very accurate, have excellent properties for lower resistance values and high power ratings, and high precision wire wound resistors are often used in calibration equipment.

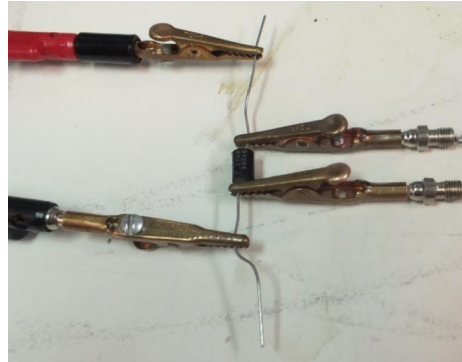


**Figure 16. The Calibration Resistor Connected to the Testing Set-up.**

After this "calibration resistor" was assimilated into the testing set-up, a 1000 V pulse was applied to the system set-up and the resulting curve traces were captured on the oscilloscope shown above. The resulting curves representing the potential difference across the resistor between the two middle alligator clips and the current across the resistor running through the two outside alligator clips were analyzed for their average value, which was then used to calculate the measured value of the resistor. If the measured four point technique calibration value of the resistor was calculated to be within approximately 10% of the actual value of the calibration resistor, 10 k $\Omega$ , the set-up was deemed acceptable and voltage rejection calibration could be performed.

In order to determine the voltage rejection value between the voltage probes used to determine the potential difference across the testing apparatus potential electrodes, one of the voltage probes was removed from its alligator clip and attached to the same alligator clip as the other voltage probe. A 1000 V pulse was again applied to the system and the resulting curve traces were captured on the oscilloscope. If the potential difference measured across the same point on the calibration resistor was less than approximately 10 V, the set-up was deemed acceptable and specimen testing could begin. Additionally, the scale used to measure sample

mass during testing was checked for accuracy and re-calibrated, if necessary, prior to each discrete testing session.

After recording the day's data correction values, the calibration resistor was removed from the testing set-up and the testing apparatus was reassembled. Specimens to be tested during each testing session, following the order prescribed by the testing record sheet, were weighed and measured dimensionally for length, average width, and average thickness before they were placed in the testing apparatus. Each specimen tested was tested only once throughout its lifetime, due to the fact that the impacts of this kind of electrical impulse on specimens' material and electrical properties was not well understood at the time of testing. For the purposes of this investigation, it was assumed that each specimen tested was considered damaged or unusable after being electrified.

The testing output data shown on the oscilloscope for each specimen was recorded on a digital copy of the testing record sheet. Using the Excel document prepared to electronically record data, including sample dimensions, mass, and electrical input and output values, ensured that data could be easily recorded, stored, preliminarily analyzed, and saved for later data analysis and manipulation.

Additionally, detailed records were made in a testing notebook during each experimental testing period regarding testing operations, samples tested, results of oscilloscope measurements, and any significant testing occurrences (mistakes, delays, stoppage, anomalies, etc.) that could affect results. Any curve traces presented on the oscilloscope that were deemed interesting or different in any way from the expected curve traces were captured for later analysis.

Following the recording of the oscilloscope output data, sample resistivity was calculated directly within the Excel testing record sheet using a calculation equation in one of the sheet columns. The volume resistivity for each specimen tested was calculated using Equation 2 shown below,

$$R = \frac{Vwdk}{Il} \quad (2)$$

where  $R$  is the sample volume resistivity [ $\Omega\text{-m}$ ],  $V$  is the potential difference across potential electrodes [ $V$ ],  $I$  is the current through the current electrodes [ $A$ ],  $w$  equals the width of a test specimen [in or mm],  $d$  equals the thickness of a test specimen [in or mm],  $l$  equals the fixed distance between the testing apparatus potential electrodes [in or mm], and  $k$  is a correction factor dependent on the units in which  $w$ ,  $d$ , and  $l$  are measured;  $k$  is 0.001 if measured in millimeters and 0.0254 if measured in inches.

After all raw data was recorded and visually inspected, it was apparent that there were several outliers in the data sets. Instead of eliminating these outliers, which would have either left some samples with only one data point at certain voltage values, or eliminated a few of the samples flats tested completely, it was decided that these outliers would be identified using some criteria and selected for retest, instead of being thrown out, in order to preserve the size of the data set taken.

Following a 10% trimmed mean approach, the rounded, top and bottom 5% of calculated resistivity values of the specimens from the raw data collected for each group of additives were identified for retest in random order. This “trimmed mean looks to reduce the effects of outliers on the calculated average,” and is a method that “is best suited for data with large, erratic deviations or extremely skewed distributions” [45]. The number of specimens to be retested totaled 24, including 10 tungsten specimen, 10 copper specimen, two carbon black specimen, and two non-additive specimen. Specimens were re-weighed and new testing masses, along with new electrical output values were recorded; outlier specimens were not re-dimensioned.

Following the completion of data collection and the outlier evaluation, all specimens were weighed and their final “end of testing” mass was recorded on the testing record sheet. After all of the tested specimens had been weighed, they were left in their flat molds, sealed in a new, relabeled plastic bag, and placed inside of the desiccator, which was then filled with new desiccants, a new humidity indicator strip, and sealed with grease in order to preserve samples for later use. All testing hardware and equipment required for the testing set-up described above was broken down and put away, as specified by lab personnel.

*Procedures for Data Calibration Correction*

The subsection above, Procedures for Calibration and Data Collection, reviewed the procedures for taking five calibration data points: a Fluke DMM reading of the calibration resistor and the current measurement resistor, and the oscilloscope readings for mean voltage across the potential electrodes, mean voltage across the current measurement resistor, and for voltage rejection based on a 1000 V pulse. Based on the equipment used during this investigation and on the testing set-up, both DMM readings and both mean voltage readings, used to compute a measure value for the calibration resistor, were considered verification calibration readings. These readings were all completed and recorded in order to ensure that the resistor used for the testing set-up and the testing set-up including the testing apparatus were connected and functioning properly. These four readings were not applied to the raw data before or after collection.

The recorded oscilloscope readings for voltage rejection are the only calibration data points collected that were used to later alter the raw data collected during this study. Based on the testing set-up shown and described in Chapter 3, the recorded measurement of voltage across the potential electrodes was a combination of both a differential and a common mode component.

$$V_{out} = V_{DM} + V_{CM} \quad (3)$$

Had the output of the pulse generator been measured during the calibration portion of each testing session, this value would have been used to calculate the differential mode gain. Since this value was not measured, it was assumed throughout the calibration correction process that the differential mode gain,  $G_{DM}$ , was equal to a value of one. This is illustrated in the equation below, where  $V(1)$  and  $V(2)$  represent the difference between the two input terminals, the two potential electrodes.

$$V_{DM} = G_{DM}(V(1) - V(2)) = 1(V(1) - V(2)) \quad (4)$$

Since the voltage rejection values, or the voltage measured when both voltage probes were placed on the same potential electrode, were measured and recorded from oscilloscope readings, they were used to calculate the common mode gain and applied to the final bulk volume resistivity

calculation as a calibration correction. If more than one set of calibration data was taken for a discrete testing session, voltage rejection readings were either averaged if they were taken during the beginning of a testing session, or applied to only the samples that were tested after measurements were recorded if they were taken throughout the testing session.

$$V_{CM} = G_{CM} \left( \frac{V(1) - V(2)}{2} \right)$$

$$= \left( \frac{\text{Voltage Rejection Measurement}}{\text{Pulse Generator Voltage Setting}} \right) \left( \frac{\text{Pulse Generator Voltage Setting}}{2} \right) \quad (5)$$

The final equation used to calculate the calibration corrected potential electrode voltage readings is as follows:

$$V_{out} = 1(V(1) - V(2)) - G_{CM} \left( \frac{V(1) - V(2)}{2} \right)$$

$$= \text{Voltage Across Potential Electrodes Oscilloscope Reading} \quad (6)$$

$$- \left( \frac{\text{Voltage Rejection Measurement}}{\text{Pulse Generator Voltage Setting}} \right) \left( \frac{\text{Pulse Generator Voltage Setting}}{2} \right)$$

The calibration correction was performed in the same Excel spreadsheet in which all of the raw experimental data was stored and the final values for calibration corrected voltage across the potential electrodes were used to recalculate the values for electric propellant bulk volume resistivity.

M	N	O	P
Pulse Generator Voltage [V]	Voltage Rejection Correction [V]	Voltage Across Electrodes [V] = "mean [i]"	Calibration Corrected Voltage Across Potential Electrodes [V]
2200	-2.75	329	=O2+((N2/M2)*(M2/2))
600	-2.75	94.2	92.825
2200	6.8	350.1	353.5
1800	6.8	261.9	265.3

**Figure 17. Screen Capture of the Calibration Correction Portion of the Excel Testing Record Sheet.**

The equation above, for final corrected potential electrode voltage, assumes that the voltage rejection measurement, taken once during the calibration portion of each testing session across a specific pulse generator input voltage, did not vary significantly over the course of that testing session. Calibration testing procedures and the calibration correction procedure described above were set up this way in order to simplify the amount of measurements that needed to be taken for each specimen electrified during a testing session. Additionally, because the testing session was prohibited from proceeding further unless the measured voltage rejection value was less than 10

V, equivalent to a maximum change in calibration corrected measured voltage value of approximately 1.7%, the error attributed to a non-zero common mode gain is small compared to other sources of experimental error present in this investigation. Error propagation methodology for this testing set-up is discussed below.

### *Response Surface Methodology*

In order to analyze such a large amount of data in a timely and efficient manner, a statistical software package called Minitab® 17 was used, as it provided all of the necessary tools for analyzing the data collected for this investigation. The response surface equation modeled to the data collected and input into Minitab shows how changes in variables affect a response of interest; in this case the changed variables include the additive, percent loading of additive, and additive particle size, and the response of interest is the electric propellant bulk volume resistivity.

Data from the outlier and calibration corrected Excel testing record document was cut down and edited in a separate sheet tab so that it could be properly formatted and transferred into the Minitab Worksheet space, as shown in Figure 18. Only columns for additive resistivity, additive percent loading, additive particle size, and resulting propellant resistivity were needed for the Minitab analysis performed for this investigation.

	C1	C2	C3	C4
	Additive Resistivity [Ω-m]	% Loading	Particle Size [μm]	Bulk Volume Resistivity [Ω-m]
1	0.0000005600	0.050	0.000149	152.827
2	0.0000005600	0.050	0.000149	105.480
3	0.0000001690	0.023	0.000005	128.237
4	0.0000001690	0.023	0.000005	159.556
5	0.0000001690	0.023	0.000149	99.031

**Figure 18. The Minitab Worksheet Where Experimental Data Was Entered.**

In order to be properly analyzed in Minitab, additive type was replaced with the value of electrical resistivity for each additive used in this set of experiments. Additive resistivity for the non-additive samples was set equal to zero, the resistivity values for tungsten and copper were set to those values provided in Table 1 of Chapter 2, and the carbon black/graphite resistivity values was estimated to be approximately equal to  $1 \times 10^{-6} \Omega\text{-m}$ , as no resistivity data was provided or available for the material. The largest given value of particle sizes in each size order



was formatted for use in Minitab and was used in place of the range of particle sizes; “5” for the 1-5 micron additive particle sizes, “44” for the -325 mesh, and “149” for the -100 mesh. Additionally, the units of particle size were converted from micron/mesh to meters and the values for percent loading were converted to decimal place numbers in order to ensure that the resulting regression equation developed in Minitab had correctly scaled units.

Several design of experiment response surface statistical functions are provided by Minitab. For the data entered into Minitab, partially shown above in Figure 18, data was first analyzed for normality and then the corresponding response surface was analyzed; various data-specific results, including ANOVA tables and several factorial, surface, and contour plots, were used to draw conclusions regarding the results of this set of experiments.

As discussed in the Introduction section of this Chapter, the purpose of this screening-type experiment and response surface interpretation was to identify any of the electric propellant formula additive variables that could have significant effects on propellant properties or performance. The response surface design options in Minitab are capable of fitting a second-order (quadratic) prediction equation using the measured input responses. The quadratic terms included in this equation model the curvature in the response function (or at least in the response function created by the measured data), allowing for the visualization of unique extrema in the response. This method of imposing a quadratic function on the measured responses forces a revealing structure with local perturbations (the maximum, minimum, or range of values, depending on what is desired) that could be important; these features are what could possibly indicate or hint at an optimal combination of electric propellant formula additive variables, or explanatory factors.

#### Error Analysis

In any experimental investigation, it is important to understand and account for the fact that all measurements of physical quantities are subject to uncertainty. In the case of this investigation, experimental response values for bulk volume resistivity were determined indirectly, calculated using an equation composed of other measured physical and electrical quantities. Based on the description of the results above, it is clear that experimental error exists within the

response values obtained, however the quantification of all of this error is almost impossible given the most likely sources (mixing non-homogeneity, etc.). However, because the test measurement system was set up using equipment and hardware with known (or able to be estimated) associated uncertainties, the error contribution from the testing measurements themselves can be propagated through the resistivity calculation equation and analyzed to determine the impact on response results.

In order to determine the error propagation through the testing set-up, all known equipment and hardware errors/tolerances/uncertainties were gathered, or estimated, as shown in the table below, and were used as the measurement error values throughout the resistivity error propagation calculations.

**Table 4. The Error Values Used as the “Prime” Values for Testing Set-up Error Propagation.**

<b>Error Term</b>	<b>Error Value</b>
Pulse generator error	±3% of set output voltage value
Voltage probes	100:1 ± 1.75%
Differential amplifier	1:1 or 10:1 ± 1%
Current measurement resistor DMM error	100Ω, 5% = 5Ω ± 2% + 1
Specimen width, Specimen thickness	± 0.5mm based on rubber quality of specimens
Distance between potential electrodes	$l' \ll w', d'$ , Assumed negligible
Correction factor	N/A

Using the values for error gathered in Table 4 and the equation for resistivity (Equations 2 and 6), the equation for error propagated through the resistivity testing set-up detailed in Chapter 3 was determined. The first step of determining the equation for testing equipment and hardware error propagation through the resistivity measurement, assuming all variables are independent of each other and neglecting any correlations, was to write out the full error propagation equation to be used, shown in Equation 7.

$$(\partial R)^2 = \left(\frac{k}{l}\right) \left[ \frac{wd^2}{I} \partial V^2 + \frac{Vd^2}{I} \partial w^2 + \frac{Vw^2}{I} \partial d^2 + \frac{-Vwd^2}{I^2} \partial I^2 \right] \quad (7)$$

Following the definition of the equation to be used for error propagation, it was necessary to determine the equations of several terms and subsequent terms within Equation 7 in order to fully define calculations required to complete this error propagation. These equations were for the uncertainty in both the voltage and the current measurements (Equations 8 and 9, respectively), and subsequently for the uncertainty of the voltage values used to compute the final voltage measurement, which was then used to calculate the bulk volume resistivity of each specimen tested (Equation 10).

$$(\partial V)^2 = \left[ (1)^2 \partial V_{oscope}^2 + \left(\frac{1}{2}\right)^2 \partial V_{rej}^2 \right] \quad (8)$$

$$(\partial I)^2 = \left[ \left(\frac{-V_{oscope}}{R_{CM}}\right)^2 \partial R_{CM}^2 + \left(\frac{1}{R_{CM}}\right)^2 \partial V_{oscope}^2 \right] \quad (9)$$

$$\begin{aligned} (\partial V_{oscope})^2 &= (\partial V_{rej})^2 \\ &= \left[ (G_{probes} G_{diff amp})^2 \partial V_{pgen}^2 + (V_{pgen} G_{diff amp})^2 \partial G_{probes}^2 \right. \\ &\quad \left. + (V_{pgen} G_{probes})^2 \partial G_{diff amp}^2 \right] \quad (10) \end{aligned}$$

Once equations were fully defined, they were all input into separate cells of the same outlier and calibration corrected Excel testing record document discussed above and testing equipment and hardware contributed uncertainty values for each of the 189 bulk volume resistivity measurements made during this investigation were determined.

#### Summary

This chapter detailed the methodology used throughout this investigation to prepare samples and specimens for testing, to set up and calibrate the testing apparatus, hardware, and equipment, to take resistivity measurements on specimens and record resulting measurements, to test for outliers and correct raw data with calibrations measurements, to preparing responses surfaces, and finally to calculating the error, or uncertainty, values imparted on each resistivity

measurement based on the testing hardware and equipment. Each of these methods was either created specifically for this investigation and approved, such as the methods for sample and specimen preparation and testing procedures, or was followed based on previous work, on outlines provided by ASTM standards, or in the case of error analysis, widely accepted practice.

The following chapter of this document details the results of the experiments outlined above, produced by following the methodology discussed in this chapter.

## CHAPTER 4

### RESULTS

#### Introduction

Using the equipment and following the methods detailed in Chapter 3, 21 sample flats were mixed, cast, dehydrated, and prepared for testing. Detailed qualitative and quantitative resulting data for each of the 189 specimens considered for this experiment was recorded during the testing process, and the final experimental outcomes have been processed and are presented below.

#### Sample Results and Test Preparation

##### *Pre-Mixing Sample Manufacturing*

As discussed in the Manufacturing Pilot Studies and Sample Manufacturing subsections of Chapter 3, a testing sample pre-mixing plan was created and carried out over a period of approximately one month. The results of this pre-mixing plan were carefully reviewed in order to determine the best set of mixing and curing instructions for each of the 22 sample formulations required for this investigation.

The first set of samples produced during this pre-mixing plan were variations of the non-additive propellant sample formulation; the set of four samples made for this formulation were the most informative set of samples mixed during this time. Each of the four samples made, manufactured to the 70% perchlorate oxidizer solution to 30% PVA formulation, had the same ratio of ingredients and were hand mixed for approximately the same amount of time, but were mixed in the Thinky mixer for varying amounts of time. The two most noticeable differences between each of the resulting four samples were the number of voids visible within the samples (relatively easy to gauge, as there was no additive included so the samples were transparent) and the tendency of the finished samples to relax out of their 6 inch by 0.5 inch by 0.25 inch mold shape when removed from their molds. The non-additive sample that was hand mixed, but not mixed in the Thinky mixer had the most voids, bubbles, and undissolved sections of PVA visible, and was the most susceptible to relaxing out of its original mold shape. The non-additive samples mixed for a Thinky mix time equal to six minutes, had the least amount of visible voids and had

relaxed the least when compared to the other samples. The non-additive samples mixed in the Thinky mixer for one and three minutes confirmed the following trend: the more time a batch of propellant was mixed in the Thinky (and the longer it was under vacuum), the warmer the propellant got during mix time, the fewer voids, bubbles and unmixed PVA within the propellant sample, and the less likely the propellant sample was to relax.

Following the non-additive mix trials, each of the three carbon black additive samples formulations were test manufactured. The light and medium loaded carbon black additive samples were fairly easy to manufacture as long as the initial hand mix of the ingredients was done carefully so as not to lose any of the carbon black additive. Due to the difficulty experienced when mixing the amount of carbon black required for the 5% loading carbon black sample with the formulated amounts of dissolved perchlorate oxidizer and PVA, the set of samples to be manufactured to the 5.0% CB Volume Fraction formulation presented in Figure 10 was ultimately eliminated from this study.

In order to preserve materials and decrease time to complete test mixing, only the -100 mesh tungsten and copper formulations were prepared, in addition to the three carbon black samples loaded at different amounts and the test samples with no included additive. The -100 mesh samples were chosen because they contained the largest additive particle sizes, and it was assumed that if any of the additive particle sizes were to negatively affect the rheological properties of the propellant, it would be the largest particle sizes that made the propellant more difficult to mix and extrude, and that may settle or sink within the sample after being allowed to set in a mold. This was later disproved, as the formulations that included additives of smaller particle size were the most difficult to manufacture.

All of the metallic additive samples made during this mix study were easily mixed by hand and then by the Thinky, and easily cast into molds. It was observed after a few weeks' time, however, that each of the samples' susceptibility to relax out of its desired shape increased with the increased amount of metallic additive particle loading.

Following the completion of mixing all of the test samples for this pre-mixing plan, and based on the amount of relaxation observed for each of the samples, it was decided that added

dehydrating time was absolutely necessary in order for the samples to retain their required shape. Additionally, all sample formulations, with the exception of the tungsten formulation at 2.3% particle loading, were adjusted so their PVA to perchlorate oxidizer solution volume ratio matched that of the baseline formulation at 2.3% tungsten particle loading as closely as possible; these are the samples formulas presented in Figures 7 through 10. This was done to ensure that the desirable mechanical properties of the 2.3% tungsten particle loading formulation (hardness, resistance to relax, ease of mixing and extruding) were preserved across the entire sample population. One of each of the 22 samples formulation, minus the heavily loaded carbon black sample, was produced using these updated sample formulations and was finished with additional time in a dehydrator in order to test the influence of dehydration time on each of the sample's propensity to cold flow. The final sample manufacturing procedure used for this investigation was described above in the Manufacturing Pilot Studies and Sample Manufacturing subsection of Chapter 3.

In addition to improving sample manufacturing techniques, the sample size, in accordance with ASTM standards, and the sample mold shape were also updated based on the pre-mixing results. Samples made during the pre-mixing study were extruded into 3D printed molds of ASTM standard specified sample shape 6 in by 0.5 in by 0.25 in, however as the testing apparatus designed for this experiment matured, sample size was decreased dramatically, but still kept within the allowable ASTM standards, down to 2.75 in by 0.5 in by 0.125 in, in order to continue to preserve material and allow for quicker testing sample manufacturing. It was also decided that extruding and pressing syringe mixed propellant into sheets, referred to as "flats," that could then be cut down would be more time efficient in terms of manufacturing all of the required test samples, and would, again, decrease material waste.

#### *Pilot Study Results*

Following the pre-mixing plan, and prior to taking any electrical measurements, the left over material from each sample manufactured for the pre-mixing study described above was set aside and later configured for open atmosphere on/off test firing to verify that each formulation retained the on/off abilities of the baseline propellant formulation.

Using aluminum tape, insulated wire, and a wooden stir, leftover sample material was configured into small, (~10 to 30 grams of propellant) improvised coaxial electrode thrusters. Each of these test thrusters was connected to an 800 VAC power source with interrupted current using an alligator clip. The improvised thrusters were then fired continuously and pulsed on and off until the insulated wire and propellant around it had burned back to the top strip of aluminum tape. All of the samples produced during the mix trial were able to lend leftover material to this pilot study, and all of the improvised thrusters tested were able to be fired continuously and pulsed on and off several times. Noted during sample mixing and pilot study testing, was that samples with alternate formulations, when compared to the baseline electric propellant formulation, did not show any indication of properties or behavior different from that of the baseline formulation other than in variations in sample texture due to the amount of solids loading in each formulation.



**Figure 19. An Improvised Coaxial Electrode Thruster Shown After Being Pulsed Several Times.**

Unfortunately, and as mentioned previously, no pressurized testing set-up was available during this investigation, so improvised sample thrusters could not be tested under varied pressurized conditions. Again, this may be desired as a follow up experiment, as the determination of such may provide vital clues to the propellant burning and control mechanisms. It is possible that not all formulations being studied retain their ability to extinguish over a range of pressures, as detailed in the patent invented by Villarreal and Loehr containing the baseline formulation, and discussed in Chapter 1.



*Sample Manufacturing and Preparation*

The flats of propellant tested for this investigation were manufactured over a period of three days, spread across four weeks due to availability, however, care was taken to ensure that manufacturing across all samples was consistent and unbiased. The finished, unprepared sample flats are all shown below in Figures 20-26.



**Figure 20. (Left) The Unprepared Non-Additive In-Mold Sample Flat. (Middle) The Unprepared 1.5% Loaded Carbon Black In-Mold Sample Flat. (Right) The Unprepared 2.3% Loaded Carbon Black In-Mold Sample Flat.**

The unprepared non-additive flat, shown Left in Figure 20, is the most telling regarding the amount of variation within the flats, given the random, patchy concentrations of perchlorate oxidizer (pink areas) and PVA binder (clear areas). Additionally, the varying sizes of voids and bubbles are visually unobstructed in this sample, when compared to those samples with an additive included. Both of the carbon black samples, Middle and Right, are perhaps the best two mixed samples of all 21 prepared samples. However, upon further inspection, both samples did contain several unmixed lumps of PVA. All three of the samples picture in Figure 20 were the lightest in weight out of the 21 samples manufactured for this study due to either their lack of an additive, or due to the fact that their additive was the lightest additive by weight used in this investigation.



Figure 21. The Unprepared 1.5% Loaded Tungsten (Left) 1-5 Micron, (Middle) -325 Mesh, and (Right) -100 Mesh In-Mold Sample Flats.

The three 1.5% loading tungsten samples all turned out fairly well, with the Left 1-5 micron tungsten sample turning out to be the best mixed of the three, most likely due to the smaller particle size. The Right -100 mesh sample was, however, one of the least well mixed samples due to the amount of variation in the concentration of the tungsten additive across the sample.

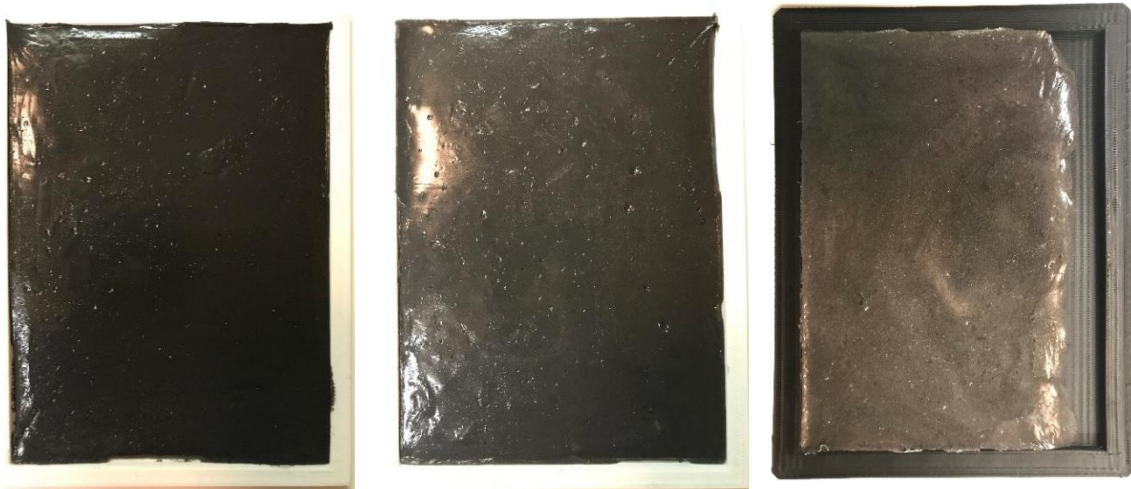


Figure 22. The Unprepared 2.3% Loaded Tungsten (Left) 1-5 Micron, (Middle) -325 Mesh, and (Right) -100 Mesh In-Mold Sample Flats.

Figure 22 shows the three 2.3% tungsten loading samples; these are the three samples most closely resembling the baseline electric propellant formulation. The Left 1-5 micron sample is probably one of the most well mixed samples, next to the two carbon black samples and the

extreme amount of variation in tungsten concentration within the -100 mesh sample, shown Right, is comparable to that of the 1.5% -100 mesh sample shown in Figure 21.



**Figure 23. The Unprepared 5% Loaded Tungsten (Left) 1-5 Micron, (Middle) -325 Mesh, and (Right) -100 Mesh In-Mold Sample Flats.**

Due to the large percentage, by mass, of tungsten particles required to make the 5% loaded tungsten sample formulations, none of the three sample flats manufactured to the 5% tungsten loading formulations were able to entirely fill a flat mold, however at least 9 specimen were obtained from each flat when cut, so samples were deemed acceptable. Apparent in the texture of the 1-5 micron tungsten flat, pictured Left, are some of the unmixed PVA lumps described throughout this document when discussing the non-homogeneity/non-uniformity of these sample mixtures (see left half of sample flat).



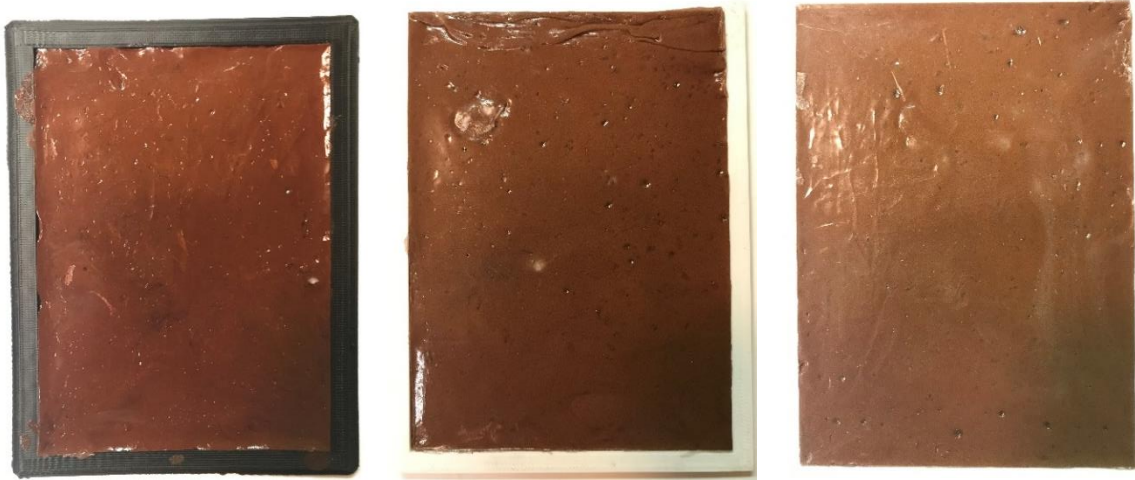


**Figure 24. The Unprepared 1.5% Loaded Copper (Left) 1-5 Micron, (Middle) -325 Mesh, and (Right) -100 Mesh In-Mold Sample Flats.**

The 1.5% copper samples manufactured using the -325 and the -100 mesh copper particles were both some of the more poorly mixed samples out of the 21 prepared for this investigation due to the amount of unmixed PVA in both samples. These PVA lumps are very visible in the Middle -325 mesh sample (see upper left corner of sample flat) and were made even more apparent when both propellant sample flats were held up to the light for further inspection. The 1-5 micron sample, again most likely due to the particle size, was not deemed to be as poor of a mixture as the other two copper particle flats in its loading percentage category.



**Figure 25. The Unprepared 2.3% Loaded Copper (Left) 1-5 Micron, (Middle) -325 Mesh, and (Right) -100 Mesh In-Mold Sample Flats.**

All three of the 2.3% copper loading flats were mixed fairly well, and are the most comparable in formulation to the baseline tungsten propellant formulation. Variation in the concentration of the 1-5 micron copper additive is apparent in the 5% loading copper sample shown Left in Figure 26. Also apparent in the texture of the -100 mesh 5% loading copper sample is the amount of unmixed PVA (see bottom half of sample flat).



**Figure 26. The Unprepared 5% Loaded Copper (Left) 1-5 Micron, (Middle) -325 Mesh, and (Right) -100 Mesh In-Mold Sample Flats.**

Following their removal from the dehydrator, each sample flat was placed in a labeled plastic bag and all sample flats were relocated to the lab space used for testing samples for storage inside of a laboratory desiccator near the testing set-up. Prior to entry into the desiccator, each sample flat was examined for its post-cure batch inspection and any observations made were recorded on the corresponding batch sheets used to document sample heritage.

Variations in the homogeneity of each of the 21 sample flat images provided in Figures 20 through 26 are visually obvious, and indicate a short coming in the version of the electric propellant mixing procedures followed to manufacture each flat. By visual inspection only, it appears that the non-additive sample flat is the most nonhomogeneous mixture of all of the flats prepared, followed by the 1.5% and 2.3% loading flats made with the -100 mesh tungsten and the 1.5% loading -325 and -100 mesh copper flats. These variations in mixture homogeneity, discussed in detail below, have definitely impacted the variation in sample resistivity results across each flat. However, the degree of variability due to poor mixing is currently unknown and

should be a subject that is revisited after the electric propellant mixing process has been improved. The quality of mixing of each of the samples and across the entire specimen population tested for this investigation could be further investigated using a coded “quality of mix” scale, which could then be taken into account during statistical analysis in order to account for a portion of the variation within the results further discussed below. This coded mix scale analysis is further described in the Recommendations section of Chapter 5.

Following their post-cure batch inspection, sample flats were cut, using a scoring blade and scissors, into between 9 and 14 specimen depending on the amount of propellant that filled each flat. (Some sample flats were not entirely filled due lack of volume based on the sample’s high additive loading and of that additive’s high density.) Once a sample flat had been cut into the allowable number of correctly sized specimens, specimens to be tested were randomly chosen, removed from the flat mold, and the specimen’s testing number was written on the part of the mold showing in the void with a paint pen. This was done to prevent the need to mark directly on the samples and to prevent the need for storing samples individually, which could have allowed them to relax as they would have been out of their original molds for several weeks during testing. Figure 27 shows an example of a sample flat of prepared specimens.



**Figure 27. A Prepared Sample Flat and Storage Bag, with a Randomly Chosen Specimen Removed from Flat Mold to Display the Specimen Labeling Technique.**

With testing numbers assigned to each specimen to be electrified, specimen serial numbers could be finalized. Following the finalization of specimen identification and prior to entry into the

lab desiccator, the pre-desiccator mass of each of the 189 specimen to be tested for this set of experiments could be established and recorded to be used later for comparison with the pre-testing mass to ensure that specimens were not losing any considerable amount of mass in the desiccator over a long period of time and for later possible density assessment, if required. As discussed in Chapter 3, since the effects of water absorption on electric propellant resistivity are still unknown, any absorption or loss of water within the samples could have affected experimental resistivity measurements and made the researched hypothesis developed for this experimental investigation difficult to prove or disprove. All prepared sample flats were left sealed in the laboratory desiccator for a period of approximately four weeks prior to the start of testing.

#### Pre-Response Surface Results and Analysis

##### *Data Collection and Initial Raw Data Visualization*

Data collection was broken up into discrete testing sessions conducted over a period of several weeks, due to the large number of specimens to be tested, but was kept as consistent as possible in order to maintain the integrity of the experiments. Data collection was carried out following the methodology discussed in Chapter 3.

Voltage values of 600 V, 1800 V, and 2200 V were chosen for the low, mid-level, and high pulse generator input voltage values, and the 10 k $\Omega$  calibration resistor was measured at each of the voltage input values chosen in its calibration configuration to verify that the wide spread of input voltage values did not affect the accuracy of the testing set-up. These three voltage values were chosen for this set of experiments for several reasons including the larger size of the tested specimens compared to any previous testing specimen size and the fact that, in practice, higher voltage values would most likely be used to drive the operation of this material. This experiment could be repeated using lower voltage values, as this material should be understood across the full spectrum of operating values, however the higher values chosen above aligned more closely with research interests at the time during which testing was carried out.

Following the completion of data collection across all 189 prepared specimens, all of the raw Excel testing data was plotted for visualization and determination of general trends in the data

prior to the application of calibration corrections, to determine if outlier re-testing was required, and in order to preliminary predict response surface results.

The raw testing data collected from the non-additive set of nine specimen was the first set of data plotted visually in Excel, as it was believed that this would be the data most equivalent to a “control” to compare all of the additive results with despite the extreme variation in sample homogeneity.

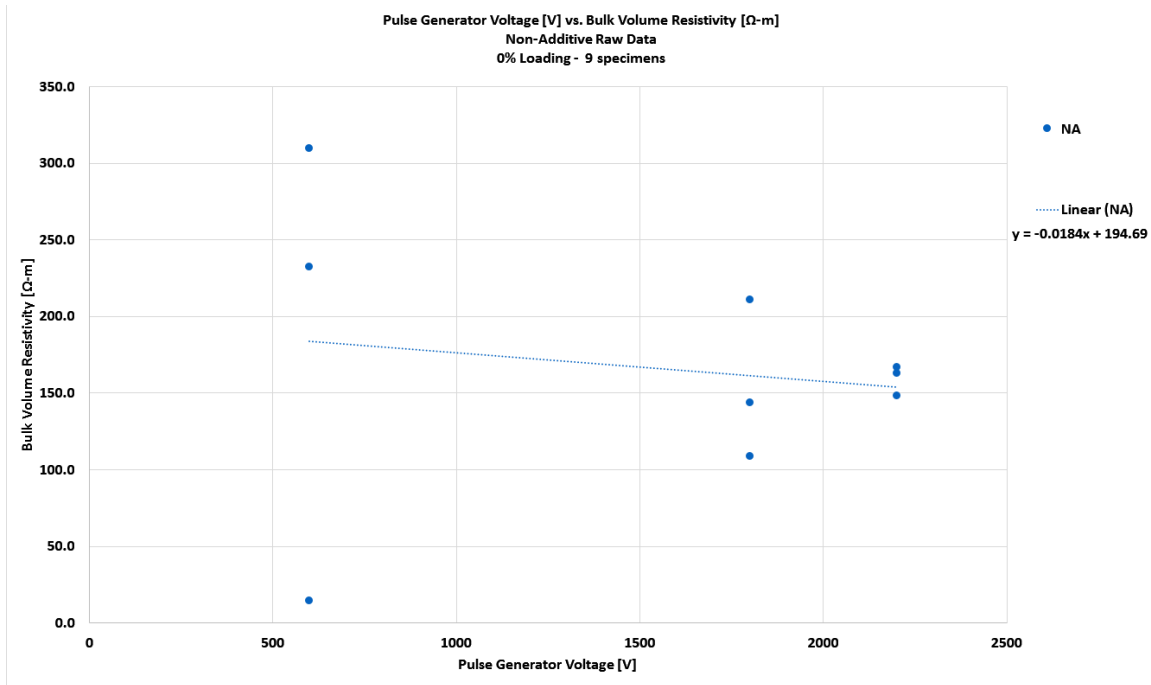


**Figure 28. Values for Bulk Volume Resistivity of the Non-Additive Specimens Plotted as a Function of Pulse Generator Input Voltage.**

Linear fits were chosen for each of the initial raw data visualizations shown only in order to obtain a general idea of the behavior of the results. Quadratic and/or exponential fits could have also been utilized, given the fact that three sets of data points are available; however it is unlikely at this point in the investigation that anything more specific or precise than a linear fit would be useful at this time, given the amount of data and related variation available.

As directed, a linear fit was applied to the nine non-additive specimen data points plotted above, in order to determine if there was a significant relationship between measured specimen bulk volume resistivity and pulse generator input voltage. The y-intercept of this linear fit, or the estimated value of the bulk volume resistivity of this electric propellant formulation at a 0 V pulse



generator input voltage value, was approximated by Excel to be equal to 194.69  $\Omega$ -m; the slope of the line generated by excel was given as -0.0184, indicating that as input voltage value increases, resistivity is expected to decrease only slightly. However, the value of the slope of this line is so close to zero that it should not be considered statistically significant, and it can be said that, given the current amount of data, the resistivity of this non-additive electric propellant sample does not seem to be related to or significantly affected by pulse generator input voltage values.

Notable in the plot shown in Figure 28 is the wide spread of data points across resistivity values. Given that this propellant formulation only has three ingredients, with no additive of any kind, and that the sample flat was not well mixed (see Figure 20), the variation in this data could most likely be explained by the variability in mixture homogeneity. Although it is less likely, and the determination of which is out of the scope of this investigation, interactions and percolation between the perchlorate oxidizer and the PVA could have also contributed to this variation, and would affect all of the other samples examined during this investigation regardless of their additive. However, more data would be and is required to officially determine these relationships, and to possibly help with the identification of the variation in measured resistivity.

In Figure 29, the results of the eighteen different carbon black specimens were plotted on the same axes as the non-additive specimens shown above and grouped by their additive particle loading percentage values. The y-intercept of the line fitted to the carbon black specimens loaded at 1.5% is approximated at 42.345  $\Omega$ -m, with a slope of 0.0083, and the y-intercept of the line fitted to the specimens loaded at 2.3% is approximately 53.81  $\Omega$ -m, with a slope of 0.0043. Interestingly, the y-intercept values of the carbon black samples were significantly lower than the non-additive sample y-intercept value, and as the particle loading percentage of the carbon black samples increases, so does the y-intercept value of each linear fit. Similar to the slope of the non-additive sample data linear fit, the slopes of both of the carbon black fitted lines are close enough to zero that the interaction between resistivity and input voltage can be considered statistically insignificant, given the data collected. Again, more data should be gathered across varying

loading percentages and across an increased number of pulse generator input voltage values, and is required to conclusively determine these relationships.

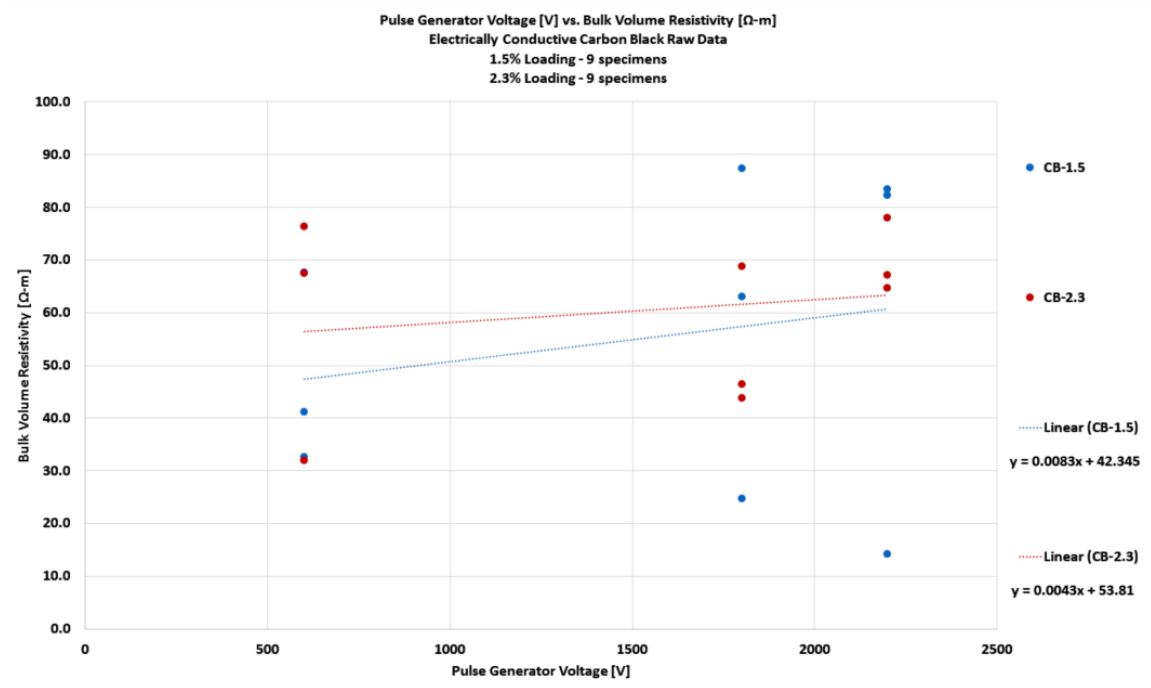


**Figure 29. Values for Bulk Volume Resistivity of the Carbon Black Specimens Plotted in Groups of Percent Additive Loading as a Function of Pulse Generator Input Voltage.**

Variation in the measurements of resistivity across this plot are also noticeable, however, as shown by the lines representing the linear fit of each loading group, the Excel fits do indicate that all of the data points measured for the 2.3% loaded samples do appear to be, on average, slightly higher in resistivity values, given that the plotted (red) line for the 2.3% sample group is higher than the linear fit (blue) line for the 1.5% sample group.

Additionally, the variation shown in Figure 29 across all eighteen of the carbon black specimens spans from approximately 30 to 80 Ω-m compared to the approximately 15 to 310 Ω-m spread of the non-additive specimen data. This reduction in the overall spread of resistivity values measured for the carbon black specimens could indicate either that the carbon black sample flats were much more well mixed than the non-additive flat, that the addition of carbon black somehow aided in the tightening of variation across measured samples, or some combination of both. Additional visualization of measured specimen resistivity results over particle loading percentage could indicate some evidence of whether or not the added carbon black is

showing the effects of percolation, however, with data at only two loading percentages available, the evidence would need to be backed up later with more specimens tested at different loading percentages.

Figure 30 details the resistivity results of all of the tungsten specimens, grouped by additive loading percentage, but not by additive particle size. The twenty-seven specimens manufactured with a 1.5% loading of tungsten particles, when given a (blue) linear fit, show a y-intercept value of approximately 102.96  $\Omega$ -m and a slope of 0.0037, compared to the 2.3% loading y-intercept of 126.93  $\Omega$ -m and a slope of 0.0031 (red fit), and to the 5% loading y-intercept of 173.59  $\Omega$ -m and a slope of 0.0157 (green fit). These linear fits, along with the lines plotted for the particle loading percentage fits, indicate that as the tungsten particle loading in samples increases, so does the propellant samples' average value of bulk volume resistivity.

The slopes of all three linear fit lines, all relatively close to zero, indicate, similar to the carbon black specimens above, that there does not seem to be a relationship between pulse generator input voltage and measured sample bulk volume resistivity. Additionally, given how flat and close together the 1.5% and 2.3% loading linear fit lines are, the statistical difference between the two sets of data is questionable, which may mean that percolation may have more of an effect on the variation across the measured resistivity of all of the tungsten specimens when compared to the carbon black specimens. However, no data exists for the carbon black sample at 5% loading, so this is only speculation and more data is needed to confirm.

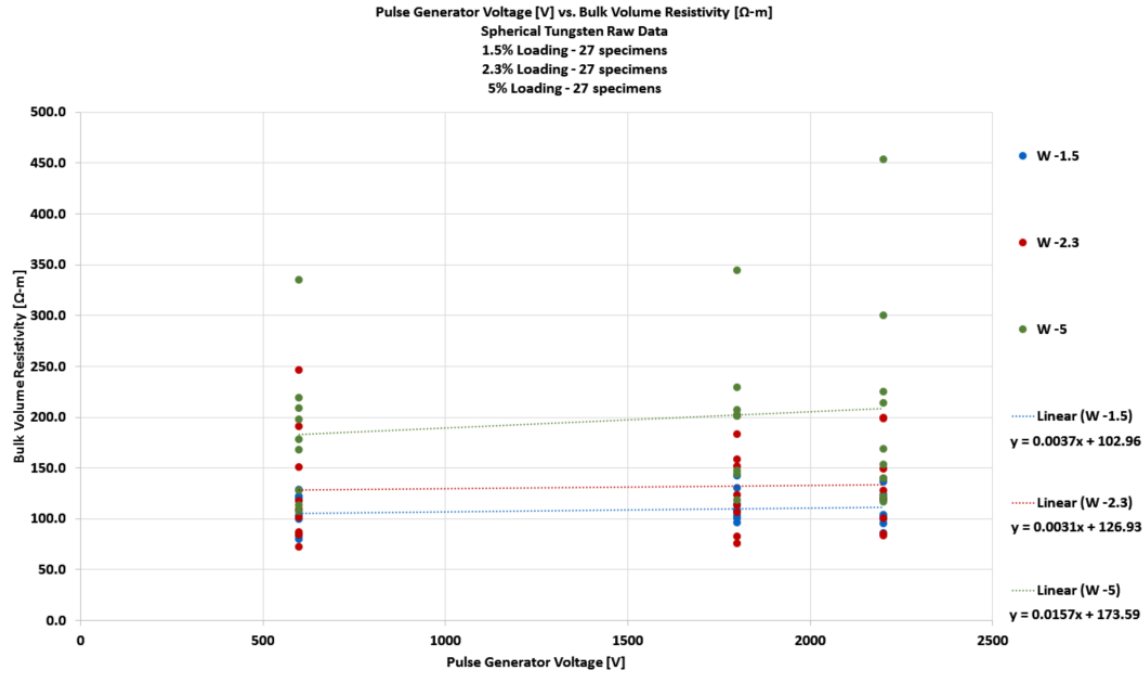


**Figure 30. Values for Bulk Volume Resistivity of the Tungsten Specimens Plotted in Groups of Percent Additive Loading as a Function of Pulse Generator Input Voltage.**

Given that the 5% particle loading linear fit line is further above the 2.3% loading line, the estimation of a percolation threshold of approximately 3.4%, discussed in Chapter 2, could hold valid for electric propellant samples with a tungsten additive. However, the approximately 75-350 Ω-m spread of measured resistivity values is indicative of the largest variation across one of the additive data sets studied during this investigation. Since the spread of variation is so large, additional data or new data measured from specimens manufactured with better mixing quality could help to later pinpoint the true source of variation in results.

Results of the measured resistivity of the copper specimens are shown in Figure 31. The twenty-seven specimens manufactured with a 1.5% loading of copper additive particles, when given a (blue) linear fit, show a y-intercept value of approximately 126.27 Ω-m and a slope of -0.0024, compared to the 2.3% loading group's (red linear fit) y-intercept of 123.16 Ω-m and slope of -0.0063, and to the 5% loading group's (green linear fit) y-intercept of 163.81 Ω-m and slope of 0.0047. Given that the 1.5% and 2.3% loading linear fit lines are closer than the same fit lines produced for the tungsten results at the same particle loading percentages, percolation theory could also hold true for the copper additive as well. Even though the y-intercept and linear fit line

for the 1.5% loading data are higher than the 2.3% results for both, the debatable statistical difference between the two lines given the slopes is an indication that the switch in the fit line order compared to the tungsten results could be insignificant. However, a similar amount of variation in the data exists when compared to that of the tungsten data, which could explain why the 1.5% and 2.3% fit lines are not the same, brings into questions the validity of percolation theory given the mixture quality of each flat.

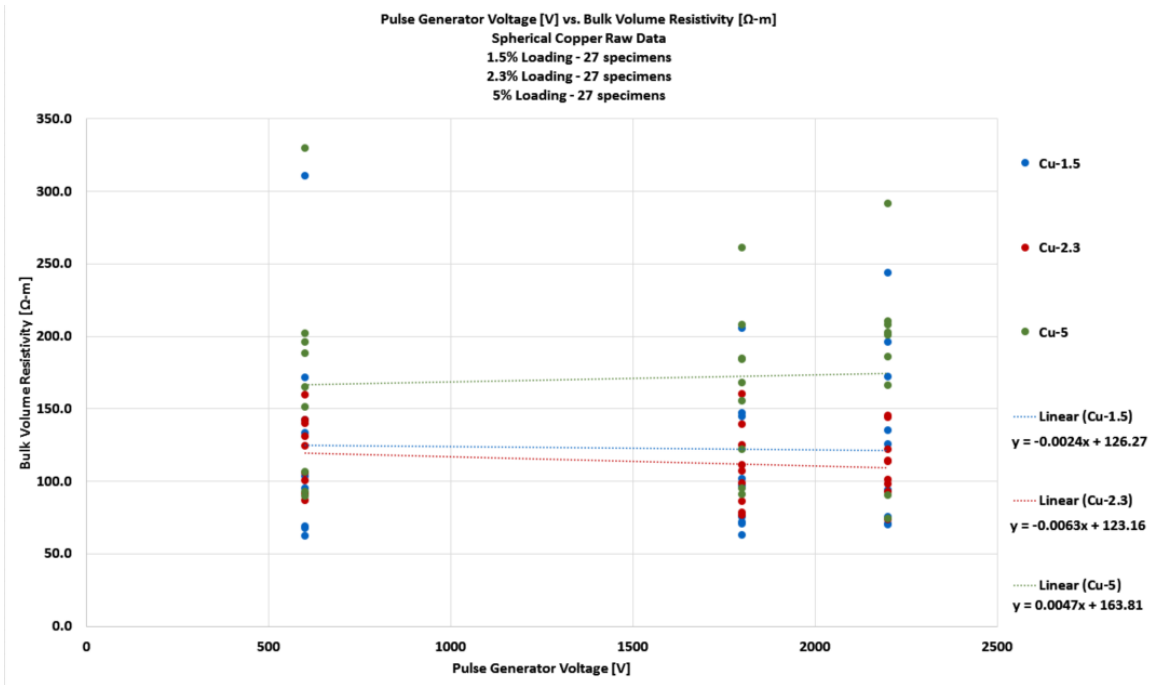


**Figure 31. Values for Bulk Volume Resistivity of the Copper Specimens Plotted in Groups of Percent Additive Loading as a Function of Pulse Generator Input Voltage.**

Trends noticeable across all sets of samples, regardless of additive, include the lack of a relationship between resistivity and pulse generator input voltage value, as indicated by slopes approximately equal to zero on a plot of pulse generator input voltage value versus bulk volume resistivity, bulk volume resistivity values between ~40-400 Ω-m, and a large amount of variation across each plotted data set with noticeable outliers in each additive group of specimens. Given the amount of variation across the resulting resistivity data and the data outliers made obvious with data visualization, it was decided that a certain set of specimens would be re-measured for electrical resistivity based on the outlier identification criteria used for a trimmed mean approach, specified in Chapter 3.

*Outlier Identification, Re-Testing, and Visualization*

The outliers for each additive data set were chosen for retest by sorting the resistivity values for each data set from low to high so the top 5% and bottom 5% of measured specimen resistivity values could be identified; equivalent to a total of 10% of the results for each additive data set to be identified for retest. Specimens were chosen for retest rather than elimination due to the limited size of each data set collected and to the amount of data required for the response surface results detailed below. The total number of specimens to be re-tested, 24 in all, included the following: two non-additive specimens, two carbon black specimens, 10 tungsten specimens, and 10 copper specimens.

During the outlier retesting process, each of the outlier specimens retested were photographed outside of their flat with all of the other specimens identified for retesting, if any, in the same flat removed. This was done in order to inform any later analysis and discussion surrounding the mix quality of each the flats and to contribute information to the discussion of current overall electric propellant mixing procedure effectiveness and/or avenues of possible improvements.



**Figure 32. Two Prepared Sample Flats, Both with at Least Four Specimens Identified as Outliers.**

Interestingly, only two out of the 24 specimen identified as outliers for retest were unique to their sample flat. This suggests that, at least in the flats with more than one specimen identified for retest, there is a good chance that the variation in mixing observed previously in all of the flats,

but notable in those that contained outliers, is a significant contributor to variation in electrical resistivity values. However, where there were groups of outlier specimens identified close together in position within their sample flat, the measured resistivity values of each of the specimens was approximately the same. So while the specimens identified for retest may have been outliers within the additive groups as a whole, within their flats, and compared to each other, resistivity values were consistent. This also indicates that the testing set-up and procedures, when followed appropriately and consistently across each testing session, are able to produce consistent results. The table below details the measured values of volume resistivity for each outlier before and after retesting.

**Table 5. All 24 Raw, Outlier Specimen Bulk Volume Resistivity Values Before and After Retesting.**

<b>Specimen Serial Number</b>	<b>Original Resistivity Value [<math>\Omega</math>-m]</b>	<b>Re-measured Resistivity Value [<math>\Omega</math>-m]</b>	<b>Percent Difference [%]</b>
NA-1	14.5	173.1	1093.8
NA-3	309.5	222.8	28.0
CB-1.5-5	87.2	73.9	15.3
CB-1.5-9	14.1	13.8	2.1
W-1.5-1-5-1	79.5	78.6	1.1
W-1.5-1-5-3	83.4	64.9	22.1
W-2.3-1-5-2	72.5	44.4	38.8
W-2.3-1-5-4	75.9	66.8	11.9
W-2.3-1-5-5	82.4	63.3	23.8
W-2.3-325-5	246.6	170.4	30.9
W-5-1-5-1	334.5	241.4	27.8
W-5-1-5-5	344.5	174.3	49.4
W-5-1-5-8	299.8	170.0	43.3
W-5-1-5-9	453.1	221.4	51.1
Cu-1.5-1-5-1	67.8	40.4	40.4
Cu-1.5-1-5-2	61.9	56.4	8.9

Specimen Serial Number	Original Resistivity Value [ $\Omega$ -m]	Re-measured Resistivity Value [ $\Omega$ -m]	Percent Difference [%]
Cu-1.5-1-5-3	68.4	46.5	32.0
Cu-1.5-1-5-4	62.9	56.5	10.2
Cu-1.5-1-5-8	69.9	74.7	6.9
Cu-1.5-100-1	310.7	227.5	26.8
Cu-1.5-100-8	243.4	119.8	50.8
Cu-5-1-5-6	261.0	186.6	28.5
Cu-5-1-5-8	291.2	285.3	2.0
Cu-5-325-3	329.9	220.2	33.3

In the table shown above, only five of the outlier specimens retested for resistivity (CB-1.5-9, W-1.5-1-5-1, Cu-1.5-1-5-2, Cu-1.5-1-5-8, and Cu-5-1-5-8) remained within 10% of their original resistivity measurement, and three of the specimens' measured values (NA-1, W-5-1-5-9, and Cu-1.5-100-8) changed by at least 50% or more. The reason for such a variation in the original versus the outlier retest resistivity measurement is unknown, as all of the outlier's chosen for retest were originally measured across seven testing sessions and in random order with the rest of the 165 specimens tested. Variation could be explained by further examining the specimens to see if large concentrations of one ingredient made up more of certain specimens than others within their flat; which would make sense given that most of the outliers were from the same flats and were located close together within those flats. These outlier specimen measurements and a detailed explanation of possible causes are further discussed in the Interpretation of the Findings section of Chapter 5. After outlier testing was complete, re-measured values were substituted in place of the raw data for original outlier results and the specimen resistivity results were again plotted on axes of pulse generator input voltage versus bulk volume resistivity values to visually compare the differences in outlier measurements.

The resistivity values of the two non-additive outliers retested, both at an input voltage value of 600 V, changed dramatically. Both values converged closer together and closer to the measured resistivity value for the third specimen measured at 600 V, lessening the variation in



resistivity of the specimens measured at the lowest test voltage. The slope of the line fitted to the data is now more negative as input voltage value increases and the y-intercept value of the line is approximately 227.41  $\Omega$ -m compared with the original y-intercept value of 194.69  $\Omega$ -m. Although these changes may seem significant, it is important to remember that this is the experimental data set with the smallest amount of data points and thus is the data set most susceptible to changes in trends given any applied data correction. More resistivity data collected for non-additive electric propellant samples would result in more stable and more reliable data.

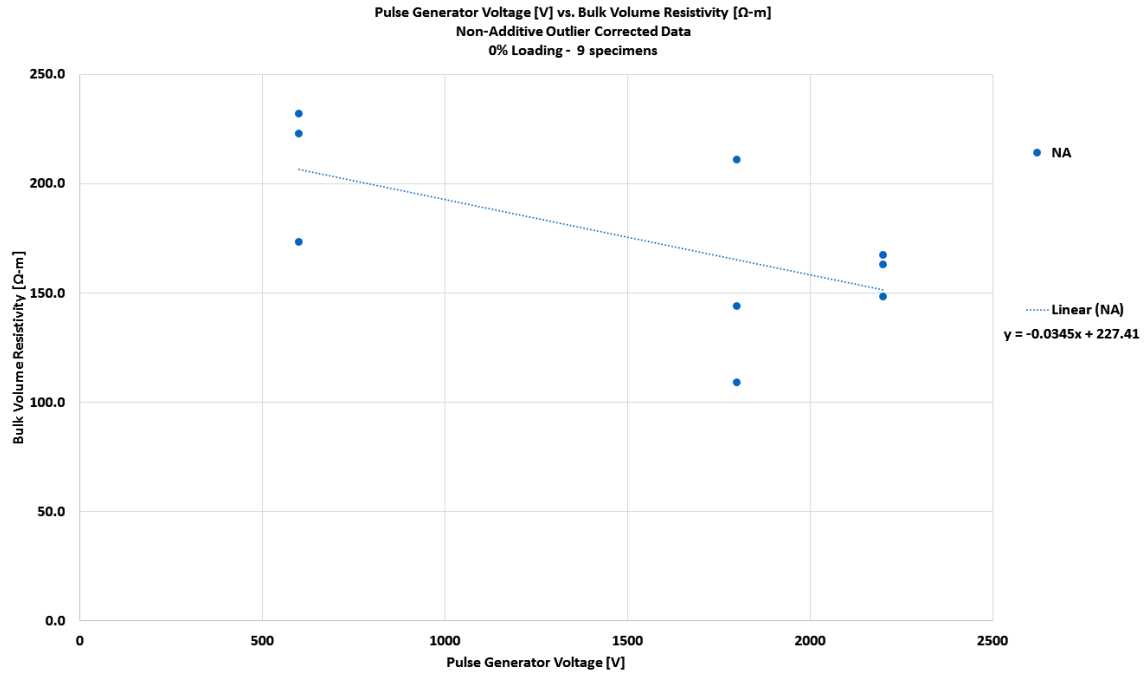


**Figure 33. Values for Bulk Volume Resistivity, Including the Two Data Points That Have Been Retested as Outliers, of the Non-Additive Specimens Plotted as a Function of Pulse Generator Input Voltage.**

The changes in resistivity values of the two carbon black specimens that were retested, both from the 1.5% loading flat, were much less dramatic than that of the non-additive specimens and did not significantly affect the y-intercept location or the slope of the 1.5% loading linear fit line. The outlier corrected data for both carbon black sample flats still has the lowest amount of variation in resistivity values compared to all of the other outlier corrected additive data sets, at a spread of approximately 50  $\Omega$ -m.

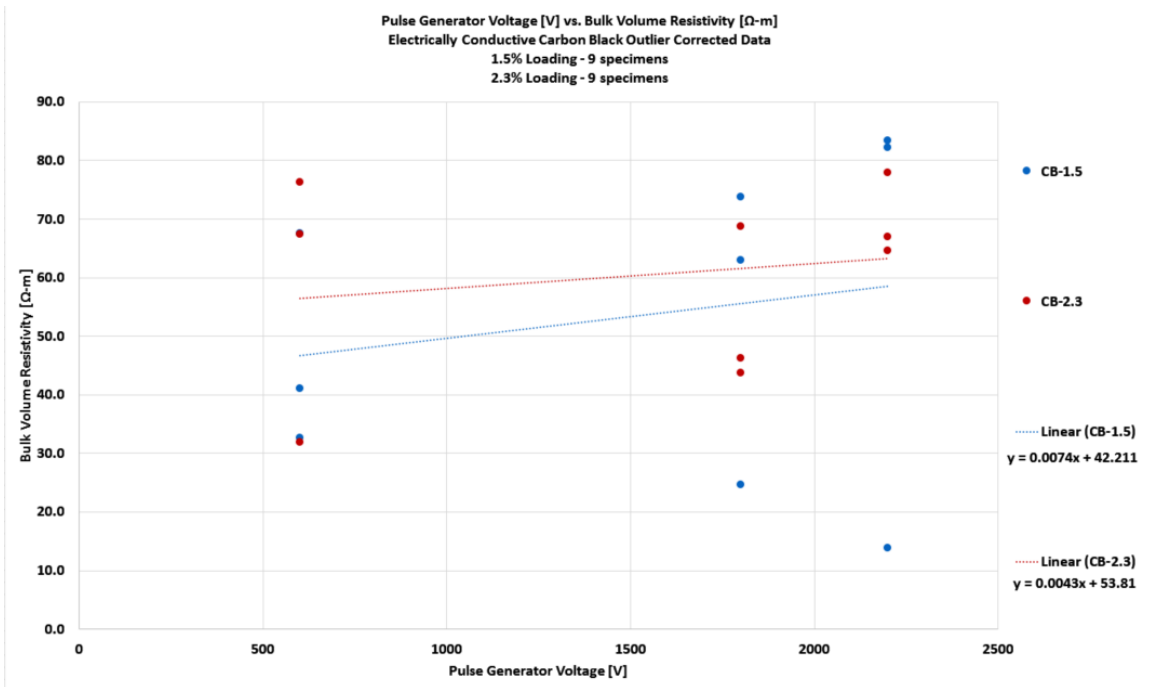


**Figure 34. Values for Bulk Volume Resistivity, Including the Two Data Points That Have Been Retested as Outliers, of the Carbon Black Specimens Plotted in Groups of Percent Additive Loading as a Function of Pulse Generator Input Voltage.**

The linear Excel fits for the carbon black data still indicate that all of the data points measured for the 2.3% loaded samples do appear to be, on average, slightly higher in resistivity values than the 1.5% loading group, given that the plotted line for the 2.3% sample group is higher than the linear fit line for the 1.5% sample group. However, whether or not the lines are statistically different, given the amount of variation across all of the measurements, is still under consideration.

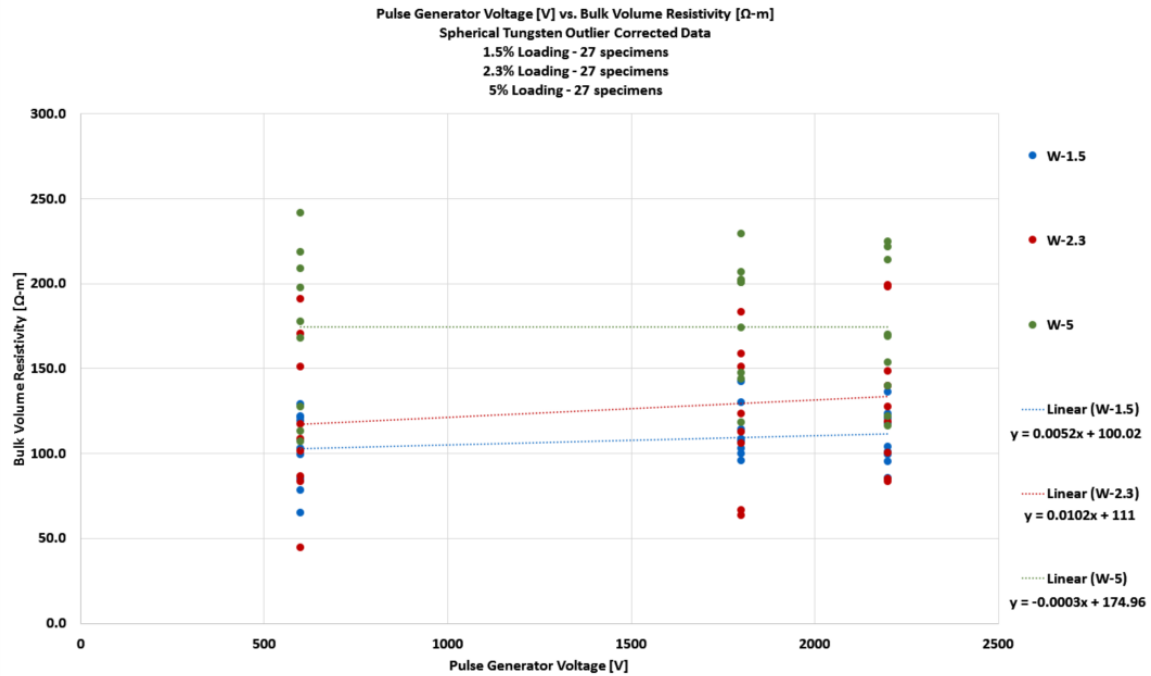


**Figure 35. Values for Bulk Volume Resistivity, Including the 10 Data Points That Have Been Retested as Outliers, of the Tungsten Specimens Plotted in Groups of Percent Additive Loading as a Function of Pulse Generator Input Voltage.**

The set of tungsten samples saw the most dramatic of the 5% loading group outliers fall back in with the rest of the data set after retesting. Given the updated spread of 5% loading sample measurements, the loading group’s linear fit slope increased positively, only slightly decreasing its y-intercept value, but compared to the linear fit equation generated for the raw 5% loading tungsten data, there was no significant change. The 1.5% loading groups’ linear fit slope positively increased and its y-intercept value decrease slightly as a result of outlier retesting, but the overall change in the linear fit equation was, again, negligible. The 2.3% loading group’s linear fit slope decreased, increasing its y-intercept slightly, and resulting in the most significant change, even though small, in the outlier-corrected tungsten linear fit equations.

The set of 1.5% copper samples contained the largest number of outliers for re-testing and saw a range of change in initial to retested bulk volume resistivity values of approximately 7 to 51%. As a result, the slope of the linear fit changed from slightly negative to slightly positive and the linear fit equation’s y-intercept increased. Overall, the change did not dramatically affect the position of the line created by the linear fit on the plot in Figure 31, and the question of statistical

significant between the 1.5% and the 2.3% loading samples sets still stands. No 2.3% loading group specimens were re-tested as outliers, so the 2.3% linear fit remains the same as shown in the raw data plots, and with the correction of three 5% outlier specimen measurements, the 5% loading linear fit positively increased in both slope and in y-intercept value.

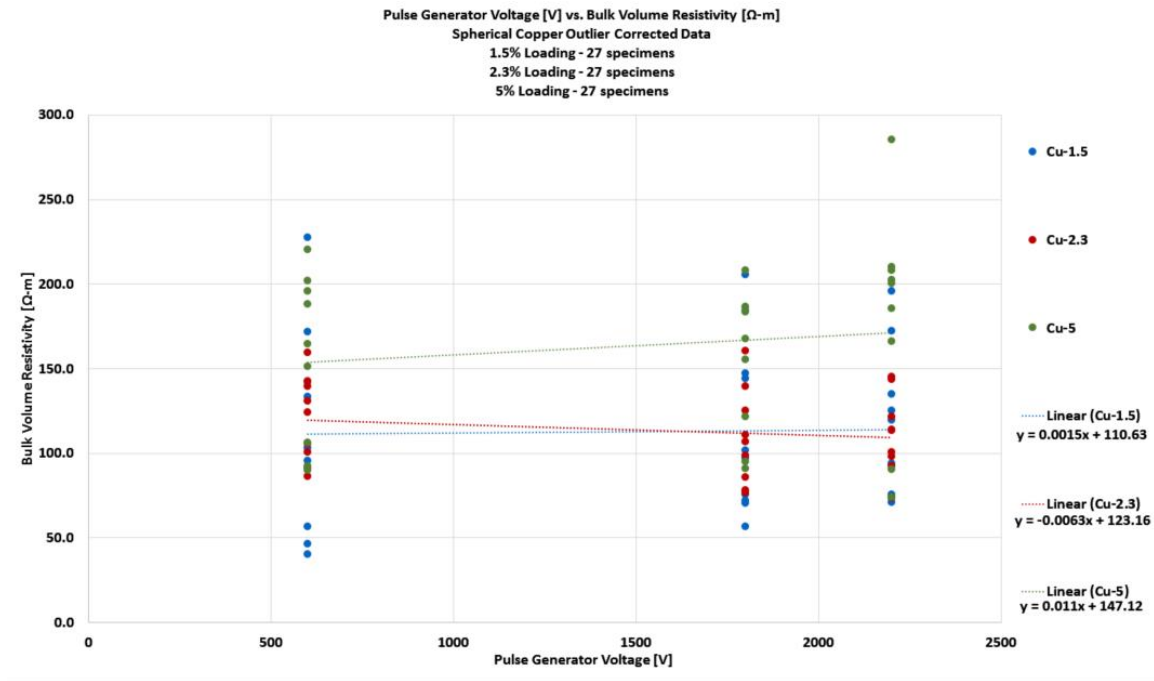


**Figure 36. Values for Bulk Volume Resistivity, Including the 10 Data Points That Have Been Retested as Outliers, of the Copper Specimens Plotted in Groups of Percent Additive Loading as a Function of Pulse Generator Input Voltage.**

Additional plots produced with raw and outlier corrected data include bulk volume resistivity versus particle loading percentage and versus particle size. These plots have not been included above, but they were done with calibration corrected data and are presented below.

#### *Additional Observations*

Following outlier retesting and prior to beginning data visualization and analysis, a column for calculated density was added to the Excel testing record sheet in order to be used for later data analysis if needed, as it was speculated throughout testing as specimen were visually inspected prior to being electrified, that even between specimen from the same sample flat, there was a wide variation of specimen dimensions and masses. A small amount of this variation could be attributed to inconsistencies in specimen size, as cutting sample flats with scissors was not a

precise specimen shaping method, but is most likely due to a combination of variation of homogeneity within the sample flat and of voids within the samples. Voids of varying sizes were observable within all of the specimens tested and throughout all of the propellant flats manufactured, but are most apparent in the non-additive sample flat, as there is no additive included to visually obscure the voids.

Combined, both of these observations (the fact that the majority of the specimen selected as outliers were from the same flats and the fact that voids within the samples were, if nothing else, at least present and creating density consistency issues) indicate the need for mixing process improvement. While care was taken to ensure that the procedures used to mix all of the sample flats used for this investigation were thoroughly followed, noticeable voids, non-homogeneously mixed flats, and unmixed PVA throughout samples implies the need for improved propellant mixing techniques.

Additionally, as outliers were re-tested, images of the resulting oscilloscope traces were taken and archived for later comparison to “normal” trace results and any additional required analysis. These traces are not provided in this document, as this analysis work is outside of the scope of this investigation, however the traces resulting from sample electrification are important; an understanding of these responses and the underlying physics driving these responses will be required for a complete understanding of the fundamental science surrounding this material and for later implementation into and operation of a system utilizing this material.

#### *Calibration Corrections and Visualization*

The testing set-up voltage rejection values, or the voltage measured when both voltage probes were placed on the same potential electrode, were measured and recorded from oscilloscope readings during the calibration portion of each discrete testing session. The values were then used to calculate the common mode gain of the circuit used to measure potential difference voltage values, which was then applied to the final bulk volume resistivity calculation as a calibration correction.

**Table 6. All of the Measured Values for Voltage Rejection Taken During Sample Testing Sessions. (Some testing session were broken up into several smaller specimen measurement sessions and have several voltage rejection values.)**

Testing Date	Voltage Rejection Value(s) [V]
January 18, 2018	-2.75 (Average of -2.6, -2.9)
January 23, 2018	6.8
January 25, 2018	1.05 (Average of 1.9, 0.2)
January 26, 2018	-20.8
January 31, 2018	5.15 (Average of 5.5, 4.8), 5.6, 6.2
February 01, 2018	-0.6, -1.5, 4.1, 5.1, 4.0
February 02, 2018	1.8, 4.5, 4.7, 5.2, 4.8, 4.1, 4.6, 4.0, 6.7
February 05, 2018	-9.0, 2.1, 4.9, 4.2, 3.8, 5.7, 5.2
February 15, 2018 (Outlier Testing)	5.1, 6.1, 4.2, 4.5

As shown above, almost all of the values recorded for voltage rejection were under the arbitrarily selected 10 V limit, with the exception of the -20.8 V reading from the January 26, 2018 testing session. Prior to this testing session, the oscilloscope's "Auto Zero" function was not being utilized during testing procedures. After this testing session, due to erroneous equipment readings, the testing instructions were altered slightly to include the "Auto Zero" function as a regular part of testing. After this inclusion, no other erroneous readings were identified. Additionally, it is not believed that these erroneous equipment readings or their cause had significantly affected the accuracy of results measured prior to the inclusion of this procedural step.

The final outlier corrected, raw data calibration correction was performed in the same Excel record sheet in which all of the raw experimental data was stored. The final values for calibration corrected voltage across the potential electrodes were calculated and then used to recalculate the final values for electric propellant bulk volume resistivity. After applying calibration corrections, all of the newly corrected data was plotted similarly to the raw and outlier corrected shown above and in further detail shown below.

The first set of plots made for each of the replacement additives are similar to those shown above of pulse generator input voltage versus the measured bulk volume resistivity response. When compared with the previous plots made with the outlier corrected data, the four plots shown below in Figures 37 through 40 show that while the final bulk volume resistivity values did change, they only changed by a small percentage and the overall trends in data have not been altered with the addition of the calibration correction.

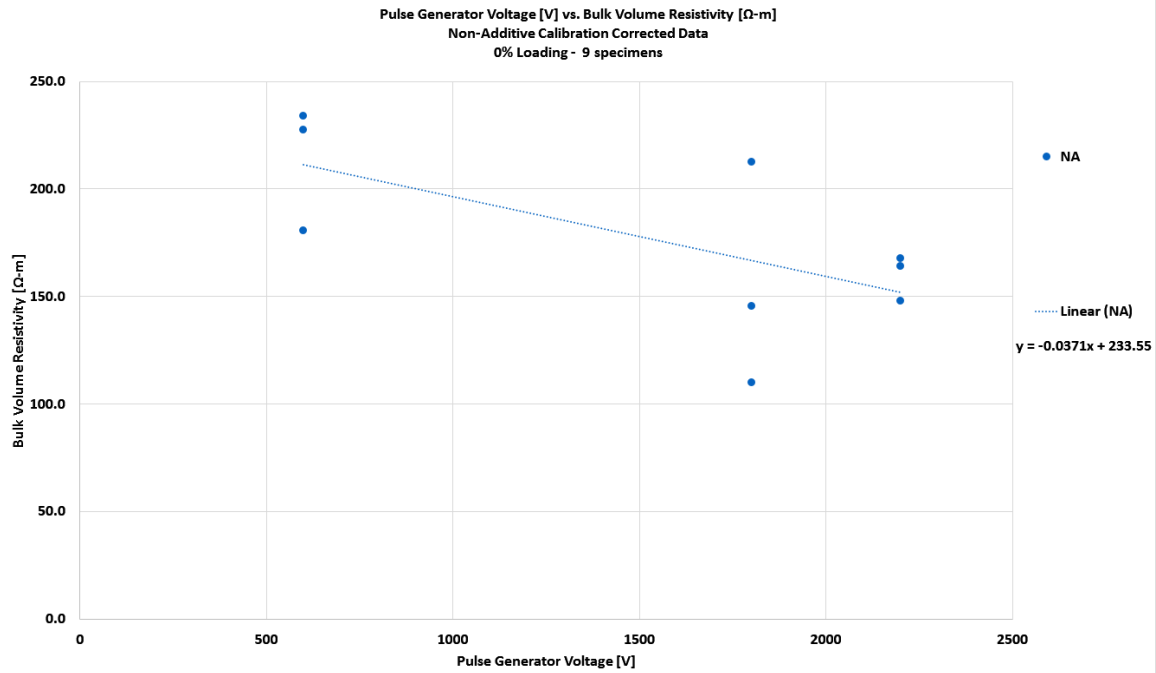


**Figure 37. Calibration Corrected Values for Bulk Volume Resistivity, Including the Two Data Points That Have Been Retested as Outliers, of the Non-Additive Specimens Plotted as a Function of Pulse Generator Input Voltage.**

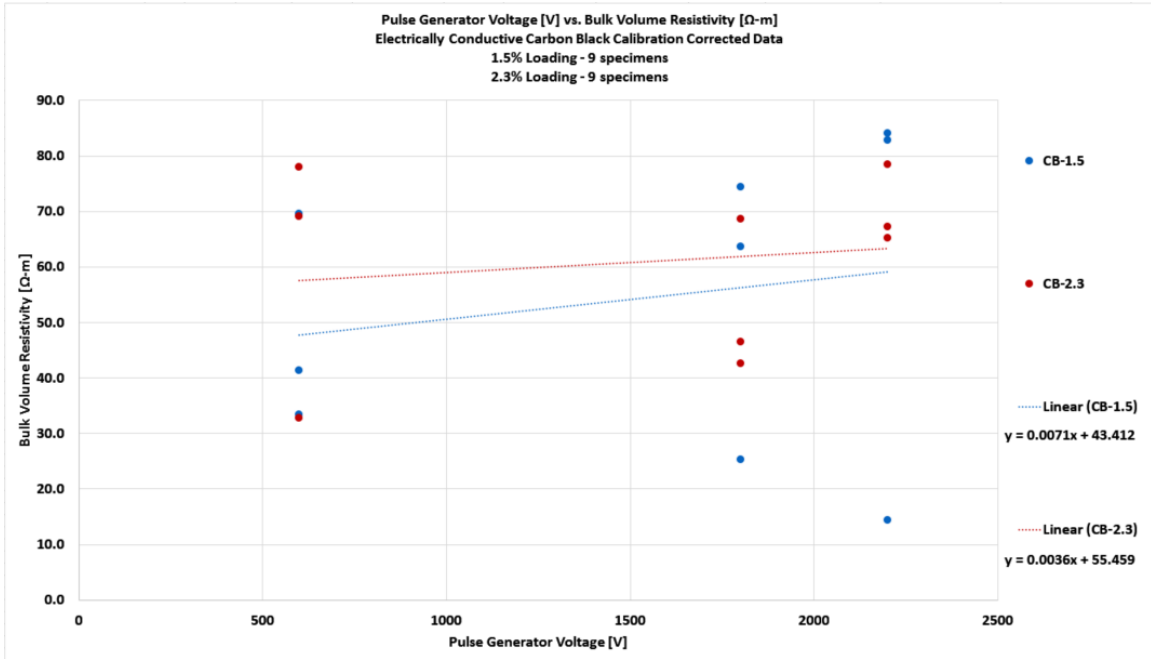


Figure 38. Calibration Corrected Values for Bulk Volume Resistivity, Including the Two Data Points That Have Been Retested as Outliers, of the Carbon Black Specimens Plotted in Groups of Percent Additive Loading as a Function of Pulse Generator Input Voltage.

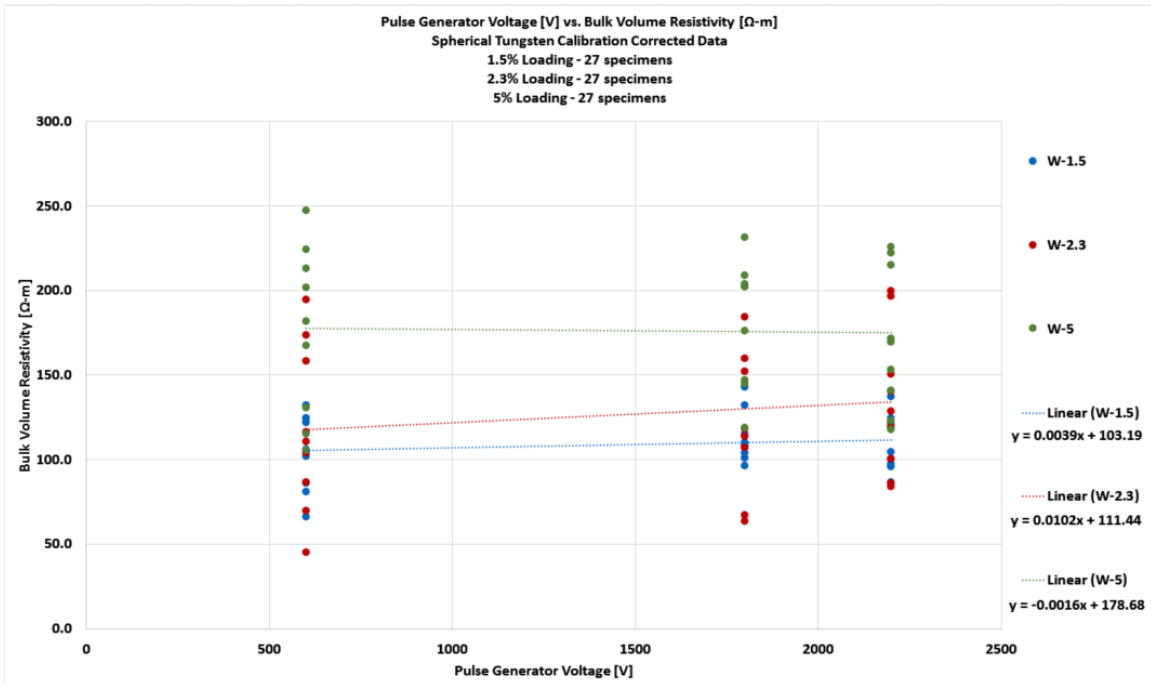
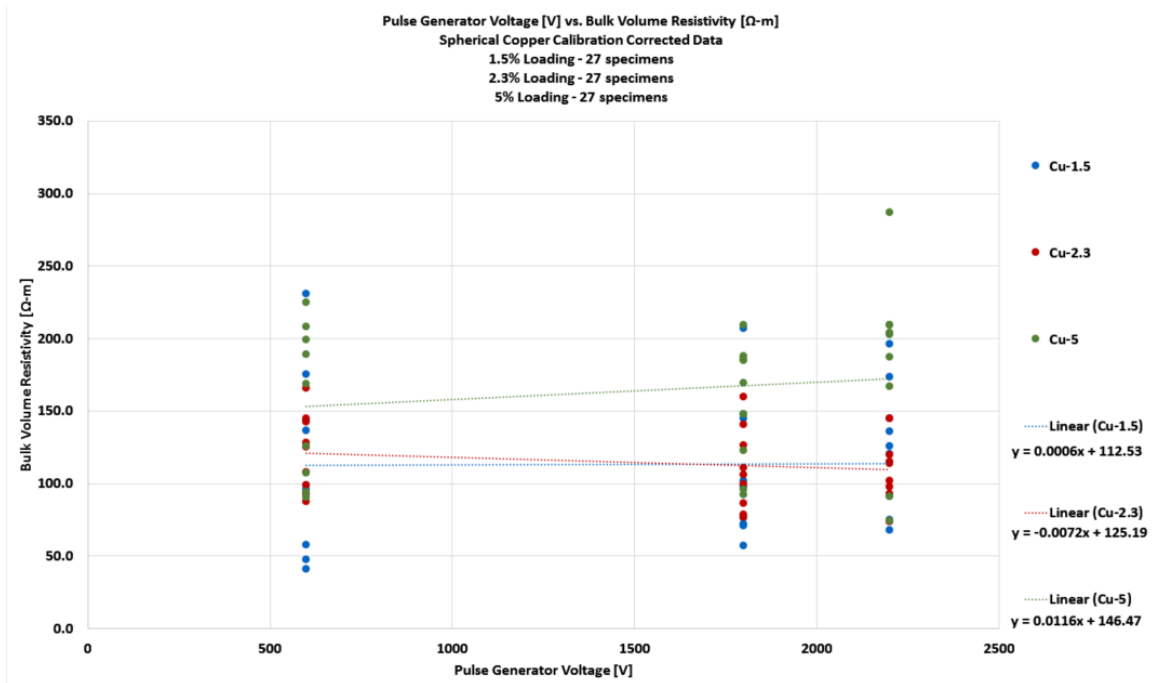


Figure 39. Calibration Corrected Values for Bulk Volume Resistivity, Including the 10 Data Points That Have Been Retested as Outliers, of the Tungsten Specimens Plotted in Groups of Percent Additive Loading as a Function of Pulse Generator Input Voltage.





**Figure 40. Calibration Corrected Values for Bulk Volume Resistivity, Including the 10 Data Points That Have Been Retested as Outliers, of the Copper Specimens Plotted in Groups of Percent Additive Loading as a Function of Pulse Generator Input Voltage.**

Based on Figures 37 through 40 above, and on the previously plotted raw and outlier corrected resultant data, the data collected for this investigation shows that the electric propellant bulk volume resistivity for all of the samples tested is not dependent on the pulse generator voltages at which it's resistivity value was being tested/measured. The same data has also indicated a large variation of bulk volume resistivity values across all of the samples tested for this set of experiments. Before moving on to generating response surface results using this calibration corrected data, additional data visualization was completed in an effort to preliminarily predict the response surface results and to use for later verification.

The first of these additional visualizations included plotting the resulting bulk volume resistivity values across the values for additive particle loading percentage in order to check for the existence of a relationship between the two variables and to show variation among loading percentage groups. Results for the non-additive set of nine specimens, all plotted at a particle loading percentage value of zero, show the variation of bulk volume resistivity values between approximately 100 and 250 Ω-m, with an average value of 176.6 Ω-m. Given that there are only

nine data points to show for the non-additive electric propellant formulation, and that all of these nine data points have been taken from the same, poorly mixed sample flat, more data from flats with a better distribution of ingredients throughout is definitely required in order to claim and/or confirm an approximate value of bulk volume resistivity for the non-additive propellant formulation.

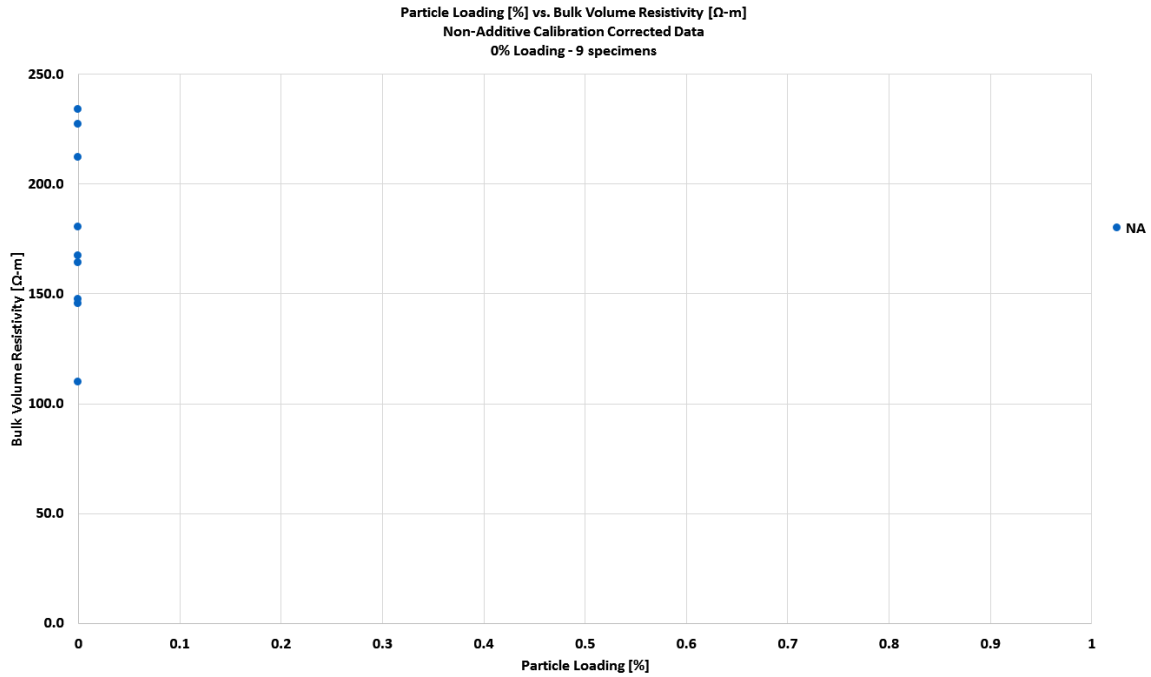


**Figure 41. Calibration Corrected Values for Bulk Volume Resistivity, Including the Two Data Points That Have Been Retested as Outliers, of the Non-Additive Specimens Plotted as a Function of Particle Loading Percentage Value.**

The bulk volume resistivity values of each of the 18 carbon blacks specimens were also plotted across the values for additive particle loading percentage and the resulting plotted values of both the 1.5% and the 2.3% loading percentage values showed significantly less variation than that present in the non-additive set of specimens.

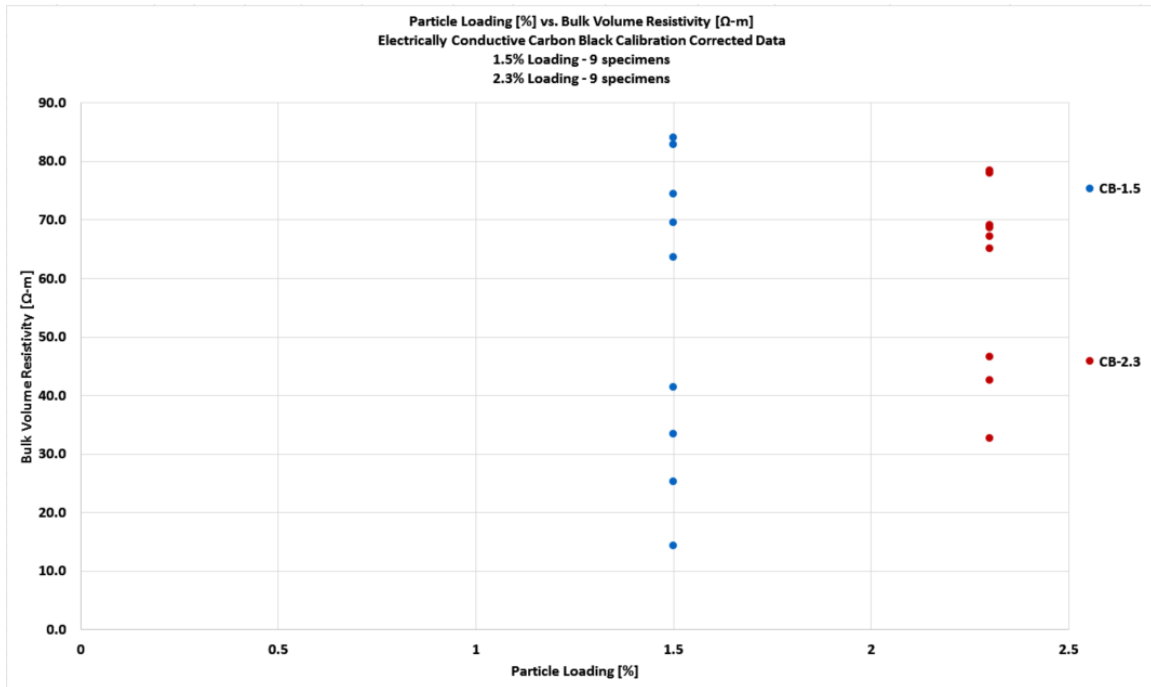


**Figure 42. Calibration Corrected Values for Bulk Volume Resistivity, Including the Two Data Points That Have Been Retested as Outliers, of the Carbon Black Specimens Plotted in Groups of Percent Additive Loading as a Function of Particle Loading Percentage Value.**

Since the overall average value for the 1.5% loading sample set was 54.3  $\Omega$ -m and the overall average value for the 2.3% loading sample set was 60.9  $\Omega$ -m, it is possible that the resistivity value of electric propellant samples containing carbon black could increase as the loading percentage of carbon black is increased, however, these value of resistivity are so close to each other that more data at both loading points tested for this investigation and at additional loading percentages is still needed to confirm.

Looking at the results of the 27 different tungsten specimens plotted across particle loading percentages, a definite increase in average bulk volume resistivity is visible as particle loading percentage increases; this trend is confirmed with the overall average values of bulk volume resistivity for the 1.5%, 2.3%, and 5% particle loadings at 109.2  $\Omega$ -m, 127.1  $\Omega$ -m, and 176.3  $\Omega$ -m, respectively. When shown across loading percentage, all of the measured tungsten specimens also show the smallest amount of variation in volume resistivity values next to the carbon black specimens.

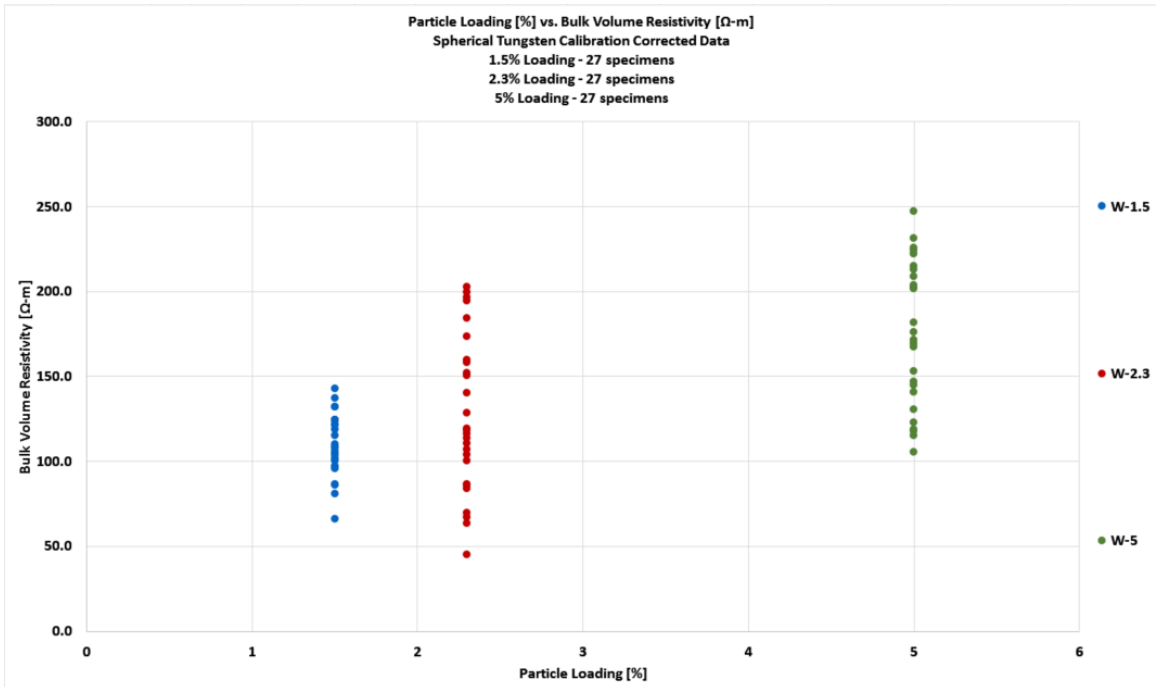


Figure 43. Calibration Corrected Values for Bulk Volume Resistivity, Including the 10 Data Points That Have Been Retested as Outliers, of the Tungsten Specimens Plotted in Groups of Percent Additive Loading as a Function of Particle Loading Percentage Value.

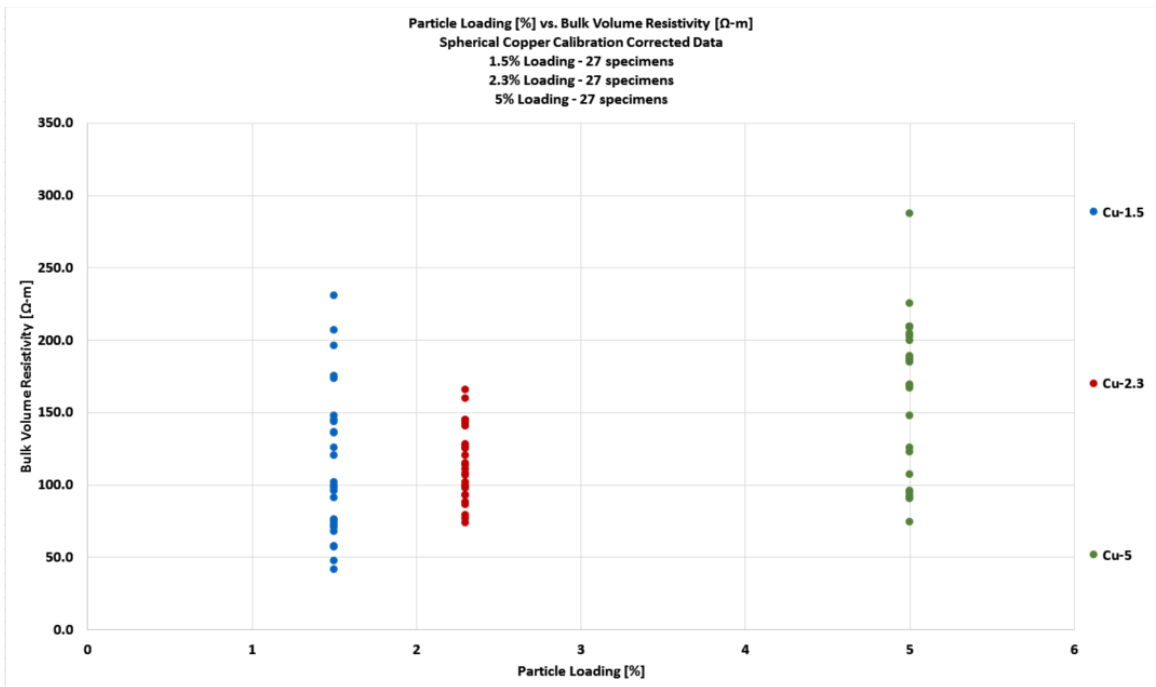
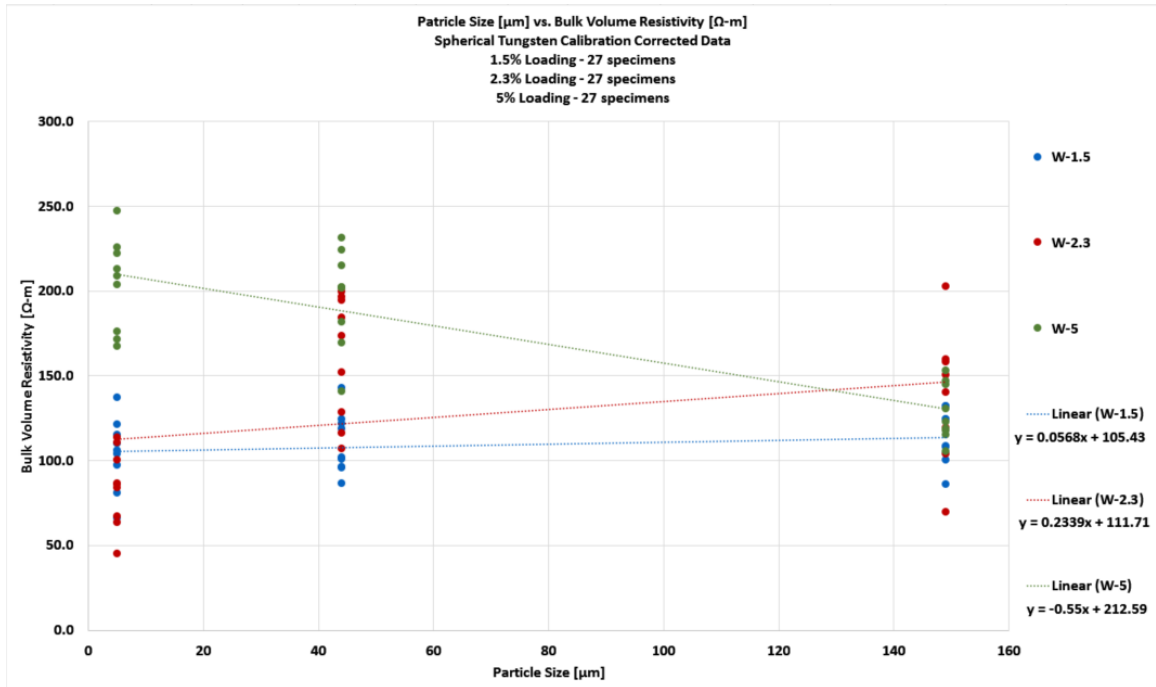


Figure 44. Calibration Corrected Values for Bulk Volume Resistivity, Including the 10 Data Points That Have Been Retested as Outliers, of the Copper Specimens Plotted in Groups of Percent Additive Loading as a Function of Particle Loading Percentage Value.

The copper loading samples appear to follow the same overall trend of increasing electrical bulk volume resistivity with increasing additive particle loading, although the average difference between the 1.5% and 2.3% loading groups is difficult to gauge just looking at the plot shown in Figure 44. This trend is confirmed in the copper specimens, however, with the calculation of the overall average bulk volume resistivity values of 113.5  $\Omega$ -m, 114.2  $\Omega$ -m, and 164.3  $\Omega$ -m for the 1.5%, 2.3%, and 5% particle loading sample sets, respectively.

Given the fact that both the tungsten and copper sets of specimens follow the same trend of increasing resistivity with increasing particle loading, it is possible, given the current set of data, that percolation theory is applicable and could be used to explain a portion of the measured results observed for some of the samples studied in this investigation. Samples measured across several additional values of particle loading percentages would be needed in order to verify whether or not percolation is governing sample response on some level.

Based on the results of this set of experiments, whether or not particle size contributes to a change in bulk volume resistivity as a primary or secondary effect is not able to be exactly determined due to the types of powdered additives used, as detailed below.



**Figure 45. Calibration Corrected Values for Bulk Volume Resistivity, Including the 10 Data Points That Have Been Retested as Outliers, of the Tungsten Specimens Plotted in Groups of Percent Additive Loading as a Function of Additive Particle Size.**

The resulting data for the set of tungsten specimens in the 5% loading group, shows, as displayed in Figure 45, a linear decrease in bulk volume resistivity as particle size increases from 1-5 microns to -325 and -100 mesh sizes. This same trend is also seen in the copper 5% loading group, shown in Figure 46. For both sets of 5% loading data, the plotted linear fit line indicates a higher value of expected resistivity for samples with particle sizes of 1-5 micron and shows a decrease in expected values of resistivity as the line moves through the data plotted for both the -325 mesh and -100 mesh samples. The expected value of resistivity indicated by this line at particle sizes of -100 mesh, or 149 micron and below, is on the order of that predicted by the linear fits lines for both the 1.5% and 2.3% particle loading groups. These results, however, are questionable due to the fact that the -100 and -325 mesh sizes of particles were used instead of discrete particles sizes, as mesh is not a precise measurement or particle sizes because it includes the range of particles that fit through a specifically sized mesh screen.

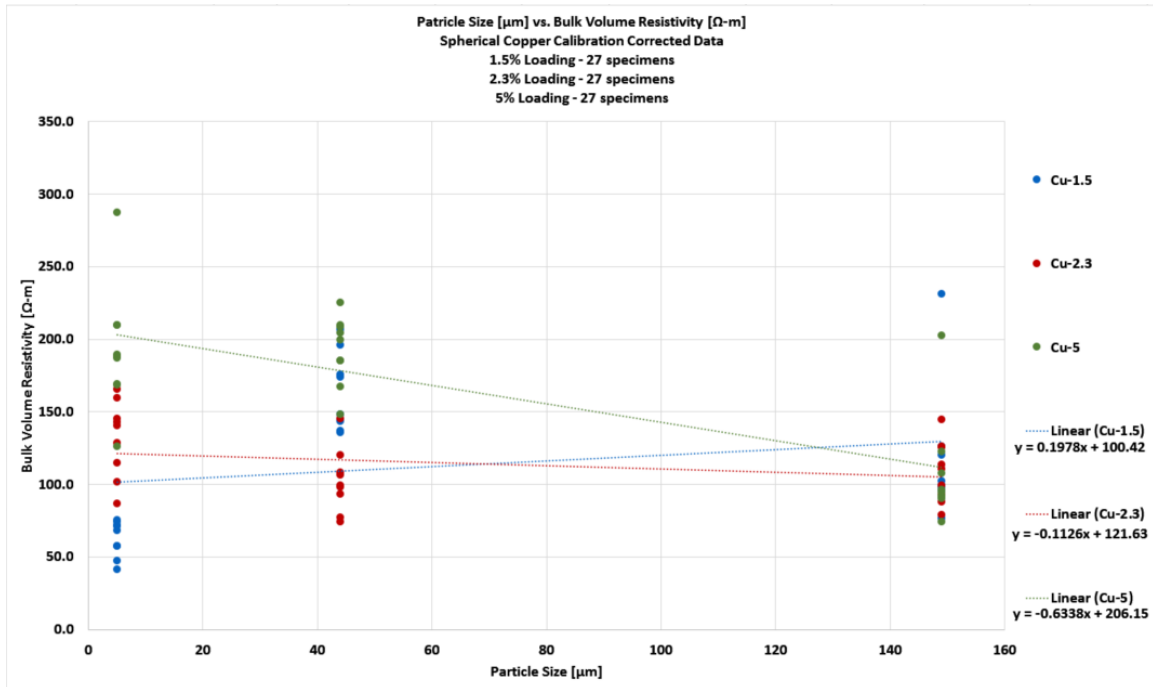


**Figure 46. Calibration Corrected Values for Bulk Volume Resistivity, Including the 10 Data Points That Have Been Retested as Outliers, of the Copper Specimens Plotted in Groups of Percent Additive Loading as a Function of Additive Particle Size.**

More data is needed in order to determine if this decrease in resistivity with an increase in particle size is truly occurring with particle size (and not as a function of the mesh sized particle additives) and if it is actually significant enough to affect resistivity results. However, the trend observed with mesh sizes is interesting and should be remembered later when more detailed particle size research is to be performed.

The ASTM D991 standard indicates that the median value for each of the three specimens measured at each specific pulse generator input voltage value for each of the cells originally shown in Table 3 of Chapter 3 should be reported as the value for measure bulk volume resistivity. Following this standard, the values for bulk volume resistivity of each of the three voltages at which the specimens were tested are reported below.

**Table 7. The Median of the Three Measured Bulk Volume Resistivity Values at Each of the Three Test Voltages Measured from Each Sample Flat.**

<b>Median Bulk Volume Resistivity Values [<math>\Omega</math>-m]</b>				
<b>Additive/ Particle Size</b>	<b>Non-Additive</b>	<b>Tungsten</b>	<b>Copper</b>	<b>Carbon black</b>
	Zero Loading			
<b>No Applicable Particle Size</b>	@600V = 227.4 @18000V = 145.5 @2200V = 164.1	-	-	-
	Light Loading (1.5%)			
<b>1-5 micron</b>	-	@600V = 80.8 @18000V = 110.1 @2200V = 121.3	@600V = 47.5 @18000V = 71.0 @2200V = 74.0	-
<b>-325 mesh</b>	-	@600V = 121.8 @18000V = 100.8 @2200V = 95.9	@600V = 143.3 @18000V = 148.0 @2200V = 173.7	-
<b>-100 mesh</b>	-	@600V = 124.2 @18000V = 108.8 @2200V = 104.6	@600V = 99.2 @18000V = 98.0 @2200V = 120.2	-
<b>Aggregate</b>	-	-	-	@600V = 41.4 @18000V = 63.7 @2200V = 82.8
	Medium Loading (2.3%)			
<b>1-5 micron</b>	-	@600V = 86.4 @18000V = 67.3 @2200V = 85.8	@600V = 142.5 @18000V = 140.5 @2200V = 114.8	-
<b>-325 mesh</b>	-	@600V = 173.5 @18000V = 152.2 @2200V = 196.6	@600V = 107.9 @18000V = 99.2 @2200V = 97.8	-
<b>-100 mesh</b>	-	@600V = 103.9 @18000V = 159.8 @2200V = 140.5	@600V = 99.0 @18000V = 110.7 @2200V = 113.7	-
<b>Aggregate</b>	-	-	-	@600V = 69.0



<b>Median Bulk Volume Resistivity Values [<math>\Omega</math>-m]</b>				
<b>Additive/ Particle Size</b>	<b>Non-Additive</b>	<b>Tungsten</b>	<b>Copper</b>	<b>Carbon black</b>
				@18000V = 46.6 @2200V = 67.2
	Heavy Loading (5.0%)			
<b>1-5 micron</b>	-	@600V = 212.9 @18000V = 203.5 @2200V = 222.4	@600V = 168.7 @18000V = 187.8 @2200V = 209.3	-
<b>-325 mesh</b>	-	@600V = 201.7 @18000V = 202.4 @2200V = 169.7	@600V = 208.4 @18000V = 184.9 @2200V = 204.2	-
<b>-100 mesh</b>	-	@600V = 115.3 @18000V = 145.0 @2200V = 122.8	@600V = 94.4 @18000V = 96.0 @2200V = 91.2	-
<b>Aggregate</b>	-	-	-	-

### Regression and Response Surface Results

#### *Introduction and a Note on the Normality of the Data*

In order to analyze such a large amount of data in a timely and efficient manner, a statistical software package called Minitab® 17 was used, as it provided all of the tools necessary for ANOVA analysis, regression equation building, and for response surface, etc. visualization of study results.

After all of the study results were input into Minitab in the format shown in Figure 18 of Chapter 3, Minitab's "DOE>Response Surface>Analyze Response Surface Design..." function was used to create the response surface regression model discussed below.

An analysis of variance, or ANOVA, was performed with collected study data to test hypotheses regarding the effect of main factors and their interactions on results. Minitab was used to perform this analysis and as a result, outputs an ANOVA table, shown in Figures 48-50. Before discussing these initial Minitab results, it is important to note that the ANOVA analysis performed using the sets of experimental data gathered for this investigation was performed with

several limiting assumptions. These assumptions include: that the specimens have each been randomly selected for test and that the specimen response results are independent of all other specimens, that the experimental errors within the data gathered are normally distributed, and that the variance between different groups/treatments/etc. is similar.

In order to verify the assumption of normally distributed data, a probability plot, or a graphical method used to determine whether collected specimen data conforms to a hypothesized distribution or not, can be made in Minitab for visual examination. This verification of a normal data distribution was performed using a probability plot, rather than a histogram plot (even though a histogram plot was also produced), because a probability plot is usually considered more reliable than a histogram for small or moderately sized sample sets.

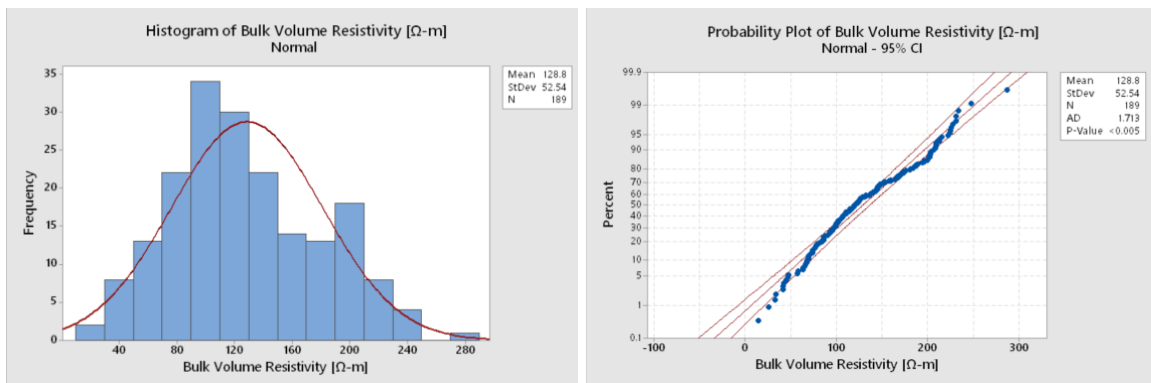


**Figure 47. (Left) A Histogram Plot of All of the Values Measured for the Bulk Volume Resistivity Response Shown with a Normal Distribution Curve for Comparison. (Right) A Probability Plot of the Bulk Volume Resistivity Responses Used to Verify the Normality of the Response Data.**

The right image in Figure 47 shows the probability plot for the bulk volume resistivity response variable measured during the data collection portion of this study. The Minitab single variable probability plot creates and estimates a cumulative distribution function from all of the specimen data chosen by plotting the value of each observation against that observation's estimated cumulative probability; if the data points plotted fit a positively sloped straight line, then the data is perfectly normal. In this case, the response variable data points plotted show a tailed distribution that is left-skewed at higher bulk volume resistivity values and right-skewed at lower resistivity values. The goodness-of-fit Anderson-Darling (AD) statistic run on the response data in order to create the probability plot is a measure of the area between the fitted line based on a

normal distribution and the data point based empirical distribution function; the AD statistic is used by Minitab to calculate a P-value for determining whether or not the plotted data follows a normal distribution. Based on the plot shown right in Figure 47 with a P-value equal to less than 0.05, or 5%, it has been concluded that the response data does not follow a normal distribution [46].

Given that the response data gathered during this investigation is not normally distributed and that one of the three assumptions governing the validity of ANOVA results does not hold up, it is possible that the chances of getting falsely negative results for the response surface analysis, performed using this data and described below, are increased given that this analysis may be underpowered. Based on this information, the robustness of the response surface regression ANOVA analysis could be called into question. However, since the calculated AD-value is equal to 1.713, the fact that larger AD-values indicate non-normally distributed data and the fact that the ANOVA test makes inferences about mean values (or expected average responses at chosen factor levels) and not about the tails of the distribution, it was decided to proceed with response surface regression analysis.

#### *Initial Regression and Response Surface Results*

Minitab outputs ANOVA tables with columns as follows: "Source" represents the source of variation being analyzed, "DF" indicates the number of degrees of freedom, or the amount of information in the data, of the Source, and the "Contribution" term indicates the percentage that each Source in the ANOVA table contributes to the total Seq SS values. The "Seq SS" term, or the sequential sum of squares term, are the measures of variation for the different components of the model and take into account the order of the terms in the model. Each Seq SS term represents the increase in the model sum of squares compared to a model with only the above ANOVA terms. The adjusted sum of squares, or the "Adj SS" term, indicates the measures of variation for different components of the model and each term quantifies the amount of variation in the response data that the corresponding term in the model explains. The adjusted mean squares, or "Adj MS" term, measures how much variation a term or model explains, assuming that every other terms is also in the model, and unlike the Adj SS term, the Adj MS term takes

into account the DF information. The “F-Value” of a term contains the test statistic used to determine whether or not that term is associated with the overall response; a larger F-Value represents a higher statistical significance. Finally, the “P-Value” of a term indicates the probability that measures the evidence collected against the null hypothesis, where lower probabilities provide stronger evidence against the null hypothesis and in support of the research hypothesis.

Analysis of Variance

Source	DF	Seq SS	Contribution	Adj SS
Model	9	305768	58.92%	305768
Linear	3	188583	36.34%	12484
Additive Resistivity [Ω-m]	1	100786	19.42%	3511
Loading [%]	1	63686	12.27%	379
Particle Size [m]	1	24110	4.65%	4180
Square	3	61202	11.79%	91164
Additive Resistivity [Ω-m]*Additive Resistivity [Ω-m]	1	281	0.05%	994
Loading [%]*Loading [%]	1	40173	7.74%	66986
Particle Size [m]*Particle Size [m]	1	20748	4.00%	20215
2-Way Interaction	3	55984	10.79%	55984
Additive Resistivity [Ω-m]*Loading [%]	1	2267	0.44%	1636
Additive Resistivity [Ω-m]*Particle Size [m]	1	3168	0.61%	4168
Loading [%]*Particle Size [m]	1	50549	9.74%	50549
Error	179	213219	41.08%	213219
Lack-of-Fit	11	75061	14.46%	75061
Pure Error	168	138158	26.62%	138158
Total	188	518987	100.00%	

Source	Adj MS	F-Value	P-Value
Model	33974.3	28.52	0.000
Linear	4161.5	3.49	0.017
Additive Resistivity [Ω-m]	3510.7	2.95	0.088
Loading [%]	378.9	0.32	0.573
Particle Size [m]	4179.9	3.51	0.063
Square	30388.0	25.51	0.000
Additive Resistivity [Ω-m]*Additive Resistivity [Ω-m]	993.6	0.83	0.362
Loading [%]*Loading [%]	66985.7	56.24	0.000
Particle Size [m]*Particle Size [m]	20215.4	16.97	0.000
2-Way Interaction	18661.3	15.67	0.000
Additive Resistivity [Ω-m]*Loading [%]	1636.3	1.37	0.243
Additive Resistivity [Ω-m]*Particle Size [m]	4168.4	3.50	0.063
Loading [%]*Particle Size [m]	50548.9	42.44	0.000
Error	1191.2		
Lack-of-Fit	6823.8	8.30	0.000
Pure Error	822.4		
Total			

Model Summary

S	R-sq	R-sq(adj)	PRESS	R-sq(pred)
34.5133	58.92%	56.85%	236142	54.50%

**Figure 48. The ANOVA Table That Minitab Generated Using the Data Collected for This Set of Experiments.**

The Contribution column of the ANOVA table detailing the Minitab model fit for the data collected during this investigation indicates that the model generated accounts for approximately 58.92% of all of the variation in the electric propellant resistivity responses collected. A large

majority, 36.34%, of the sources accounting for this variation come from a linear fit model with additive resistivity, then additive loading percentage, and lastly, additive particle size each accounting for a lesser portion of the variation in the order they were listed. Both the square and the 2-way interaction model account for about the same amount of response variation, 11.79% and 10.79%, respectively, with the additive percent loading squared term and the additive percent loading multiplied by the additive particle size term accounting for the most variation in each model, respectively.

The Contribution column also indicates that approximately 41% of the variation in the recorded resistivity response results is due to error. The error is parsed out into two categories: the first, as a result of the model's lack of fit to the recorded data, accounting for 14.46% of the total variation in response, and the second source of error, a result of random error, accounts for 26.62% of the total variation in response. Both of these model error contributions make sense, as only a few of the electric propellant additive explanatory factors have been explored during this investigation, and as described throughout this document, a significant portion of the error and/or variation present in this set of experiments is due to sample mixing non-homogeneity, among other known and unknown contributors, which cannot easily be quantified at this point. Additionally, the restricted experimental domain could also be contributing to both of these error components, however, since this study was intended to be a screening experiment, this was to be expected.

Based on the relationship used to calculate P-Values from F-Values, it can be said that higher F-Values lead to smaller P-Values, which suggests stronger statistical evidence against the null hypothesis. (The research hypothesis, from Chapter 1, states that there exists some replacement additive for the electric propellant formulation that will both preserve the operating mechanisms of the propellant and reveal the nature of the electrical resistivity of the altered propellant samples with regard to the presence of percolation theory. That is, that some percolation curve exists for each replacement additive used that will reveal some limiting critical threshold percolation value, beyond which no added benefit of particle size or amount can be shown. The corresponding null hypothesis would indicate that there is no replacement additive

that can be used in the electric propellant formulation that will preserve the operational mechanisms and/or that would reveal any effects of percolation.) With regard to the statistical analysis performed in Minitab, this null hypothesis corresponds to the fact that the model fit to all of the data gathered for this experiment does not explain any of the variation in the observed responses, and this is where looking at P-Values becomes important.

By comparing a standard chosen significance level of 5%, or 0.05, to the P-Values calculated for this set of data, the null hypothesis can be assessed by determining how well the model explains variation in the observed responses. If the P-Value being analyzed is less than or equal to the chosen significance level then it can be concluded that the model is likely to be able to explain the variation observed, otherwise, if the P-Value is greater than the significance level, the lack of fit of the model could be statistically significant and it may not correctly specify the relationships between provided independent and response variable data.

The P-Value of the model is shown as 0.000 (which means that the estimated probability is not zero, but beyond the number of significant digits presented), a P-Value less than the 0.05 significance level value, meaning that, overall, the model itself is statistically significant and does account for a significant amount of the variation observed in the experimental results.

Additionally, the P-Values of each of the fits, linear, square, and 2-way interaction, are also all below the significance level, meaning they too all contribute to the model being able to explain the observed variation in response. Models and terms that are significant based on their P-Values include: the linear fit model, the square fit model, the additive percent loading squared term, the additive particle size squared term, the 2-way interaction model, and the additive percent loading multiplied by the additive particle size term [47].

Finally, the ANOVA table presents the outputs of several “goodness of fit” statistics. The first statistic is an “S” values that represents how well the model describes the response and is intended to be used in place of the R<sup>2</sup> value to compare model fit with those models that do not have a constant value. In this case, the S value is fairly low, at 34.5133  $\Omega$ -m, (the lower the S value, the better the model describes the response) but since this is the first attempt at a

regression model for data of this kind, there is nothing valuable that could be compared to the S value for this model.

The last three statistics that were analyzed in this figure were the three R<sup>2</sup> model summary values. The first of these values, “R-sq” or R<sup>2</sup>, is a statistical measure of how closely the data matches the fitted model for which the higher the value of R<sup>2</sup> the better the model fits the data. This statistic will usually increase in value when additional predictors are included in the model, but is most useful when compared to models of the same size. An R<sup>2</sup> value of 0% indicates that the fitted model does not explain any of the variation in the observed responses, and a value of 100% indicates that the model accounts for all of the variability in the response results. For the data gathered during this investigation, Minitab predicts an R<sup>2</sup> value of 58.92%, which is fairly high considering that this experiment was only conducted using one of the four electric propellant ingredients and using only a subset of available additive replacements, percentages, and particle sizes.

The next value for “R-sq (adj),” or the adjusted R<sup>2</sup> value, is the value intended for use when comparing models with different numbers of predictors. Again, since no model similar to this one exists yet, this value should be saved and used later after more work has been done to explore electric propellant formulations and corresponding resistivity. However, it should be noted that the value for adjusted R<sup>2</sup> is equal to 56.85%, only a -2.07% difference from the actual model R<sup>2</sup> value.

Lastly, the value shown for the predicted R<sup>2</sup>, or “R-sq (pred),” indicates how well the fitted model will predict responses for new observations in the data. For this model, the predicted R<sup>2</sup> value is 54.50%, a -4.52% difference from the actual model R<sup>2</sup> value. A predicted R<sup>2</sup> value that has a substantially lower value than the model R<sup>2</sup> value could possibly indicate that the model is over-fit or has a number of added terms that account for population effects that are not important, meaning the model could be tailored to the specific set of data to which it was fitted and a poor population response predictor. This is not the case with the model fitted for this investigation given its ~4.5% difference from the fitted model R<sup>2</sup> value [48].

Minitab outputs the Coded Coefficient portion of its ANOVA tables, shown in Figure 49, with columns as follows: the "Effect" column includes Effect values that describe the magnitude and direction of the relationship between a term and the chosen response variable, and the "Coef" column contains values that describe the magnitude and direction of the relationship between a term in a specific model and the response variable, half the size of the value in the Effect column. The "SE Coef" column contains values for the estimated variability of the coefficient estimates that would be obtained if samples from the same population were repeatedly retested; the smaller the values of the standard error of the coefficient, the more precise the estimate is. The "95% CI" column details the ranges of values that are likely to contain the actual value of the coefficient for each modeled term. The "T-Value" is a measurement of the ratio between the coefficient and its standard error and the "P-Value," as discussed previously is the probability that measures evidence against the null hypothesis. Lastly, the "VIF" (variance inflation factor) values describe how much the variance of a particular coefficient has been inflated based on the correlations among model predictors.

Given that the T-Values for all of the model terms are relatively low, the standard error for each of the calculated coefficients can be deemed sufficiently large, meaning that the coefficient estimates are not very precise. Combined with the computed P-Values that are less than the chosen significance level, these statistics indicate that the following coefficients are statistically significant: the constant value term, the additive loading percentage squared term, the additive particle size squared term, and the additive loading percentage multiplied by the additive particle size interaction term. Terms that had an assigned P-Value slightly above the significance level of 0.05 (which could or could not be considered marginally significant) included the following: the linear additive resistivity and additive particle size terms and the additive resistivity multiplied by additive particle size interaction term.



Approved for Public Release DOPSR 19-S-0112  
Placed in the Public Domain Per E18-9TPV

Coded Coefficients

Term	Effect	Coef	SE	Coef
Constant		219.4		54.7
Additive Resistivity [Ω-m]	277.8	138.9		80.9
Loading [%]	27.4	13.7		24.3
Particle Size [m]	290.9	145.4		77.6
Additive Resistivity [Ω-m]*Additive Resistivity [Ω-m]	93.7	46.9		51.3
Loading [%]*Loading [%]	145.77	72.88		9.72
Particle Size [m]*Particle Size [m]	-65.92	-32.96		8.00
Additive Resistivity [Ω-m]*Loading [%]	59.8	29.9		25.5
Additive Resistivity [Ω-m]*Particle Size [m]	312.4	156.2		83.5
Loading [%]*Particle Size [m]	-70.88	-35.44		5.44

Term	95% CI	T-Value	P-Value
Constant	( 111.5, 327.3)	4.01	0.000
Additive Resistivity [Ω-m]	( -20.8, 298.6)	1.72	0.088
Loading [%]	( -34.2, 61.6)	0.56	0.573
Particle Size [m]	( -7.8, 298.6)	1.87	0.063
Additive Resistivity [Ω-m]*Additive Resistivity [Ω-m]	( -54.4, 148.1)	0.91	0.362
Loading [%]*Loading [%]	( 53.70, 92.06)	7.50	0.000
Particle Size [m]*Particle Size [m]	(-48.75, -17.17)	-4.12	0.000
Additive Resistivity [Ω-m]*Loading [%]	( -20.4, 80.2)	1.17	0.243
Additive Resistivity [Ω-m]*Particle Size [m]	( -8.6, 321.0)	1.87	0.063
Loading [%]*Particle Size [m]	(-46.17, -24.70)	-6.51	0.000

Term	VIF
Constant	
Additive Resistivity [Ω-m]	335.36
Loading [%]	35.81
Particle Size [m]	638.05
Additive Resistivity [Ω-m]*Additive Resistivity [Ω-m]	2.87
Loading [%]*Loading [%]	2.86
Particle Size [m]*Particle Size [m]	1.29
Additive Resistivity [Ω-m]*Loading [%]	34.05
Additive Resistivity [Ω-m]*Particle Size [m]	710.73
Loading [%]*Particle Size [m]	1.31

Regression Equation in Uncoded Units

$$\begin{aligned}
 \text{Bulk Volume Resistivity } [\Omega\text{-m}] = & 158.8 - 281805605 \text{ Additive Resistivity } [\Omega\text{-m}] \\
 & - 5061 \text{ Loading } [\%] + 1215759 \text{ Particle Size } [\text{m}] \\
 & + 187401216575959 \text{ Additive Resistivity } [\Omega\text{-m}]*\text{Additive Resistivity } [\Omega\text{-m}] \\
 & + 116613 \text{ Loading } [\%]*\text{Loading } [\%] \\
 & - 5938542914 \text{ Particle Size } [\text{m}]*\text{Particle Size } [\text{m}] \\
 & + 2391904217 \text{ Additive Resistivity } [\Omega\text{-m}]*\text{Loading } [\%] \\
 & + 4193688095212 \text{ Additive Resistivity } [\Omega\text{-m}]*\text{Particle Size } [\text{m}] \\
 & - 19027419 \text{ Loading } [\%]*\text{Particle Size } [\text{m}]
 \end{aligned}$$

**Figure 49. A Continuation of the ANOVA Table That Minitab Generated Using the Data Collected for This Set of Experiments.**

VIF values can be used to describe how much correlation between predictors (multicollinearity) exists in a regression model. A VIF value equal to 1, usual in most factorial designs, indicates that predictors have no correlation between them, and a VIF value of greater than 5 indicates that predictors are highly correlated. Five out of the nine model terms included in the generated regression equation, discussed below, have VIF values significantly greater than 5; “highly correlated predictors are problematic because the multicollinearity can increase the variance of the regression coefficients,” making them unstable. This could mean that some of the regression equation coefficients “can seem to be not statistically significant even when an

important relationship exists between the predictor and the response,” and “removing any highly correlated terms from the model will greatly affect the estimated coefficients of the other highly correlated terms” [49].

Following the Minitab Coded Coefficients table is the Minitab generated response surface Regression Equation. The equation shown in Figure 49 has been output by Minitab in uncoded units due to the fact that the model generated for the data is hierarchical. A hierarchical model is one in which, “for each term in the model, all lower order terms contained in it must also be in the model.” When interpreting this regression equation in uncoded units, “interpret the coefficients using the natural units of each variable” [50, 51].

The last set of data output by Minitab as part of the response surface regression analysis is the table shown below in Figure 50 of Fits and Diagnostics for Unusual Observations. This table details all of the unusual, or influential, observations that have an unequal impact on the ANOVA analysis and/or on the regression model; these observations are important to identify, as they could produce misleading results. The unusual observations detected in the data set fed to Minitab for this investigation are all of the outlier, or large residual, type, meaning that they are values that are considered extreme in the y-direction when compared to the fitted regression line. These observations are denoted extreme standardized residuals by the “R” value shown in the unusual observations table.

Fits and Diagnostics for Unusual Observations

Obs	Bulk Volume Resistivity [Ω-m]	Fit	SE Fit	95% CI	Resid	Std Resid	Del Resid	HI
27	125.97	196.11	8.15	(180.02, 212.19)	-70.13	-2.09	-2.11	0.0557757
36	202.62	112.69	9.15	( 94.64, 130.75)	89.92	2.70	2.75	0.0702748
88	199.51	125.04	5.73	(113.73, 136.34)	74.48	2.19	2.21	0.0275391
90	206.85	137.57	5.83	(126.07, 149.06)	69.28	2.04	2.05	0.0284870
113	202.84	111.05	7.21	( 96.83, 125.28)	91.78	2.72	2.77	0.0436484
127	196.57	125.04	5.73	(113.73, 136.34)	71.54	2.10	2.12	0.0275391
130	233.96	158.80	10.66	(137.76, 179.83)	75.17	2.29	2.32	0.0953859
157	194.64	125.04	5.73	(113.73, 136.34)	69.60	2.04	2.06	0.0275391
169	227.38	158.80	10.66	(137.76, 179.83)	68.58	2.09	2.11	0.0953859
176	41.27	109.87	5.64	( 98.75, 120.99)	-68.60	-2.01	-2.03	0.0266628
185	231.02	122.35	8.20	(106.17, 138.53)	108.67	3.24	3.33	0.0564485
189	287.29	196.11	8.15	(180.02, 212.19)	91.18	2.72	2.77	0.0557757

Obs	Cook's D	DFITS	
27	0.03	-0.513145	R
36	0.06	0.756425	R
88	0.01	0.372222	R
90	0.01	0.351866	R
113	0.03	0.591680	R
127	0.01	0.357152	R
130	0.06	0.752597	R
157	0.01	0.347251	R
169	0.05	0.684911	R
176	0.01	-0.336371	R
185	0.06	0.814909	R
189	0.04	0.672987	R

R Large residual

**Figure 50. A Continuation of the ANOVA Table That Minitab Generated Using the Data Collected for This Set of Experiments.**

The observations denoted in the Fits and Diagnostics for Unusual Observations table refer to 12 different data points, or specimen, that seem unusual given the rest of the data collected. The specimen corresponding to the observations above have been tabulated below. Interestingly, four out of the 12 unusual observations (observations 169, 176, 185, and 189) were identified as outliers and retested as detailed above in the Outlier Identification, Re-Testing, and Visualization subsection.

**Table 8. The Specimen Serial Numbers Corresponding to the Minitab Identified Unusual Observations.**

Minitab Unusual Observation	Specimen Serial Number
27	Cu-5-1-5-2
36	Cu-5-100-8
88	W-2.3-325-8
90	Cu-1.5-325-4

<b>Minitab Unusual Observation</b>	<b>Specimen Serial Number</b>
113	W-2.3-100-4
127	W-2.3-325-7
130	NA-2
157	W-2.3-325-1
169	NA-3
176	Cu-1.5-1-5-1
185	Cu-1.5-100-1
189	Cu-5-1-5-8

In order to verify whether or not the observations noted above have had an influential effect on the regression results, the model would have to be fit with and without each of the observations and values including those for P-Values, R2 values, and additional model significance indicators considered important would have to be analyzed. If significant changes in the models occur when one or more of the noted observations is removed, then those observations should be checked for error (in entry, measurement, etc.) and a decision as to whether or not the data point should be omitted, re-tested, or if more data needs to be collected all together needs to be made in order to determine a model resolution [52]. This analysis, however, was outside of the scope of this study.

The first set of plots generated in Minitab for data visualization and interpretation included the main effects and interaction plots for the bulk volume resistivity response values shown below.

The main effects plot “displays the means for each group within a categorical variable, with a line connecting the points for each variable. When this connecting line is horizontal, there is no main effect present; the steeper the slope of a non-horizontal line, the larger the magnitude of the main effect. Interestingly, additive resistivity and additive particle size both have a positively increasing slope, although curved oppositely, while the additive loading percentage categorical variable has a “U” shaped curve. The ANOVA and response regression detailed above have

already verified that the main effects of additive resistivity and particle size, at least for this model, are important. This main effects plot, however, details that percolation may be having an effect on bulk volume resistivity response. The curve shown for additive loading percentage could be “U” shaped, or could represent one side of the typical “S” curve (discussed for carbon black in plastics in Chapter 2). In order to verify this, more data for additive loading percentage values on either side of the additive loading percentage values chosen for this investigation would be needed.

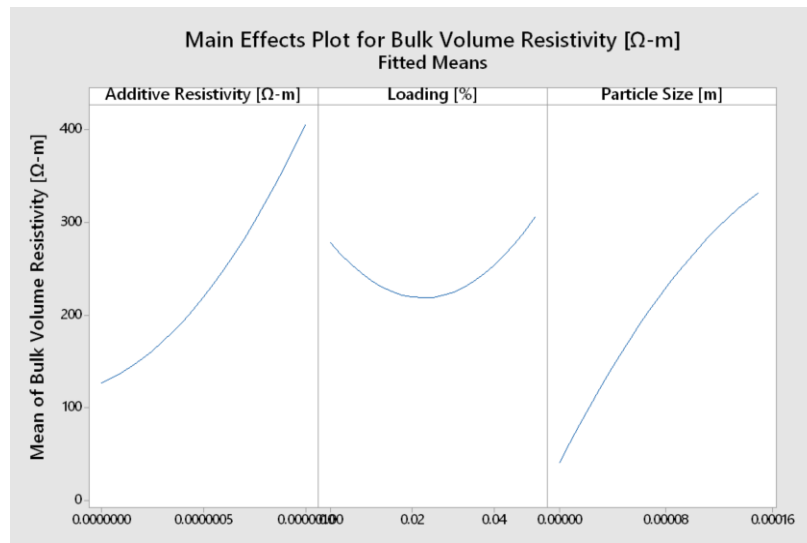


**Figure 51. The Minitab Generated Fitted Means Main Effect Plot for the Bulk Volume Resistivity Response Variable.**

An interaction plot is used to show the relationships between one categorical factor and a response variable that depends on the value of a second categorical factor; the lines on the interaction plots are to be evaluated in order to determine interactions. If the plotted lines are parallel, no interaction occurs, and if the plotted lines are non-parallel or intersecting, an interaction occurs, where the strength of the interaction is determined by how non-parallel the lines are.

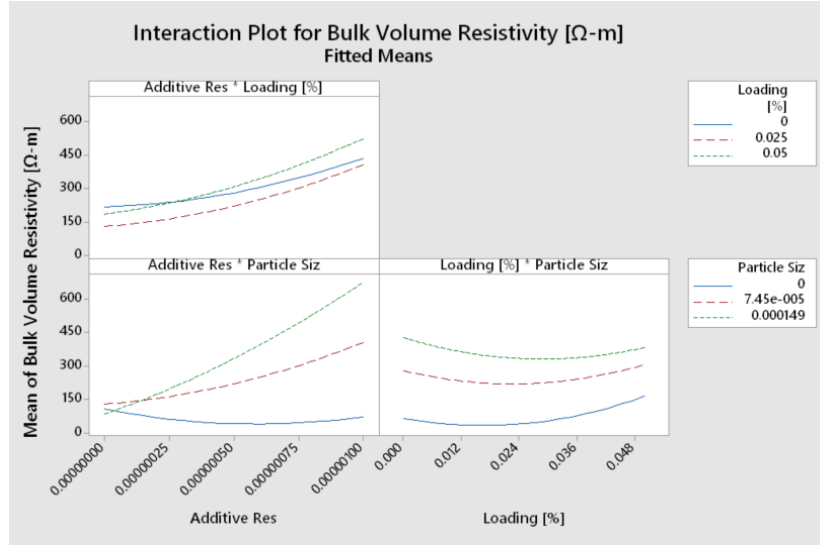


**Figure 52. The Minitab Generated Fitted Means Interactions Plot for the Bulk Volume Resistivity Response Variable.**

The top left plot, of additive resistivity and additive loading percentage, shows two parallel lines (representing a 0.025 and a 0.05 loading percentage) with one line (representing a 0 loading percentage) intersecting the 0.05 loading percentage line on the left hand side on the plot, and possibly intersecting the 0.025 loading percentage line off of the plot to the right. The bottom left plot, of additive resistivity and particle size, shows interaction between all three particle size lines and shows lines each with a significant difference in slope. The last plot on the bottom right, additive loading percentage and particle size, shows three nearly parallel lines that do not intersect, indicating no significant interaction. However, these line could possibly show an intersection further off of the plot to the right if the data set were to be expanded [53].

Upon further inspection of the fitted means main effects plot above, specifically the additive resistivity plot, the fitted mean bulk volume resistivity point representative of the carbon black specimens is dramatically higher compared to the actual response value data. This is also true for the fitted mean values shown in the interactions plot. It is believed that this error could be due to the fact that tungsten, copper, carbon black, and the non-additive samples were all analyzed in Minitab under the assumption that they all included additives, or a lack of additives, that could be compared on the same scale across all of the analysis work performed. In order to remedy this, a nested analysis would have to be performed, however, this would have required sufficient effort

and it is preferred that this analysis be completed when more data is available so conductive and non-conductive metallic and non-metallic combinations could be equally analyzed separately and then compared for review. This is further discussed in Chapter 5. 2D contour plots of the data were also generated in Minitab, however these plots exhibit a similar error as described above and are not shown, however, their form can be inferred from the surface plots shown below.

Due to the effect described above, two different sets of surface plots were generated in Minitab: those shown as green surfaces below were generated using the Minitab DOE Response Surface option and those shown as a blue/grey mesh surface were generated using the actual measured values collected during testing.

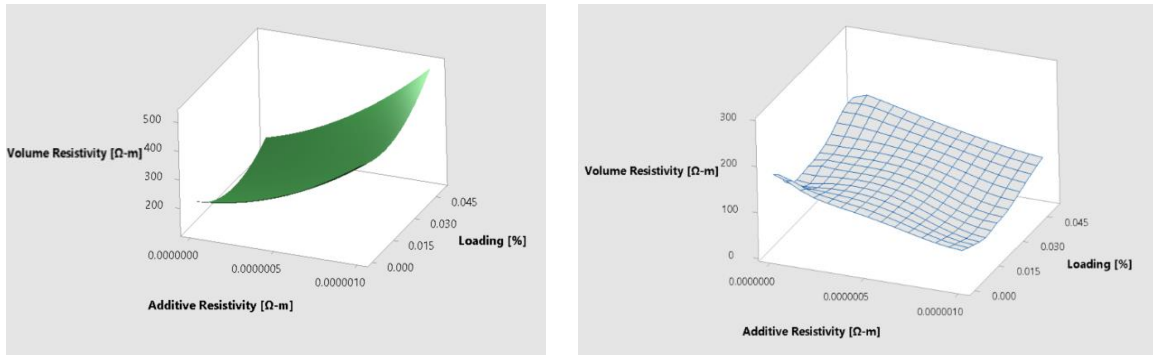


**Figure 53. Surface Plots of Bulk Volume Resistivity (z-axis) Versus Additive Resistivity (x-axis) and Particle Loading Percentage (y-axis), with an Additive Particle Size Hold Value Equal to 0.0000745m.**

The surfaces shown in the figure above detail the bulk volume resistivity response values over the plane of additive resistivity values versus additive loading percentages. In the plot on the left (the Minitab surface) the plotted bulk volume resistivity response surface clearly increases with increasing additive resistivity and has a slight “U” shape corresponding to additive loading percentage where the lowest point in the “U” shape occurs at a loading value of approximately 0.023, or 2.3% percent.

The surface shown to the right (the surface representing the actual data point values) shows this similar “U” shape corresponding to additive resistivity only at lower values of resistivity (where the metallic additive resistivities occur) and transitions into more of a downward curve as additive resistivity increases. Peaks in bulk volume response resistivity appear to occur at low values of additive resistivity and either very low or very high (within the domain tested) values of

additive loading percentage. Valleys in the response variable appear to occur at low additive resistivities and mid-level additive loading percentages and higher additive resistivity values and low additive loading percentages.

The portion of the surface shown in Figure 53 representing the actual data point values corresponding to the tungsten and copper additive resistivity values appears to mirror the results found above in the initial data visualization done in Excel. The slope of the response surface increases slightly between the 1.5% and 2.3% additive loading percentages, and slightly more between the 2.3% and the 5% additive loading percentages.

The two surfaces plotted to show the bulk volume resistivity response value over the plane of additive loading percentage versus additive particle size shows an incredible difference in predicted response values as particle size increases. The Minitab surface shown in Figure 54 indicates that as particle size increases, so does the bulk volume resistivity response across all additive loading percentage values. However, more realistically, given the values of mesh sizes that were used for two out of the three particle size levels, the actual data shown in the meshed surface only shows that particle size has an impact at lower values, where the 1-5 micron particle sizes used for this experiment exist. This end of the response also details the “U” shaped additive loading percentage curve discussed above.

The initial data visualization in Excel detailed that, for a 5% additive loading percentage, a decrease in resistivity with an increase in particle size was observed using a linear fit. This behavior is small, but observable in the surface shown in Figure 54 representing the actual data point values at a loading percentage of approximately 5%.



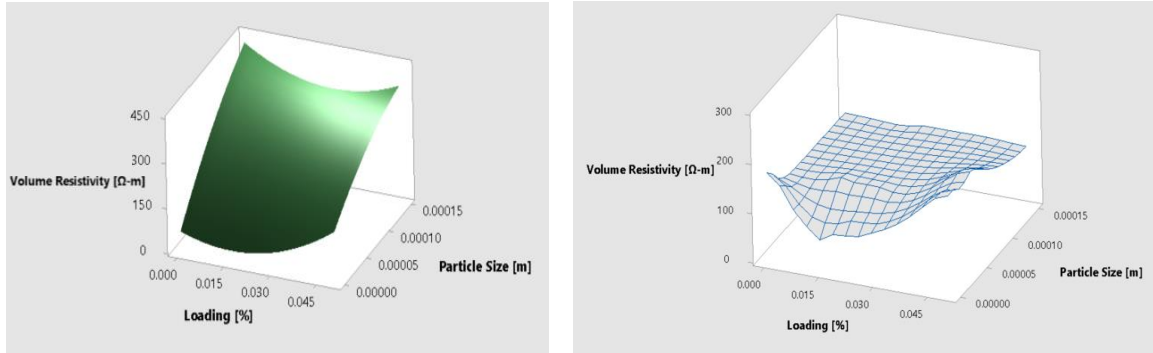


**Figure 54. Surface Plots of Bulk Volume Resistivity (z-axis) Versus Additive Loading Percentage (x-axis) and Additive Particle Size (y-axis), with an Additive Resistivity Hold Value Equal to 0.0000005Ω-m.**

The last surface plotted, showing the bulk volume resistivity response values over the plane of additive resistivity versus additive particle size, only seems to differ between the Minitab and data-based surfaces at values of high particles size and high additive resistivity. Unfortunately, the initial data visualization done in Excel detailed inconclusive results in bulk volume resistivity response relationship based on the interactions between the additive resistivity and additive particle size explanatory factors, most likely due to mesh sizes. This inconclusively in measured response was carried through to the response surface representing the actual measured data points, as the majority of the surface is flat.

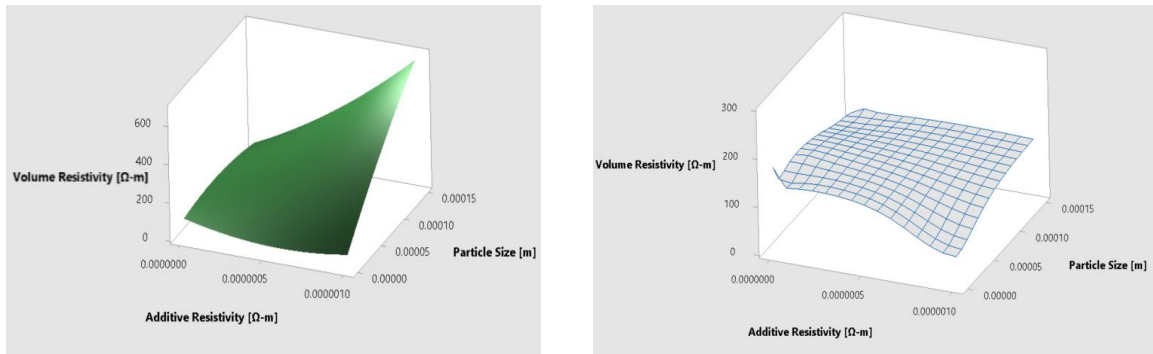


**Figure 55. Surface Plots of Bulk Volume Resistivity (z-axis) Versus Additive Resistivity (x-axis) and Additive Particle Size (y-axis), with an Additive Loading Percentage Hold Value Equal to 0.025.**

*Updated Regression and Response Surface Results*

Based on the Coded Coefficients P-Values and VIF values detailed in the initial regression analysis table shown above, the modeled terms for additive resistivity squared and the additive resistivity multiplied by the additive loading percentage interaction term were removed from the

response surface analysis design and a new regression model was created. Both the additive resistivity squared and the additive resistivity multiplied by the additive loading percentage terms had high P-Values and low VIF values, meaning that their inclusion in the overall model was not statistically significant and that neither of them were collinear enough to consider allowing them to remain in the model. Given that the regression model above was determined to be hierarchical only these terms were removed, as they were not included in any higher order terms and their constituent linear terms were left alone.

The updated response surface regression model was generated following the same procedure as the regression model shown above. The first table, the ANOVA table, output by Minitab shows an R2 value equal to 58.41% compared to the R2 value of 58.92% from the initial analysis; by removing only two non-collinear, statistically insignificant variables, the regression equation output by Minitab was simplified and in the process, only 0.51% of the model's contribution to variation was lost and reallocated to the model's error contribution percentage.

Approved for Public Release DOPSR 19-S-0112  
Placed in the Public Domain Per E18-9TPV

Analysis of Variance

Source	DF	Seq SS	Contribution	Adj SS	Adj MS
Model	7	303131	58.41%	303131	43304.4
Linear	3	188583	36.34%	31577	10525.6
Additive Resistivity [ $\Omega$ -m]	1	100786	19.42%	2735	2735.0
Loading [%]	1	63686	12.27%	6911	6910.9
Particle Size [m]	1	24110	4.65%	4266	4266.2
Square	2	59910	11.54%	88903	44451.3
Loading [%]*Loading [%]	1	38509	7.42%	83040	83039.8
Particle Size [m]*Particle Size [m]	1	21401	4.12%	19203	19202.7
2-Way Interaction	2	54639	10.53%	54639	27319.3
Additive Resistivity [ $\Omega$ -m]*Particle Size [m]	1	4549	0.88%	4264	4263.6
Loading [%]*Particle Size [m]	1	50089	9.65%	50089	50089.2
Error	181	215856	41.59%	215856	1192.6
Lack-of-Fit	13	77699	14.97%	77699	5976.8
Pure Error	168	138158	26.62%	138158	822.4
Total	188	518987	100.00%		

Source	F-Value	P-Value
Model	36.31	0.000
Linear	8.83	0.000
Additive Resistivity [ $\Omega$ -m]	2.29	0.132
Loading [%]	5.79	0.017
Particle Size [m]	3.58	0.060
Square	37.27	0.000
Loading [%]*Loading [%]	69.63	0.000
Particle Size [m]*Particle Size [m]	16.10	0.000
2-Way Interaction	22.91	0.000
Additive Resistivity [ $\Omega$ -m]*Particle Size [m]	3.58	0.060
Loading [%]*Particle Size [m]	42.00	0.000
Error		
Lack-of-Fit	7.27	0.000
Pure Error		
Total		

Model Summary

S	R-sq	R-sq(adj)	PRESS	R-sq(pred)
34.5337	58.41%	56.80%	235516	54.62%

**Figure 56. The ANOVA Table That Minitab Generated Using the Data Collected for This Set of Experiments, with the Additive Resistivity Squared and Additive Resistivity Multiplied by Additive Loading Percentage Terms Removed from the Analysis.**

The updated Minitab Coded Coefficients table details only one model term with a P-Value significantly higher than the chosen significance level value, 0.005, for additive resistivity, which has increased significantly from the first regression analysis done using the same data. However, because this model is hierarchical and the VIF value for this term is still high, the term must remain in the analysis and in the resulting regression equation.

Approved for Public Release DOPSR 19-S-0112  
Placed in the Public Domain Per E18-9TPV

Coded Coefficients

Term	Effect	Coef	SE Coef	95% CI
Constant		210.7	53.9	( 104.5, 317.0)
Additive Resistivity [ $\Omega$ -m]	174.6	87.3	57.6	( -26.4, 201.0)
Loading [%]	-31.83	-15.92	6.61	(-28.96, -2.87)
Particle Size [m]	202.5	101.2	53.5	( -4.4, 206.9)
Loading [%]*Loading [%]	150.90	75.45	9.04	( 57.61, 93.29)
Particle Size [m]*Particle Size [m]	-64.04	-32.02	7.98	(-47.77, -16.28)
Additive Resistivity [ $\Omega$ -m]*Particle Size [m]	218.2	109.1	57.7	( -4.8, 222.9)
Loading [%]*Particle Size [m]	-70.43	-35.21	5.43	(-45.93, -24.49)

Term	T-Value	P-Value	VIF
Constant	3.91	0.000	
Additive Resistivity [ $\Omega$ -m]	1.51	0.132	169.98
Loading [%]	-2.41	0.017	2.65
Particle Size [m]	1.89	0.060	302.94
Loading [%]*Loading [%]	8.34	0.000	2.47
Particle Size [m]*Particle Size [m]	-4.01	0.000	1.28
Additive Resistivity [ $\Omega$ -m]*Particle Size [m]	1.89	0.060	338.85
Loading [%]*Particle Size [m]	-6.48	0.000	1.31

Regression Equation in Uncoded Units

$$\begin{aligned}
 \text{Bulk Volume Resistivity } [\Omega\text{-m}] = & 155.4 - 43593014 \text{ Additive Resistivity } [\Omega\text{-m}] \\
 & - 5264 \text{ Loading } [\%] + 1226926 \text{ Particle Size } [\text{m}] \\
 & + 120723 \text{ Loading } [\%]*\text{Loading } [\%] \\
 & - 5769430904 \text{ Particle Size } [\text{m}]*\text{Particle Size } [\text{m}] \\
 & + 2928522678752 \text{ Additive Resistivity } [\Omega\text{-m}]*\text{Particle Size } [\text{m}] \\
 & - 18906073 \text{ Loading } [\%]*\text{Particle Size } [\text{m}]
 \end{aligned}$$

**Figure 57. A Continuation of the Updated ANOVA Table That Minitab Generated Using the Data Collected for This Set of Experiments, Detailing Coded Coefficients and the Regression Equation Output by the Analysis.**

The values in the Coded Coefficients table Coefficients column, as described in the subsection above, detail the size and direction of the relationship between the response variable and that particular term in the model, shown in coded units in order to minimize the multicollinearity among all of the model terms. In other words, a term's coefficient represents the change in the mean response associated with an increase of one coded unit in that term if all other terms are held constant; the sign of each coefficient indicates the direction of the relationship between the response and that particular term [49]. The size of the Effect value, or twice the Coefficient value, is usually a good indicator of the practical significance of the effect one of the terms in the regression has on the response variable. The updated Minitab regression equation, shown at the bottom of Figure 57, indicates that, along with the constant term, the model terms, in order of coefficient size are as follows: additive resistivity multiplied by additive particle size, particle size, additive resistivity, additive loading percentage squared, additive loading percentage multiplied by additive particle size, additive particle size squared, and finally, additive loading percentage.

Lastly, the updated Fits and Diagnostics for Unusual Observations table, shown in Figure 58, lists the all of the unusual observations that had an unequal impact on the updated ANOVA analysis and/or the regression model. When compared to the initial set of unusual observations output and shown above, only two of the initial observations (observations 157 and 176) were eliminated.

Fits and Diagnostics for Unusual Observations

Obs	Bulk Volume Resistivity [Ω-m]	Fit	SE Fit	95% CI	Resid	Std Resid	Del Resid	HI
27	125.97	194.79	7.15	(180.68, 208.90)	-68.81	-2.04	-2.05	0.0429033
36	202.62	114.53	9.06	( 96.65, 132.40)	88.09	2.64	2.69	0.0688229
88	199.51	126.66	5.46	(115.89, 137.43)	72.85	2.14	2.16	0.0249884
90	206.85	135.40	5.54	(124.47, 146.33)	71.45	2.10	2.12	0.0257133
113	202.84	110.13	7.02	( 96.29, 123.98)	92.70	2.74	2.79	0.0412660
127	196.57	126.66	5.46	(115.89, 137.43)	69.91	2.05	2.07	0.0249884
130	233.96	155.42	10.42	(134.86, 175.98)	78.54	2.39	2.42	0.0910589
169	227.38	155.42	10.42	(134.86, 175.98)	71.95	2.19	2.21	0.0910589
185	231.02	122.73	8.06	(106.83, 138.63)	108.30	3.22	3.31	0.0544351
189	287.29	194.79	7.15	(180.68, 208.90)	92.50	2.74	2.79	0.0429033

Obs	Cook's D	DFITS	
27	0.02	-0.435069	R
36	0.06	0.730918	R
88	0.01	0.345452	R
90	0.01	0.343790	R
113	0.04	0.579373	R
127	0.01	0.331176	R
130	0.07	0.765084	R
169	0.06	0.699091	R
185	0.07	0.794813	R
189	0.04	0.590433	R

R Large residual

**Figure 58. A Continuation of the ANOVA Table That Minitab Generated Using the Data Collected for This Set of Experiments, Detailing the Data Points That Minitab Has Determined to Be Unusual Observations.**

In addition to the updated set of ANOVA regression analysis tables, all of the plots shown above for the initial analysis were recreated with the updated regression model and are discussed below. The first set of plots re-made for data visualization and interpretation include the main effects and the interaction plots for the bulk volume resistivity response values shown below in Figures 59 and 60.

The main effects plot produced from the updated regression analysis has changed slightly from the same plot produced for the initial regression analysis. The curve shown for additive resistivity has gotten slightly more linear in shape, and while it overall follows the same trend, it now spans a range of bulk volume resistivity response values from approximately 125 to 300 Ω-

m. There was less of a change in shape and range observed in the curve drawn for particle size. The additive loading percentage curve has also not significantly changed in trend, but the shape of the parabolic curve has narrowed slightly, however, this is most likely due to the change in scale of these plots compared to those from the initial regression analysis.

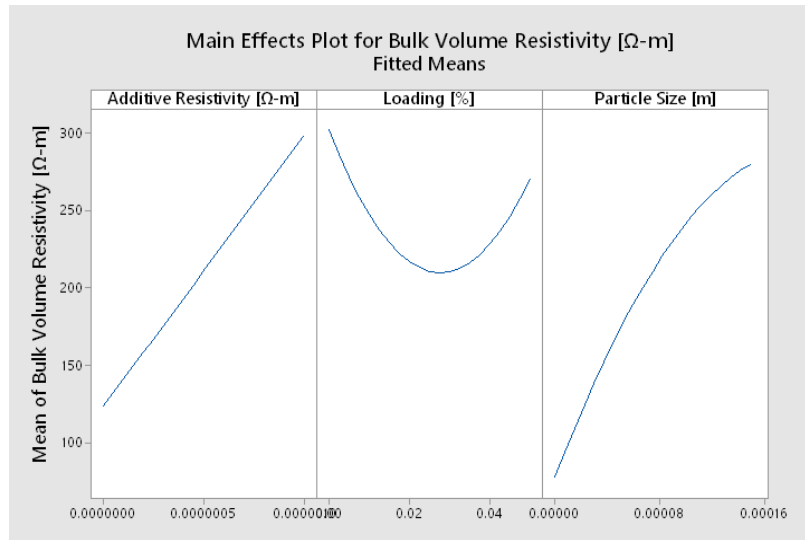


**Figure 59. The Minitab Generated Fitted Means Main Effect Plot for the Bulk Volume Resistivity Response Variable.**

The interactions plot for this updated analysis only contains two complete plots, as the interaction term for additive resistivity multiplied by additive loading percentage was removed from analysis. The trends observed in the updated interaction plots are similar to those observed in the original plots, with almost no change. There appears to be significant interaction between additive resistivity and particle size with respect to the bulk volume resistivity response, given that each of the particle size lines have different slopes and all show an intersection with the other lines. No interaction is shown in the additive loading percentage and particle size plot, and the curves all appear fairly parallel, however, the possibility of intersection could still exist off to the right of the plot, but more data would be required to either confirm or deny this speculation.

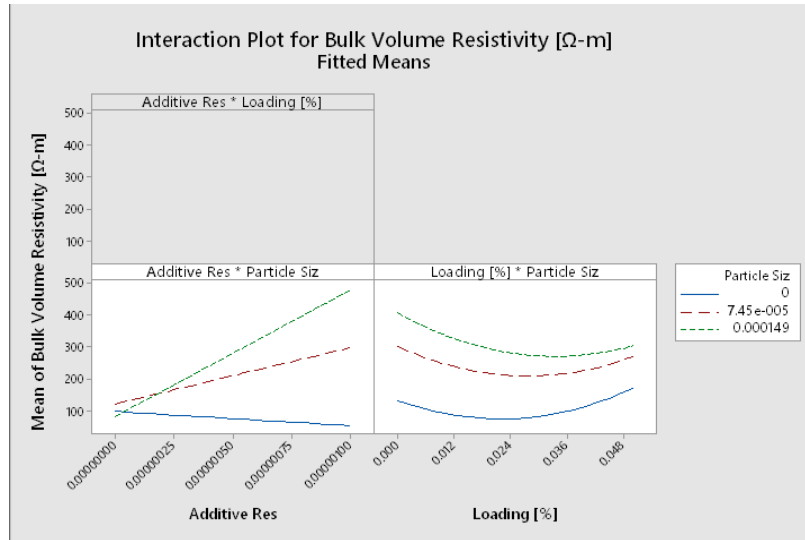


**Figure 60. The Minitab Generated Fitted Means Interactions Plot for the Bulk Volume Resistivity Response Variable.**

The response surface plots for this updated regression were also generated and are shown below next to the same blue/grey mesh surfaces generated using the actual measured values collected during testing and shown above for direct comparison.

The surfaces shown in the figure below detail the bulk volume resistivity response values over the plane of additive resistivity values versus additive loading percentages. In the plot on the left (the Minitab surface) the plotted bulk volume resistivity response surface clearly increases with increasing additive resistivity and has a distinctly parabolic shape (when compared to the original plot) corresponding to additive loading percentage where the lowest point in the “U” shape occurs at a loading value of approximately 0.023, or 2.3% percent. This surface shape indicates that additive loading percentage has a parabolic shaped relationship with measured bulk volume resistivity across the tested additive loading percentage domain and that additive resistivity has a linearly shaped relationship with bulk volume resistivity across the tested additive resistivity domain. The surface shown to the right (the surface representing the actual data point values) shows this similar “U” shape corresponding to additive resistivity only at lower values of resistivity (where the metallic additive resistivities occur).

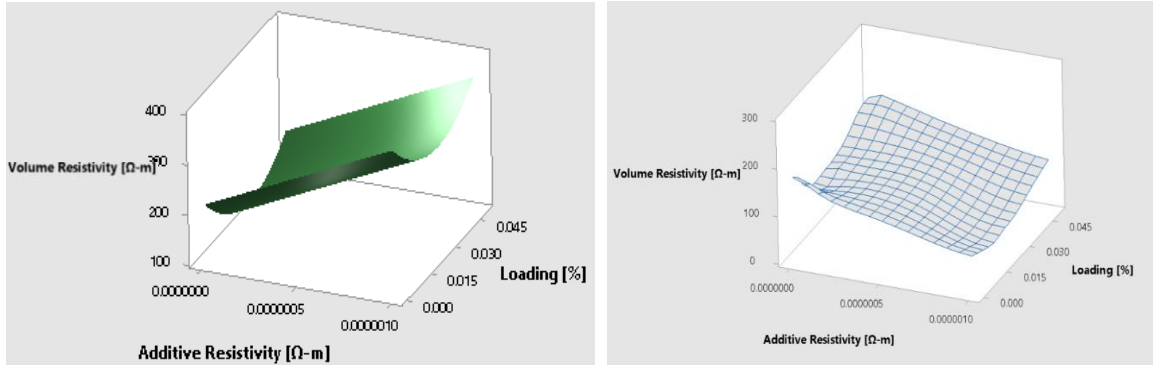


**Figure 61. Updated Surface Plots of Bulk Volume Resistivity (z-axis) Versus Additive Resistivity (x-axis) and Additive Loading Percentage (y-axis), with an Additive Particle Size Hold Value Equal to 0.0000745m.**

Following the trend of the initial results described above, the two surfaces plotted to show the bulk volume resistivity response value over the plane of additive loading percentage versus additive particle size show an incredible difference in predicted response values as particle size increases. The only observable difference in the Minitab predicted surface, when compared to the initial surface above, is the slight decrease in predicted bulk volume resistivity values when both additive particle size and additive loading percentage are large.

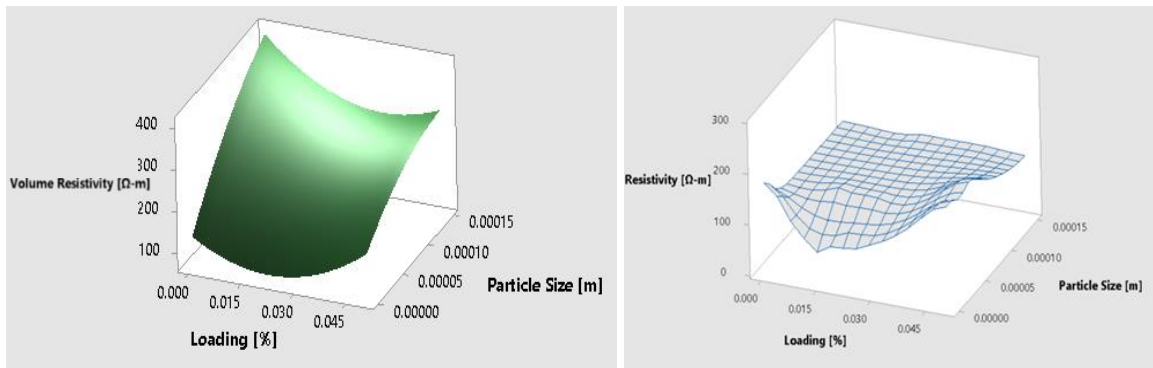


**Figure 62. Updated Surface Plots of Bulk Volume Resistivity (z-axis) Versus Additive Loading Percentage (x-axis) and Additive Particle Size (y-axis), with an Additive Resistivity Hold Value Equal to 0.0000005Ω-m.**

The final surfaces plotted, for the bulk volume resistivity response value over the plane of additive resistivity versus additive particle size, only seems to differ greatly at values of high particles sizes and high additive resistivity between the Minitab and data-based surfaces. A decrease in predicted bulk volume resistivity values by approximately 200 Ω-m is the only



observable difference, as the predicted surface shape remained the same as the initial surface shown above.

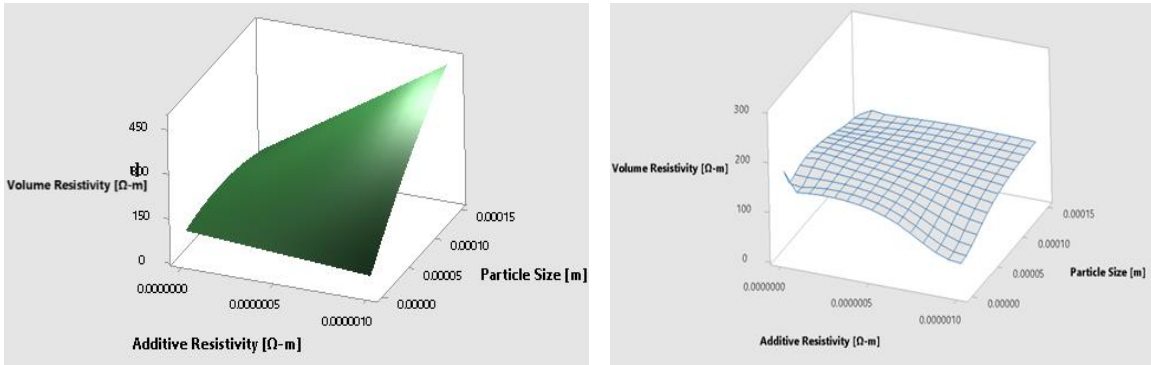


**Figure 63. Updated Surface Plots of Bulk Volume Resistivity (z-axis) Versus Additive Resistivity (x-axis) and Additive Particle Size (y-axis), with an Additive Loading Percentage Hold Value Equal to 0.025.**

### Error Analysis

Following the error analysis calculations, outlined in Equations 7-10 in Chapter 3, uncertainty values contributed to measurements from only the testing set-up measurement equipment and hardware were computed for each of the 189 specimens measured. The uncertainty values for each of the median bulk volume resistivity values presented in Table 7 have been added to Table 9 below. It is important to note that the largest of the 189 error values computed was equal to 12.6  $\Omega$ -m (computed for specimen Cu-5-1-5-8, also identified as an outlier and as one of Minitab's unusual observations).

**Table 9. The Median of the Three Measured Values at Each of the Three Test Voltages Measured from Each Sample Flat Presented with the Associated Uncertainty Value Calculated During Error Analysis.**

Median Bulk Volume Resistivity Values [ $\Omega$ -m]				
Additive/ Particle Size	Non-Additive	Tungsten	Copper	Carbon black
	Zero Loading			
<b>No Applicable Particle Size</b>	@600V = 227.4 $\pm$ 7.0  @18000V = 145.5 $\pm$ 2.9  @2200V = 164.1 $\pm$ 3.8	-	-	-

<b>Median Bulk Volume Resistivity Values [<math>\Omega</math>-m]</b>				
<b>Additive/ Particle Size</b>	<b>Non-Additive</b>	<b>Tungsten</b>	<b>Copper</b>	<b>Carbon black</b>
Light Loading (1.5%)				
<b>1-5 micron</b>	-	@600V = 80.8±1.0 @18000V = 110.1±1.7 @2200V = 121.3±2.2	@600V = 47.5±0.3 @18000V = 71.0±0.7 @2200V = 74.0±0.8	-
<b>-325 mesh</b>	-	@600V = 121.8±2.6 @18000V = 100.8±1.6 @2200V = 95.9±1.6	@600V = 143.3±3.3 @18000V = 148.0±3.8 @2200V = 173.7±5.6	-
<b>-100 mesh</b>	-	@600V = 124.2±2.6 @18000V = 108.8±2.0 @2200V = 104.6±1.7	@600V = 99.2±1.9 @18000V = 98.0±1.6 @2200V = 120.2±2.5	-
<b>Aggregate</b>	-	-	-	@600V = 41.4±0.3 @18000V = 63.7±0.6 @2200V = 82.8±1.0
Medium Loading (2.3%)				
<b>1-5 micron</b>	-	@600V = 86.4±1.3 @18000V = 67.3±0.8 @2200V = 85.8±1.5	@600V = 142.5±3.3 @18000V = 140.5±3.5 @2200V = 114.8±2.5	-
<b>-325 mesh</b>	-	@600V = 173.5±4.8 @18000V = 152.2±4.0 @2200V = 196.6±7.0	@600V = 107.9±2.0 @18000V = 99.2±1.6 @2200V = 97.8±1.6	-
<b>-100 mesh</b>	-	@600V = 103.9±1.5	@600V = 99.0±1.5	-

<b>Median Bulk Volume Resistivity Values [<math>\Omega</math>-m]</b>				
<b>Additive/ Particle Size</b>	<b>Non-Additive</b>	<b>Tungsten</b>	<b>Copper</b>	<b>Carbon black</b>
		@18000V = 159.8±4.0  @2200V = 140.5±2.9	@18000V = 110.7±2.0  @2200V = 113.7±2.1	
<b>Aggregate</b>	-	-	-	@600V = 69.0±0.7  @18000V = 46.6±0.4  @2200V = 67.2±0.7
	Heavy Loading (5.0%)			
<b>1-5 micron</b>	-	@600V = 212.9±8.6  @18000V = 203.5±7.2  @2200V = 222.4±8.4	@600V = 168.7±4.5  @18000V = 187.8±5.8  @2200V = 209.3±7.2	-
<b>-325 mesh</b>	-	@600V = 201.7±7.0  @18000V = 202.4±10.0  @2200V = 169.7±6.1	@600V = 208.4±6.3  @18000V = 184.9±5.1  @2200V = 204.2±6.0	-
<b>-100 mesh</b>	-	@600V = 115.3±2.5  @18000V = 145.0±3.2  @2200V = 122.8±2.5	@600V = 94.4±1.6  @18000V = 96.0±1.5  @2200V = 91.2±1.4	-
<b>Aggregate</b>	-	-	-	-

These calculated uncertainty values and a detailed explanation of possible causes are further discussed in the Interpretation of the Findings section of Chapter 5.

#### Summary

This chapter has detailed the qualitative and quantitative results of the experimental and analysis portions of this study for each of the 189 specimens considered for measurement.

Sample manufacturing and pilot study results were presented, as were the results of the pre-regression and response surface analysis; the resistivity response raw data, outlier corrected data, and calibration corrected data gathered during this investigation were plotted in Excel and allowed for an early interpretation of results. Following this Excel based analysis, the final calibration collected data was assessed in Minitab for normality and statistical analysis robustness, then fed through software that allowed for an initial regression and response surface examination. Once unessential contributors of variation were removed from the initial Minitab regression, an updated regression and response surface examination was conducted. Additionally, final calibration data and calibration corrected data gathered were used to calculate the amount of uncertainty present in results due to the testing equipment and hardware used for resistivity measurements.

The set of results gathered from data collection and the subsequent analysis of those results yielded a significant amount of information regarding general trends in data and raised several questions regarding the validity of the analysis performed based on sample population size and make up. Trends apparent after data analysis include: changes in propellant sample resistivity responses based on the included formulation additive, the lack of a relationship between pulse generator input voltage value and resistivity response for all samples tested, the possible effects of percolation on sample resistivity based on Excel plots detailing additive loading percentage versus bulk volume resistivity response values, and inconclusive behavior regarding the effects of particle size on sample responses. The data-based Minitab response surfaces further illustrate these trends and also offer several 3D representations of the results measured across the experimental domain. And, further statistical analysis in Minitab, based on the fitted mean and interaction plots has indicated questionable analysis predictions that should be further researched. Finally, based on the error analysis results, and on the final state of the prepared samples used for this investigation, it has been presumed that the majority of the error in measurements was most likely due to non-uniform mixing given the comparatively small calculated values of uncertainty presented.

These trends, and their implications, are further interpreted below in Chapter 5, along with a discussion of several possible avenues of research that could be carried out in an effort to further explore them.

The final result of all of the analysis completed for this investigation has yielded a regression equation, based on the data gathered and detailed above, that can be used to preliminarily predict the electrical resistivity of electric propellant samples based on the included additive's resistivity, particle size, and loading percentage. The final equation is as follows,

$$\begin{aligned} R = & 155.4 \\ & - (43593014 * \textit{Additive Resistivity}) - (5264 * \textit{Loading Percentage}) \\ & \quad + (1226926 * \textit{Particle Size}) \\ & + (120723 * \textit{Loading Percentage}^2) - (5769430904 * \textit{Particle Size}^2) \\ & + (2928522678752 * (\textit{Additive Resistivity} * \textit{Particle Size})) \\ & \quad - (18906073 * (\textit{Loading Percentage} * \textit{Particle Size})) \end{aligned} \tag{11}$$

where the final result for bulk volume resistivity and additive resistivity are in units of Ohm-meters and particle size is in units of meters.

## CHAPTER 5

### INTERPRETATION AND DISCUSSION OF RESULTS

#### Introduction

The research hypothesis under which this study was conducted, originally presented in Chapter 1, states that there exists some replacement additive for the electric propellant formulation that will both preserve the operating mechanisms of the propellant and reveal the nature of the electrical resistivity of the altered propellant samples with regard to the presence of percolation theory. That is, that some percolation curve exists for each replacement additive used that will reveal some limiting critical threshold percolation value, beyond which no added benefit of particle size or amount can be shown. This portion of the research hypothesis has been supported, as both of the replacement additives chosen for this investigation (copper and carbon black) preserved the baseline electric propellant properties at ambient pressures, and resulted in a change in propellant resistivity based upon the additive included. The various loading percentages at which these additives (including tungsten) were incorporated into the electric propellant samples manufactured for this investigation may have partially revealed the effects of percolation on propellant electrical bulk volume resistivity responses; this behavior could be further proven with added investigation, described below.

Additional statements made regarding a combination of additive properties that may negate the “electric properties” of this propellant and regarding any possible predictions about propellant performance based on electrical resistivity results were also made. The results of the bulk volume electrical resistivity responses gathered during this investigation, combined with the data gathered during the literature review conducted for this study suggest that propellant electrical resistivity responses could be loosely correlated to power consumption testing results from previous work. No conclusion can be drawn, however, regarding the negation of any electric propellant properties based on the results gathered and discussed in Chapter 4.

As discussed in Chapter 1 of this document, the significance of understanding the operational mechanism and of what improves the performance of this electric propellant formulation cannot be overstated. While the study described herein does not do this directly, until

the exact conduction and combustion mechanisms for this propellant are understood, any step taken in the direction of increasing the fundamental science surrounding the operation of this material should be considered beneficial. This chapter comprises a discussion and an interpretation of the findings detailed in Chapter 4, and will review the significant contributions of this investigation to both the understanding of the fundamental science governing the electric propellant operation and to any researchers interested in electric propellant.

#### Interpretation of the Findings

The following subsections detail an interpretation and a discussion of the significant and/or interesting outcomes described in Chapter 4, resulting from the methodologies and procedures followed or created for this study, as described in Chapter 3.

##### *Pilot Study and Sample Flat Manufacturing and Preparation Results*

The fact that the electric propellant formulations tested operate as desired with various copper additive loading percentages and particle sizes was promising to discover, as was finding out that a carbon black additive also did not affect desired propellant operation. Although no pressurized tests were done in order to confirm whether or not the on/off mechanism of the tested propellant variations is retained at higher pressures, as described in the original perchlorate oxidizer electric propellant patent, results of the pilot study completed for this investigation show that all of the 21 sample formulations tested retained the on/off operational mechanism at ambient pressures. It did not come as a surprise that all nine of the tungsten sample formulations varying in additive loading percentage and additive particle sizes maintained this ability.

Since all of the propellant variations were proven to maintain operational ability, this investigation was unable to significantly narrow in on whether or not the tungsten additive is playing a significant role based on any observed changes in propellant operating behavior based on the properties varied across the replacement additive tested (reactivity, electrical conductivity, thermal conductivity, metallic nature, etc.). Again, these pilot study tests were only performed at one input level and at one testing pressure, and it is unknown whether or not the behavior of these formulations is different than that of the baseline electric propellant formulation at varied operating conditions.

While the results of the pilot study proved interesting, the results of the sample flat manufacturing process were much more significant and perhaps point to the largest source of experimental error and possible variation in propellant properties, performance, etc. The non-additive flat produced is perhaps the most telling, due to the fact that there is no additive included to conceal the variation of perchlorate oxidizer and PVA within the sample flat. In the image of the flat shown on the left side of Figure 20 in Chapter 4, variation is apparent in the overall color of the propellant; red dye was added to the perchlorate oxidizer and deionized water solution for safety reasons, however it also serves a visual purpose, indicating where there are higher concentrations of the red dyed oxidizer solution than PVA; the PVA can be identified visually in the clearer areas of the flat and physically in the areas with a higher durometer and a hard plastic feel. Additionally, the non-additive sample flat also allows for a visual of the number of voids present in the sample due to the inability of the mixing procedure to deaerate the mixture.

The additives included in the other 20 propellant flats hinder the ability to visually determine the amount of homogeneity within each mix, however, variation in the amount of additive spread throughout several of the samples was observed by holding the sample flats up to a light. This variation can be seen in the right-most image in Figure 21 of the -100 mesh 1.5% loading tungsten sample flat. Furthermore, samples made with the smallest 1-5 micron copper additive sizes show significant variation in color and concentration across flats, most notably in the 5% loading copper sample flat shown in Figure 27. The most well mixed samples, apparent in the visualization of the data collected and discussed below, appear to be the carbon black samples. This lower variation among the resistivity results of the carbon black samples could indicate an overall better quality of mixture or could be due to the fact that since the particles/aggregates of the conductive carbon black powder were so small, and that so much was used to meet the formulation's mass requirement, that the conductive additive was much more well dispersed within the samples compared to the samples with tungsten and copper additives. The aggregate characteristics of the carbon black particles used for making these samples flats supports this idea, as particles with higher aspect ratios tend to have a higher surface area per unit volume and a more wettable surface area.



Based on the initial visual observations of the unprepared sample flats, it is clear that the mixing instructions used to produce them are lacking in ability to guide the user to a well-mixed, void-free product. This is one of the significant contributions of this investigation, as, discussed further below, it provides a starting point for the team to use to improve mixing instructions and sample homogeneity from this study forward; because the sample flats manufactured for this set of experiments have been preserved and data taken for this investigation has also been recorded and made available to the team, both can be referred to and used to determine the quality of any updated procedures and newly manufactured propellant samples.

#### *Data Collection, Correction, and Visualization Results*

Given the variation apparent in the sample flats made for specimen selection and testing, the amount of variation observed in bulk volume resistivity responses was not surprising. An initial visualization of the response results showed large differences in the responses of samples from the same flats, tested at the sample pulse generator input voltages.

Despite the amount of variation present, the linear fits applied to all of the data sets indicated, as initially found by the two-point technique analysis, performed in 2017 and described in Chapter 2, that there is no relationship between the pulse generator input voltage and the measured bulk volume resistivity response variable for any of the sample formulations tested. Interestingly, the linear fits for the 1.5% and the 2.3% data sets for carbon black, tungsten, and copper were all within a few  $\Omega\text{-m}$  of each other's y-intercept and had similar slopes approximately equal to zero, bringing into question the statistical differences between them. The 5% data sets for the tungsten and copper samples, however, had significantly higher y-intercept values and slopes approximately equal to zero, lending some credibility to the possibility of the effects of percolation theory affecting sample response.

The un-corrected data sets collected during this study do conclusively show, based on the measured resistivity of the different additives included in the formulations studied, that the removal and the replacement of the tungsten additive, in various sizes and amounts, does have some effect on the electrical resistivity of the materials that were studied. Combined with the conclusions regarding the pilot study above, this investigation was unable to narrow in on whether

or not the tungsten additive is playing a significant role based on any observed changes in propellant operating behavior given the properties that were varied across the replacement additives tested. This conclusion successfully answers the first research question established in Chapter 1 regarding whether or not the removal or replacement of the tungsten additive would yield a change in propellant electrical resistivity. This conclusion, however, does not successfully provide any supporting evidence to allow for the third research question established in Chapter 1, regarding electrical resistivity relating to propellant performance and power requirements, to be answered.

Statistically, an outlier is defined as “one or more observations in a sample that are so far from the main body of data that they give rise to the question that they may be from another population” [54]. The outliers present in this data set could have occurred due to chance, to variability in measurements taken, or could possibly indicate experimental error; after detailed inspection of the manufactured sample flats above, it is believed that any outliers present are most likely the results of variation in sample homogeneity, and identified outliers are just specimens with significantly more of one electric propellant constituent ingredient than others. Outliers can occur by chance in any distribution, but they often indicate either measurement error or that the population has a heavily-tailed distribution. In the former case, the outliers could be discarded or statistical tools that are robust to outliers could be used for analysis, and in the latter case, outliers indicate that the distribution has high skewness and that care in using tools or intuitions that assume a normal distribution should be taken. Outlier points can also indicate, in larger samplings of data, faulty data, erroneous procedures, or areas where a certain theory might not be valid.

Deletion of outlier data is a controversial practice traditionally frowned upon, and while mathematical criteria can provide an objective and quantitative method for data rejection, they do not make the practice more scientifically or methodologically sound, especially in small data sets or where a normal distribution of response results cannot be assumed. The rejection of outliers is a more acceptable practice in areas of study where the underlying model of the process being measured and the usual distribution of measurement error are confidently known; additionally, in

large data sets, a small number of outliers is to be expected (in the case of the 24 outliers chosen for retest, the number of outliers was equal to approximately 13% of the sample population). The normality of the measured resistivity response data was determined and was discussed in Chapter 4; the sample population also does not appear to have a heavily tailed or skewed distribution. Since such care was taken in performing calibration and following the testing procedures, the evidence gathered from the outliers within the same sample flats, detailed below, further indicates that mixing inhomogeneity is the most likely source of this error.

Interestingly, only two out of the 24 specimens identified as outliers for retest were unique to their sample flat and where there were groups of outlier specimens identified as close together in position within their flat, the measured resistivity values of each of the specimens was approximately the same. Again, this supports the conclusion that significant amounts of variation in observed results are due to variation in the mixed flats. Additionally, it was noted in Chapter 1, than many of the electric propellant experiments conducted in 2014 and 2015 reported that results could have been skewed due to non-uniform mixing and curing processes; it is expected, as the electric propellant mixing instructions are further refined, that variation in experimental results will decrease as propellant mixtures become more homogeneous over time. This also contributes a certain amount of credibility to the testing set-up used; as the testing set-up was able to calibrate to almost the exact value of the calibration resistor used prior to every testing session, the fact that specimens with perhaps the same kind of variation between them (based on where they were cut the sample flats) were consistently showing similar response values is promising. This coupled with the confirmation of linearity across pulse generator input voltages with a two-point resistance measurement technique is indicative of a testing set-up and a set of corresponding testing procedures that produces accurate and repeatable sample measurements that can be used to draw conclusions.

Prior to generating response surface results using the data gathered during this investigation, data visualization in Excel was completed for each phase of raw data refinement in an effort to preliminarily predict the response surface results and to use for later verification of any general trends noted during the response surface analysis. A visualization of the calibration

corrected outlier data did not show a significant amount of change in the overall trends ascertained from the non-corrected outlier data. No significant change in trends was observed across the data sets for pulse generator input voltage versus the response variable. Plots of additive loading percentage versus the response variable were created following final analysis of the pulse generator input voltage versus the response variable relationship in order to provide another way to visualize data variation. From this perspective, given the fact that both the tungsten and copper data sets follow the same trend of increasing resistivity with increasing particle loading, it is again possible that percolation theory is applicable and could be used to explain a portion of the measured results observed for some of the samples studied in this investigation. However, since the percolation threshold for this material is still unknown, as shown by the volume resistivity versus carbon black loading sloping "S" curve in Figure 3, if any of the sample sets have an additive loading near the material's percolation threshold, then measured values of electrical resistivity are likely to yield inconclusive results regarding the electrical resistivity values of that particular sample set.

Finally, plots of additive particle size versus the response variable were created, and behavior indicative of a decrease in bulk volume resistivity at an additive loading percentage of 5% as particle size increases was observed. This behavior may or may not be significant; since two different sizes of particle mesh were used at higher particle size values instead of discrete particle sizes, the this behavior could be a false result or could turn out to be much more important than originally predicted.

The final, median bulk volume resistivity results, presented in Table 7 (and Table 9) of Chapter 4, range from 41.4 to 227.4  $\Omega$ -m. The highest resistivity values measured were those measured from the non-additive sample specimens. The lowest resistivity values measured during this investigation, as shown in the Excel generated plots in Chapter 4, were those measured for the carbon black specimens; as discussed, the aggregate characteristics of the carbon black particles used for making these samples have higher aspect ratios, leading to a higher surface area per unit volume and a more wettable surface area. Both of these

characteristics would allow for an increase in electrical conductivity, and a corresponding decrease in resistivity, observed in this data set.

Recall from Chapter 2 (in the Metallic (or Otherwise) Additive, Size, and Amount subsection), Wickham's prediction that smaller particle sizes included in the electric propellant material would lead to an increase in conductivity (a decrease in resistivity). Using the average of the three median values presented for each of the pulse generator input voltage values across the reported tungsten and copper sample results and comparing, this predicted trend in resistivity is unable to be confirmed in all but the 1.5% loading tungsten samples. The non-confirmation of this trend using the resistivity values measured for this investigation could be due to the use of mesh particles sizes (of an unknown distribution), to a non-uniform dispersion of particles within samples, or both.

Experimental results indicate that the electric propellant resistivity values measured during this investigation are approximately comparable to some semiconductors with high resistivity values and some metals/metalloids with low resistivity values, as the median reported resistivity values of this electric propellant material range from the previously mentioned 41.4 to 227.4  $\Omega$ -m. The (DC) conductivity values of some of the solid polymer electrolyte compositions discussed in Chapter 2 were approximately  $10^{-3}$  -  $10^{-4}$  S/cm at 25°C, or 10 - 100  $\Omega$ -m when converted to electrical resistivity values. Provided how similar the electric propellant material ingredients are to those used in some solid polymer electrolytes, and how peculiar both mixtures are in overall composition, this result is definitely positive and promising, but was not wholly unexpected.

#### *Normality of the Resultant Data*

Due to the fact that the ANOVA analysis performed using the experimental data gathered for this investigation was performed under several limiting assumptions, the normality of the data was analyzed prior to performing the regression and response surface analysis in Minitab. As mentioned above, outliers within a data set, especially if the data set has a heavy-tailed distribution, could indicate a high skewness; if this high skewness is present, care in using tools or intuitions that assume a normal distribution should be taken. The verification of a normal data distribution was performed using a probability plot, rather than a histogram plot (even though a

histogram plot was also produced), as a probability plot is usually considered more reliable than the histogram for small or moderately sized sample sets.

Given that the response data gathered during this investigation is not perfectly normally distributed, and that one of the three assumptions governing the validity of ANOVA results does not hold up, it is possible that the chances of getting falsely negative results for the response surface analysis, performed using this data and described below, are increased. Given this information, the robustness of the response surface regression ANOVA could be called into question. However, given that the data does not appear to be heavily tailed, as detailed above, that the calculated AD-value is equal to 1.713 (larger AD-values indicate non-normally distributed data), and the fact that the ANOVA test makes inferences about mean values (or expected average response at chosen factor levels) and not about the tails of the distribution, it was decided to proceed with response surface regression analysis.

#### *Initial and Updated Regression and Response Surface Results*

The results from the initial regression and response surface analysis done in Minitab using the measured response results indicate that a quadratic regression model containing linear, square, and two-way interaction terms was able to account for approximately 59% of the variation observed in the data set studied above. The other approximately 41% of the variation observed was attributed by the analysis to error due to either a lack of fit or to pure error. The initial regression analysis R<sup>2</sup> value (the statistical measure of how closely the data matches the fitted model) of 58.92% was surprising given how limited the domain of the data set input into Minitab was; again, note that this study was meant to encompass a set of screening experiments and it is possible that some of the factor effects that could be effecting the electric propellant material's resistivity response could have been missed/not included. The contribution values determined for each term were as expected, with additive resistivity followed by additive loading percentage accounting for the most variation in the model.

The initial Excel data visualizations, plotted for the early determination of general trends, were able to separately illustrate the magnitude of the resistivity responses of each set of samples for early analysis, and preliminarily informed the comparison of all of the bulk value

responses across additive type. This turned out to be very helpful in identifying unexpected Minitab predicted results, as detailed below. Additionally, the Excel plots illustrated that the resistivity response values for the tungsten and copper samples were larger at higher additive loading percentage values, enough so to assume that this trend would have also been illustrated with the carbon black samples, even though the 5% loading sample was not able to be manufactured for testing. The Excel visualizations were also able to illustrate (although somewhat clouded by the amount of variation in the data) that the average bulk volume resistivity responses do increase as additive loading percentage increases, which could be possible evidence of the effects of percolation on this material, and may be indicative of at least part of the “S” curve detailed in Chapter 2. Finally, the Excel plots detailed some interesting, but non-conclusive trends regarding the effects of additive particle size that would not have been revealed by the response surfaces, however, whether or not these trends truly exist, and if they are indicative of overall material behavior and/or properties must still be determined. Outlier identification and re-testing may also have been done differently, perhaps using the Minitab Fits and Diagnostics for Unusual Observations table to identify outliers instead of the 10% trimmed mean approach. Overall, these initial visualizations were incredibly enlightening, as the amount of variability in the data would not have been as apparent had the response data been directly input into Minitab.

It is believed, however, that the Minitab analysis has over emphasized the value and contribution, based on fitted mean values, of particle size based on the plots shown in Figures 53, 54, and 55. Based on further inspection of both of the fitted means main effects plots shown in Chapter 4, specifically the additive resistivity plots, the fitted mean bulk volume resistivity point representative of the carbon black samples is dramatically higher compared to the actual response value data. This is also true for the fitted mean values shown in the interactions plot. The fitted means interaction plot of additive resistivity and additive particle size indicates with lines that all cross, each of a significantly different slope, that the interaction between these two variable is important. While it is possible that particle size is a more important factor than originally thought, due to its possible effect on percolation within samples, if applicable, this cannot be concluded based on the data gathered and the results produced for this investigation

due to the limited domain and the fact that mesh sizes were used in place of discrete particle sizes. The two response surface plot comparison figures (Figures 54 and 55) predict a significant increase in bulk volume resistivity response as particle size increases, when in fact, the actual collected data in the regions of responses for those same areas have been shown to be consistently flat surfaces.

It is thought that this error could be due to the fact that tungsten, copper, carbon black, and the non-additive samples were all analyzed under the assumption that they were all additives, or a lack of additive, that could be compared on the same scale across all of the analysis work done. In order to remedy this, a nested analysis would have to be performed, however, this was out of the scope of this study and it is preferred that this analysis be completed when more data is available so conductive and non-conductive metallic and non-metallic additive combinations could be equally analyzed separately and then compared for review. Future work that could be done in order to test this theory is discussed below in the Recommendations section.

Following the analysis of the initial regression and response surface results, a better understanding of which regression equation terms were actually accounting for significant contributions in variation was desired. This understanding was gained by eliminating terms from the initial regression equation that did not or could not account for significant sources of variation based on both their P- and VIF Values, which allowed for a manual simplification of the regression equation initially developed. After eliminating the additive resistivity squared term and the additive resistivity multiplied by the additive loading percentage term, as both were determined to not be as statistically significant as the other seven terms included in the initial regression equation, the updated Minitab regression analysis indicated that only 0.51% of the model's contribution to variation was lost. This is promising, as it means that the removal of these two terms was justified and would not significantly impact the predictions of any further results made using this regression equation. Additionally, the removal of these two terms revealed a significant behavior in the additive resistivity versus additive loading percentage response surface that was clouded in the initial responses. This updated response surface indicates that the 2D curved response behavior shown across additive loading percentage is consistent across all of



the additive resistivities tested. The actual data plotted in this surface format, shown next to the predicted surface in Figure 61 of Chapter 4, partially shows this behavior, however it is not as clear because it is based on actual data and is lacking in domain enough to not be fully conclusive. The predicted surface also displays a linearity of response values across additive resistivity values, which is again not conclusive in the actual response surface, and more data is needed to verify this behavior.

Both the initial and updated response surfaces generated for additive resistivity versus additive loading percentage and of additive loading percentage versus additive particle size surface show the 3D representation of the 2D curved, or parabolic, response behavior in both the initial and updated main effects plots output by Minitab. This parabola with its vertex, or lowest point, occurring at the approximately 2.3% additive loading value could be indicative evidence of the effects of percolation. The shape of the resulting parabola is not as expected compared to the "S" curve shown in Figure 3 of Chapter 2. However, this parabolic curve could prove to be only one of the halves of an "S" curve, especially given the limited number of additive loading percentages tested. If this is the case, following the collection of more data points, the two parts of the "S" curve could be analyzed as a piece-wise function made up of two quadratic curves. Furthermore, the existence of the estimated percolation threshold value of 3.4%, chosen based on information gathered during the research process for the Literature Review section of Chapter 2, cannot be confirmed based on the experimental results gathered or on the Minitab regression analysis performed for this study. Should other values of additive loading percentage, if tested in the future, be combined with this data set, and analyzed similarly, reveal an "S" or inverted "S" curve shape and/or the existence of a percolation threshold, then the behavior of this propellant, at least with the additives studied is effected somewhat by percolation theory in combination with any other conduction/combustion mechanisms that allow for its current operating behavior.

While the question of whether or not propellant properties and/or operation is in some way effected by percolation cannot be definitively stated, partial evidence of the possibility of this relationship is present in the results of this investigation. This relationship could be definitively established with the completion of some of the future work discussed below in the

Recommendations section. The second research question established in Chapter 1 of this document cannot be fully confirmed or refuted.

### *Error Analysis Results*

There are several different types of error that may contribute to the approximately 41% lack of fit/error identified by Minitab in both sets of regression analysis. Aside from the lack of fit accounting for 14.46% of the error contribution, as indicated by Minitab, a combination of both random error and systematic error could be contributing to this 41%; the types of random and systematic error that could be present in the collected data are discussed below. These possible sources of error are separate from the significant amount of variation present in the samples due to sample manufacturing and preparation, as this source of error has been thoroughly covered. Random error, or errors for which the causes are unknown could always be present, however the amount of data taken, three randomized measurements at three different pulse generator input voltage values for each propellant flat, should have allowed for the reduction of this kind of error due to the size of the data set. Errors introduced and propagated into the results from the working environment, including humidity, temperature changes, and/or electronic noise could have skewed resultant data, although care was taken to try to eliminate these errors, the negative water absorption properties of the propellant have been discussed and slight temperature changes throughout the day could have impacted resistivity measurements. Several electronic instruments were used in the testing set-up designed for this experiment to measure the values used to calculate electrical resistivity; these instruments all have finite precision of varying degrees, which limits their ability to resolve small measurement differences. The pulse generator for example, has only an analog input dial on which tick marks occur every 50 V, so an exactly accurate value of 600 V, 1200 V, or 1800 V may not have been pulsed correctly for every measurement taken. Additionally, physical variations in propellant samples tested, detailed thoroughly above, are probably the most significant contributor to the 26.62% pure error detected in the data set input into Minitab.

Based on the manner in which experimental mixing and testing was conducted (randomized across mixing days and discrete testing sessions) it is unlikely that a significant amount of

systematic error is present, as personnel technique remained the same throughout and observer bias was eliminated as much as possible. However, during the design and development of this study, the experimental designer could have failed to account for a significant explanatory or testing factor; this factor could be contributing error to the experimental results or could account for the lack of fit of the model. Again, it is important to mention here that this investigation was designed as a set of screening experiments, meant to aid in pointing researchers in a direction of study that might yield further useful results regarding the conduction and/or the operational mechanisms of the electric propellant baseline formulation and some of its variations.

As shown in the Error Analysis section of Chapter 4, some of the error identified by Minitab can be quantitatively identified via the actual or estimated uncertainties of the testing equipment and hardware used by propagating those values through the resistivity calculation. Chapter 4's Table 9 details the uncertainty values for the median reported specimen bulk volume resistivity values measured at each of the three testing voltages calculated following the error analysis methodology outlined in Chapter 3. When compared to the presented values for bulk volume resistivity, these uncertainties all appear reasonable, considering they only take into account the uncertainty propagated through the testing equipment and hardware and not errors in the propellant mixing, as those were considered too difficult to quantify for the purposes of this investigation.

It has been assumed throughout that the equations used for calculating resistivity and error propagation account for the testing set-up calibration/measurement errors that could impact the results most significantly. Based on the results presented in Chapter 3 and discussed here, it is likely that the uncertainty in measurements due to the testing equipment and hardware have contributed to the 41% error identified, however, it is unlikely that this uncertainty was the most significant contributor of error to the results of this investigation. The disadvantages of this kind of error propagation include: not accounting for any unsuspected covariances, error in which the reported value of a measurement has been altered rather than the measurement itself, and any mistakes made in propagating the error through the resistivity or error propagation formulations [55].

#### Additional Observations

The difficulty of manufacturing and the eventual elimination of the 5% loading carbon black sample flat was concisely discussed in the Pre-Mixing Sample Manufacturing subsection of Chapter 4. The failure to manufacture this sample flat was understood to be due to the wettability of the carbon black used and of the formulations' ratio of wet to powdered ingredients. "Wetting the [carbon black] pigment particles is essential for them to be finely distributed in a liquid. Air entrapped in the pigment powder must be fully removed and the pigment particle completely surrounded by the liquid medium." The process of manufacturing used for this investigation was seemingly unable to effectively wet the amount of carbon black aggregate required in the 5% loading sample flat enough to promote thorough material mixing and even additive dispersion.

It is unknown, however, whether or not the full wetting of carbon black would be advantageous in an electric propellant application that would make use of a carbon black additive. If the electrical resistivity of this propellant is dependent in any way on the additive included in the mixture, which it has at least partially proven to be, then fully surrounding each particle of the additive would effectively reduce the interactions between the additive particles, if not totally destroy the clusters allowing for the percolation phenomenon to effect the material. If the electrical resistivity of this material was only partially dependent upon the additive, or not at all dependent, but the material additive was discovered to be advantageous to properties or performance in another way, the wettability of additive particles and its influence on additive dispersion and interaction with other formulation ingredients should be considered.

The significant number of voids present in each of the sample flats manufactured for this investigation was mentioned briefly in the Data Collection and Initial Raw Data Visualization and Outlier Identification, Re-Testing, and Visualization subsections of Chapter 4. In conventional solid rocket motors, trapped air, in the form of isolated air bubbles, channels of air, or cracks, also known as voids, is normally considered intolerable. These voids can be considered uncontrolled burn rate modifiers due to the fact that the solid propellant combustion process is dependent upon burning surface area and any voids within the propellant represent local increases in the surface area available to be burnt. Voids in the propellant also decrease the overall propellant

density. The effect of voids in electric propellant operations are currently unknown, as are the effects of voids on the resistivity measurements made for this study; it was stated in Chapter 2 that several aspects of the operation of this propellant material are still unknown, including the amount of arcing occurring within propellant samples due to voids created during the mixing and casting process. However, it has been speculated that any effects could be similar in nature to those in conventional solid propellants, if not worse, given the currently suspected operational mechanisms of this electric propellant formulation. Degassing is common practice during conventional SRM propellant and hybrid fuel mixing and casting; an attempt to mirror this process using the vacuum pump embedded within the Thinky mixer exists in the current set of electric propellant manufacturing instructions, however, given the resultant state of the 21 sample flats manufactured, there is definitely room to improve with regard to void removal.

Included in some of the data written in the Literature Review section of Chapter 2, some anecdotal evidence of electric propellant formulation relating to power consumption does exist. The ninth electric solid propellant formulation sample made and tested in 2011, a mixture of 60% perchlorate oxidizer solution, 20% PVA, and 20% tungsten powder additive, or what is known today as the baseline formulation, had the lowest power consumption out of all of the RMS and DSSP samples tested in the same study. Two of the other samples tested included 80%/20% and 70%/30% perchlorate oxidizer solution/PVA mixtures, both of which had some of the highest measured values for power consumption. Based on the results from this investigation, indicating that the non-additive samples had higher resistivity values than any of the samples including a tungsten additive, credibility is given to the fact that a relationship between propellant electrical resistivity and performance and/or power requirements may exist, since the propellant samples that were previously tested had higher levels of power consumption and were shown in this study to have resistivity levels corresponding to a proportional relationship. Further information about future work that could prove or disprove this relationship can be found in the Recommendations section of this chapter. The third research questions established in Chapter 1, regarding the relationship between propellant electrical conductivity and performance, cannot be fully answered based on the results of this study, however, the above does provide some reasoning grounded in

experimental results throughout the electric propellant's lifetime that positively indicate the possibility of a relationship.

Additionally, each specimen tested was electrified and measured only once throughout its lifetime, due to the fact that the impacts of this kind of electrical impulse on specimens' material and electrical properties was not well understood at the time of testing. For the purposes of this investigation, it was assumed that each specimen tested was considered damaged or unusable after being electrified. (An exception was made here for the retesting of outliers, as this retesting was done after a significant amount of time had passed following the completion of sample testing; it was assumed that several supposed effects had diminished and samples were safe to retest. This, however, has not yet been proven.) For this reason, a total of nine specimens were tested for each cell in Table 3. Had only three specimens been assigned to each of the cells in Table 3, meaning the same specimen would have been tested at all three pulse generator input voltage values, the amount of variation in the resulting data might have been reduced. On the other hand, the variation in and across samples was a useful factor in determining the quality of overall sample mix and in solidifying some of the effects of poor mixing on testing results.

#### Revised Limitations

The majority of the limitations of this study were detailed in the Scope and Delimitations and the Limitations sections of Chapter 1, however based on the data gathered during this investigation and the discussion above, it is clear that the screening experiment delimitation discussed in Chapter 1 was even more limiting than initially predicted. In order to draw accurate conclusions regarding the effects of percolation and the correct shape of the response surfaces discussed throughout this document, more data is, without a doubt, needed. A range of loading percentages from 0% to approximately 7 or 8%, or as high as possible based on manufacturability, would most likely be sufficient for determining a definite value of the percolation threshold for this propellant based on each additive material used. Additionally, the addition of data collected from samples made with a larger selection of metallic and non-metallic additives might be able prove or disprove the assumption that all included additives, or a lack of additives, can be compared on the same scale across all of the analysis work performed.

Although more work would be required to generate this data, including creating propellant formulations with an expanded number of additive loading percentages and included additives, retesting, and updating the Minitab analysis with this new data, using the methodologies created or followed in Chapter 3 would allow for work to be done quickly and efficiently. This is further discussed in the Recommendations section below.

#### Threats to Validity

Internal threats to the validity of the results derived from this screening experiment, as discussed above include the following: the fact that distribution of the response results were not perfectly normal, which could account for any error and/or unknown false negatives in the output of the Minitab regressions, and the conclusions made based on particle size due to the fact that two mesh particle sizes (with unknown particle size distributions) were used for the larger particle size orders in place of discrete values. Particle size may turn out to be more or less important than the results above have indicated.

Additionally, there exists possible threats to the validity of the regression equations for several reasons, the first being that this set of screening experiments was only varying additive type, additive amount, and additive particle size; the regression equations produced only account for these changes in propellant formulation. Furthermore, an attempt to model a regression equation to explain resistivity behavior using one set of non-additive data, two sets of metallic additive data, and one set of non-metallic additive data may not be valid provided some of the resultant observations. Given the knowledge gained from this outcome, it may be prudent to attempt to model at least the behavior governing the change in resistivity of metallic and non-metallic propellant formulations separately and compare them to the results of this study to determine accuracy and validity. An expansion of the screening experiment domain, as mentioned in the section above and discussed further below, could help to lessen or eliminate some of these threats.

Effects of the amount of water within the tested specimens on measured specimen resistivity were briefly touched on in the Related Previous RMS Work subsection of Chapter 2 and in the Sampling and Sampling Procedures subsection of Chapter 3. Previous results have indicated that

a decreasing amount of water included in the baseline formulation caused average measured specimen resistance to decrease, this testing, however, has not been verified with a repeated experiment. As such, and with the exception of sample storage, the results of this testing were not greatly factored into the design of this investigation; samples were kept in a desiccator at approximately the same humidity values throughout the life of this set of experiments in an attempt to prevent any change in sample water content over time. Additionally, it was believed that any error in resistivity measurements due to a change in specimen water content would not have significantly altered resistivity measurements based on the magnitude of some of the other errors present in measurement data and discussed throughout this document. Another possible expansion of this set of screening experiments could include a study designed to quantify the effects of water content on the resistivity of electric propellant samples. This experiment would serve to both verify previous RMS testing results and could lend some credibility to the assumption that water content related error is not as significant as some of the other experimental errors detailed. The results of this experimental expansion would also be useful in quantifying the severity of the hygroscopic nature of the baseline formulation used in this study and its possible effects on propellant operation.

Externally, the validity of the results gathered from this investigation, as well as from other investigations of the same baseline propellant formulation and its variations, is questionable given the unique nature of this formulation and its lack of characterization outside of RMS and DSSP. However, comparisons between the electric propellant resistivity values and known industry values for the resistivity of solid polymer electrolytes and doped PVA could provide some data for triangulation and verification of results, but again, given the peculiarity of this mixture, it is unlikely that any closer verification of electric propellant resistivity values would occur in the near future.

#### Implications

The implications of the results observed and/or determined from this investigation cannot be overstated, as they indicate several previously unknown trends in the electric propellant material. Firstly, discovering that this electric propellant's on/off operating mechanism is preserved in variations of the baseline propellant formulation including the copper and carbon black additive



variations is hugely significant and could lead to additional studies/discoveries of the operational differences between these formulation variations that can be used to expand the ability to use this propellant in a variety of applications.

Although discovering that the current version of the electric propellant manufacturing instructions leaves substantial room for improvement was not very favorable, it does open the process up for advances in methodology and could/should lead to the tightening of measured variation in electrical resistivity within and across all samples made with improved manufacturing instructions. Furthermore, as described in the Literature Review section of Chapter 2, it has been shown previously that electric resistance could be used as a measure of the amount of water present in the material. Given the results detailed above, it could be said that electrical resistivity could also be used as a measure of, at least and if nothing else, the “goodness” or overall homogeneity of a propellant mixture.

Should, at a later date, it be possible to gather more experimental data to fill in the holes of the domain used for this screening experiment and discover the presence (as well as what model best represents observations) or lack of the percolation phenomenon and any local minimum and/or maximum in the newly filled in response surfaces, the information gained from understanding how additive type, amount, and particle size affects the resistivity values of this electric propellant formulation can be used to the team’s advantage later when designing propellant formulation variations for systems that utilize this type of propellant. Additionally, understanding how an additive affects the behavior of this propellant and/or its material properties may also provide evidence to support the processes believed to be occurring during the initiation and burning of the electric propellant, as theorized by Langhenry and discussed in detail in Chapter 2. It is possible that the electric propellant additive is aiding in the electro-chemical reaction that initiates burning through the generation of a fuel and an oxidizer; the additive should also relate somehow to the propellant’s resistive heating phase of operation. Furthermore, if information connecting the initial resistivity value of the propellant and its power consumption could be determined, systems could be more accurately tuned to work for particular applications.

## Recommendations

Based on the results of this study and their interpretation, several recommendations for future research that could be completed in order to expand the experimental domain and/or to further the conclusions made herein, or to aid in answering the research questions that were not able to be firmly resolved within the scope of this investigation are detailed below.

### *Pilot Study and Sample Flat Manufacturing Results*

The results of the pilot study indicated that all of the formulations created for this investigation maintained the on/off operating abilities of the baseline propellant formulation at ambient pressure. Since it is unknown, however, whether or not all of these propellant formulations maintain this capability at higher operating pressures, it is suggested that a simple study be designed to investigate this operational phenomenon. Testing each of these sample formulations at those pressures at which the baseline formulation is known to operate may reveal that all of these formulations maintain this on/off ability, in which case, they could all be advanced as possible formulations for the many applications of this material. If some of the formulations display an inability to be turned on or off, both, or neither, at higher pressures, then the differences in resistivity, as well as in the varying properties of the included additives, could indicate an area of study for researchers to explore that would help contribute to the working knowledge base surrounding electric propellant operational mechanisms.

Based on the mixing results, shown in Figures 20-26 in Chapter 4, it is clear that the current electric propellant manufacturing instructions leave some “goodness” of mix to be desired, especially with regard to mix homogeneity and voids. In the case of the voids, a more thorough degassing practice, as mentioned above, could be implemented, as could a better method for casting samples that would allow for air bubbles to be pressed out somehow. Additionally, using the pre- and post-testing mass values recorded for each of the tested specimens during this investigation, a density and/or a detailed void analysis could be performed on certain specimens which could then be fired or further tested for other electrical and/or physical properties; the additional measurements and/or performance results could hint at the effects of voids in this material. These updated measurements could also be used in a study designed to repeat and

verify the specimen resistivity and water content relationship results detailed in the Previous Related RMS Work subsection of Chapter 2.

*Data Collection, Correction, and Visualization Results*

Given the amount of variability across all of the samples flats made to be tested for this study, the recommendation/desire to improve the current electric propellant manufacturing instructions, and the suggestions made above regarding the resistivity testing procedures created for this study to possibly serve as an indicator of the “goodness” of propellant sample homogeneity, it is suggested, once manufacturing instructions have been improved, that the worst mixed sample flats from this investigation be remade and re-measured. If the variability across response variable results decreases, it would be safe to say that the new manufacturing instructions were headed in the right direction. Additionally, the newly taken data could replace the original data sets used for this investigation and response surface analysis could be redone and compared to the analysis presented in Chapter 4 to see if any overall change in trends could be identified.

As detailed in Chapter 4, the reason for such a variation in the original versus the outlier retest resistivity measurement is unknown, as all of the outlier’s chosen for retest were originally measured across seven testing sessions and in random order with the rest of the 165 specimens tested. Variation could be explained by further examining the specimens tested for this investigation to see if large concentrations of one ingredient made up more of certain specimens than others within their flat. This would make sense given that most of the outliers were from the same flats and were located close together within those flats; this could also provide further explanation of how different concentrations of propellant ingredients effect resistivity results if ingredient concentration measurements were related back to the data gathered for each specimen. Results could/would also provide further evidence in favor of updating mixing instructions.

Also detailed in Chapter 4 is the fact that, based on the initial Excel visualizations, more data is needed in order to determine if the observed decrease in resistivity with an increase in particle size is truly occurring with particle size (and is not as a function of the mesh sized particle

additives) and if it is actually significant enough to affect resistivity results. This could be done simply by remaking all of the samples manufactured with the -100 and -325 mesh particle sizes using discrete particle sizes of the correct order, retesting nine specimens from each of the newly made samples, and replacing the current mesh particle size specimen data with the newly measured discrete particle size data for analysis.

Finally, based on the results from this investigation, detailed in Chapter 5, indicating that the non-additive samples had higher resistivity values than any of the samples including a tungsten additive, credibility is given to the fact that a relationship between propellant electrical resistivity and performance and/or power requirements may exist, since the propellant samples that had been previously tested were shown to have higher levels of power consumption. This relationship could be verified using of several of the specimens from this investigation, configuring them into a testing apparatus designed to measure the power consumption of each specimen during firing, and comparing measured resistivity values to measured power consumption levels.

#### *Response Surface Model Results and Revised Limitations*

All of the results and conclusions made during this investigation have either somewhat or significantly indicated the need for more data. The addition of more data to the database completed for this study could, firstly, be used to redefine both the predicted response surfaces and the actuals shown in Chapter 4. The addition of new data to the current response surfaces would allow for further surface refinement based on actual measured responses and may reveal additional surface features not visible based on the current data set. New and denser data, especially in the areas of interest on the actual response surfaces could also help to clear up remaining questions regarding the applicability of percolation theory to the resistivity responses of this type of propellant and, if applicable, may yield a possible percolation threshold location. Furthermore, this relationship could be definitively established with the addition of several specimen measurements to the current data set made on samples manufactured with additional additive loading percentage values; these values could include, for example, any combination of additional loading percentages, for example 0.5%, 2.0%, 3.0%, 4.0%, 5.5%, and 6.0%, or otherwise as needed.

Recall, that upon further inspection of the initial and updated fitted means main effects plots shown in Chapter 4, specifically the additive resistivity plot, the fitted mean bulk volume resistivity point representative of the carbon black specimens was dramatically higher compared to the actual response value data. This was also true for the fitted mean values shown in the interactions plot. As detailed in Chapter 4, it is believed that this error could be due to the fact that tungsten, copper, carbon black, and the non-additive samples were all analyzed in Minitab under the assumption that they all included additives, or a lack of additives, that could be compared on the same scale across all of the analysis work performed.

In order to remedy this using only the current data set, a nested analysis would have to be performed in which specimen results would be nested under metallic, non-metallic, or non-additive categories. Given the limited domain and small number of additives tested during this investigation, it is recommended that instead of following a nested analysis approach using the current data set, that any repeated or further analysis be completed when more data is available so that conductive and non-conductive metallic and non-metallic additive combinations could be equally analyzed separately and then compared for review.

Due to the limited domain that was explored during this investigation, and because the Minitab regression analysis was only 2nd order (linear, squared, and two-way interactions), the final regression results have been fit to this set of data as best they could be, however, it is possible that a more accurate model with higher order terms exists. Additional work furthering the model currently fit to the data, or furthering a similar model fit to an expanded domain data set, could yield higher R<sup>2</sup> values and a model that is able to account for a greater percentage of variation within the data as long as care is taken so as not to over fit the data.

Furthermore, because the regression equation output by Minitab was only modeled to this specific set of non-additive, tungsten, copper, and carbon black data input, an overall domain expansion would serve to further generalize a regression model to the overall trends shown to be the most important in the electric propellant resistivity response behavior. Using additional metallic additives with resistivity values that differ from both tungsten and copper (such as zinc and tin) and additional non-metallic or metalloid additives that differ from carbon black (such as

germanium or silicon and boron) would allow for the separate analysis of conductive metallic and non-metallic additives. This separate analysis could then be compared with the results presented in Chapter 4 and used to determine whether or not a separate analysis of propellants formulated with varying types of additives is necessary, as it is currently believed to be.

With the current data set, further analysis work could be done in order to attempt to capture the amount of variation in the mixing of the samples, as mentioned above, by applying a coded “quality of mix” scale to all of the specimens tested. This breakdown would quantify the homogeneity of each specimen over a pre-determined scale and another regression analysis similar to the two detailed in Chapter 4 could be performed taking this scale into account.

Based on the data gathered during this investigation, and the resulting interpretations, it is clear that the screening experiment delimitation discussed in Chapter 1 was even more limiting than initially predicted. This set of screening experiments could be expanded in several ways to address the research questions established in Chapter 1 of this document and to address several of the additional questions that surfaced during the testing and/or analysis phases of this investigation. Again, with respect to the possible additives that could be used, recall that Wickham suggested investigating metallic additives with reduction potentials similar to that of tungsten, but choosing metals with different oxidation states for the purposes of determining if a metal capable of both a positive and a negative oxidation state will burn under the same conditions as the tungsten does in the current formulation. Additionally, and even though it was eliminated from this study, aluminum as a metallic additive should still be of interest due to the non-preservation of the on/off firing abilities of samples made with a powdered aluminum additive.

Since the analysis results from this investigation have revealed that particle size may be more important than it was originally believed to be (this was part of the research design justification for using meshes instead of discrete particle sizes), the effects of particle size on the resistivity response values should be further explored. The data gathered for the two mesh particle sizes used for the order  $10^1$  and order  $10^2$  particle size ranges chosen could be either replaced or expanded upon with data measured from samples made of particle sizes in discrete ranges within the desired orders (as detailed in the subsection above). This could be done for the

entire experimental domain used for this investigation or could be performed as an in-depth study of particle size done with a singular additive until the understanding of what affects the operational mechanisms of the baseline electric propellant formulation have been further advanced.

#### *Threats to Validity*

Given that this investigation was designed as a set of screening experiments and such significant amounts of room in which to expand both outwardly across the domain and deeper down into some of the more specific problems and questions addressed here exist, anything that can be done to address all of the previously identified internal threats to validity offers valid recommendations for future work. An expansion of the screening experiment domain, as detailed in the section above and discussed further below, could help to lessen or eliminate some of these threats.

In addition to expanding the domain further with varied replacement additives, an expansion of this study into alternative oxidizers, binders, etc., also suggested by Wickham, could be done in order to further understand the contributions of the propellant chemicals to its electrical resistivity response values, in which case, a comparison of results with industry studies on solid polymer electrolytes and doped PVA samples may prove more helpful. Moreover, both a study with an expanded replacement additive domain and/or an expansion of this study into the additional propellant ingredients could be set up to measure additional response variable values, electrical or otherwise, and would allow for the observation of any possible interactions between changes in the metallic additive properties/amounts and either the oxidizer solution, binder, or both. A detailed study of what is considered to be the propellant material's binder would be recommended over the propellant oxidizer based on the discussion of the major determinants for ESD sensitivity in solid rocket motors in the Literature Review section of Chapter 2. Recall that the results of Covino and Hudson's work showed that the solid propellant electrical properties were influenced the most by the hydroxyl-terminated polybutadiene (HTPB) binder and to a lesser extent, the concentration and size of the added aluminum powder particles.

## Conclusions

With respect to the research questions established in Chapter 1, the first question, meant to address whether or not a change in propellant properties or basic operation would result from an alternative additive included in its formulation, has not been answered based on the current data set, but the answer could change following the completion of some of the recommendations for future research made above. Electric propellant resistivity does change based upon the included additive, and with respect to this data set tested only at ambient pressures, no definite evolution of the understanding of the additive contributions to the electric propellant's conduction and/or combustion mechanisms was achieved.

This set of experiments and the resulting data have revealed a parabolic response behavior visible in the 2D and 3D additive loading percentage versus additive particle size visualizations. The lowest point of this parabola, occurring at an approximately 2.3% additive loading percentage value, could be indicative of the effects of percolation on this material. While the parabolic shape of this behavior does not follow the traditional "S" curve trend indicative of percolation theory, the measured responses summarized above may only be a partial piece of this expected curve. Both the hypothesis under which this investigation was conducted and the second research question established in Chapter 1 seek to examine the possible influence that percolation theory has on this material's properties and operation. The effects of percolation on the propellant have been neither confirmed nor denied given the resulting resistivity values for the additive particle loading percentage and particle size combinations tested, however, the path to expanding the current domain of resistivity results is clear and doing so may reveal conclusive evidence of the possibility of percolation affecting electric propellant resistivity values.

Finally, the response results gathered during the testing of the data set described above have been loosely correlated to power consumption testing results from previous work that may indicate that it is possible to relate propellant electrical resistivity and operating power consumptions/requirements, however more data is also required to be certain of this conclusion.

Ultimately the goals of this thesis project were two fold, the first of which was to address the three research questions and the hypothesis established in Chapter 1, and the second of which



was to provide new knowledge that could be used to aid researchers in the search for developing and understanding the fundamental science of the combustion and conduction mechanisms that drive the current perchlorate oxidizer based electric propellant formula to operate and still maintain its on/off firing abilities. This study was also able to successfully address a meaningful gap in the knowledge surrounding this electric propellant formulation and of several of its variants, and has contributed to the beginning stages of filling an industry wide gap in this area of research. The work done for this study and the results produced have provided an up to date set of mixing instructions to advance, as well as a testing set-up and the corresponding testing procedures, and an initial, resultant data set that can be used to quantify any later variations in the ESP-9 electric propellant formulation, and any other electric propellant formulation developed in the future, as well as to accurately compare with results from previously done work. While the propellant mixing procedures leave a significant amount of “goodness” of mix to be desired, moving forward, the researchers should have confidence in the ability of the testing set-up, procedures, and data analysis process used to assess propellant samples up to a certain degree of homogeneity based on the variation in propellant resistivity values.

## REFERENCES

- [1] Koehler, F. B., Langhenry, M. T., Summers, M. H., Villarreal, J. K., and Villarreal, T. W., 2016, "Electric Propellant Solid Rocket Motor Thruster Results Enabling Small Satellites," SSC17-II-02, 30<sup>th</sup> Annual AIAA/USU Conference on Small Satellites, Logan, UT, August 6-11, 2016.
- [2] Villarreal, J.K and Loehr, R.D., 2014, "Electrically Operated Propellants," U.S. Patent US-2014-0174313-A1.
- [3] Raytheon Missile Systems Internal Document 1
- [4] Raytheon Missile Systems Internal Document 2
- [5] Raytheon Missile Systems Internal Document 3
- [6] Raytheon Missile Systems Internal Document 4
- [7] Raytheon Missile Systems Internal Document 5
- [8] Raytheon Missile Systems Internal Document 6
- [9] Raytheon Missile Systems Internal Document 7
- [10] Raytheon Missile Systems Internal Document 8
- [11] Wass, J. A., Spring 2010. "First Steps in Experimental Design—The Screening Experiment," The Journal of Validation Technology, from <http://www.ivtnetwork.com/sites/default/files/First%20Steps%20in%20Experimental%20Design%E2%80%94The%20Screening%20Experiment.pdf>
- [12] Raytheon Missile Systems Internal Document 9
- [13] Sutton, G. P. and Biblarz, O., 2000, Rocket Propulsion Elements, 7th ed. Hoboken: John Wiley & Sons: pp. 512-513, 518, 521.
- [14] Puretec Industrial Water :: Ultrapure Water Solutions, 2018, Ultrapure Deionized Water Services and Reverse Osmosis Systems | Puretec Industrial Water :: Ultrapure Water Solutions, from <http://puretecwater.com/deionized-water/what-is-deionized-water>
- [15] Encyclopedia Britannica, 2018, "Polyvinyl alcohol | chemical compound," from <https://www.britannica.com/science/polyvinyl-alcohol>
- [16] Hanafy, T. A., 2012, "Dielectric Relaxation and Alternating Current Conductivity of Lanthanum, Gadolinium, and Erbium-Polyvinyl Alcohol Doped Films," Journal of Applied Physics 112, 034102.
- [17] Humble, R., 1995, Space Propulsion Analysis and Design, 1st ed. Learning Solutions, pp. 325-326.
- [18] Hammond, C. R., 2004, The Elements, in Handbook of Chemistry and Physics, 81st ed., CRC press.
- [19] Lassner, E., Schubert, and Wolf-Dieter, 1999, Tungsten: properties, chemistry, technology of the element, alloys, and chemical compounds, Springer, p. 9.

[20] Sanford, M.J, Johnson, R. T., Wallman, P.G., Bragunier, D.O, and Stiles, S. N., 2013, "High-Density Rocket Propellant," U.S. Patent US 8,545,646 B1.

[21] Armed Services Technical Information Agency, 1962, "Tungsten and Rocket Motors," Stanford Research Institute, from <http://www.dtic.mil/dtic/tr/fulltext/u2/274131.pdf>.

[22] Raytheon Missile Systems Internal Document 10

[23] Raytheon Missile Systems Internal Document 11

[24] Raytheon Missile Systems Internal Document 12

[25] International Carbon Black Association, "Particle Properties of Carbon Black," from <http://carbon-black.org/files/ICBA-Particle-CB-Factsheet-111413.pdf>

[26] Modern Dispersions, Inc., 2017, "Carbon Black Fundamentals," from [http://moderndispersions.com/CARBON\\_20BLACK\\_20FUNDAMENTALS.pdf](http://moderndispersions.com/CARBON_20BLACK_20FUNDAMENTALS.pdf)

[27] Bui, M., Chou, W.C., Shorb, J., and Yoon, Y.C., 2017, "Electrochemistry Basics," from [https://chem.libretexts.org/Core/Analytical\\_Chemistry/Electrochemistry/Basics\\_of\\_Electrochemistry](https://chem.libretexts.org/Core/Analytical_Chemistry/Electrochemistry/Basics_of_Electrochemistry)

[28] Blaber, M., 2000, "Electrochemistry—Spontaneity of Redox Reactions," from <http://www.mikeblaber.org/oldwine/chm1046/notes/Electro/Spontan/Spontan.htm>

[29] Jeraldo, P., 2005, "Critical Phenomena in Percolation Theory," from [http://guava.physics.uiuc.edu/~nigel/courses/563/Essays\\_2005/PDF/jeraldo.pdf](http://guava.physics.uiuc.edu/~nigel/courses/563/Essays_2005/PDF/jeraldo.pdf)

[30] Bentz, D.P., and Garboczi, 1991, "Percolation Theory," Cement and Concrete Research 21, 325-344, from <https://ciks.cbt.nist.gov/garbocz/paper22/node4.html>

[31] Premix, 2018, "Conductive Carbon Black," from <http://www.premixgroup.com/product-cats/conductive-compounds/conductive-carbon-black/>

[32] Kerstein, A.R., 1983, "Equivalence of the Void Percolation Problem for Overlapping Spheres and a Network Problem," J. Phys. A:Math. Gen. 16 (1983) 3071-3075, Printed in Great Britain.

[33] American Society for Testing and Materials, 2007, "Standard Test Methods for DC resistance or Conductance of Insulating Materials," D257-07.

[34] Brill, T.B., Ren, W, and Yang, V, 2000, Solid Propellant Chemistry, Combustion, and Motor Interior Ballistics, American Institute of Aeronautics and Astronautics, Inc., p. 233.

[35] Raytheon Missile Systems Internal Document 13

[36] Raytheon Missile Systems Internal Document 14

[37] Sequeira, C., and Santos, D., 2010, Polymer Electrolytes—Fundamentals and Applications, Woodhead Publishing Limited, from <https://books.google.com/books?id=vHI0AgAAQBAJ&printsec=frontcover&dq=polymer+electrolyte&hl=en&sa=X&ved=0ahUKEwjWxbLT3dXPAhUG6x4KHZ5BD9sQ6AEIjAC%20-%20v=onepage&q=polymer%20electrolyte&f=false#v=onepage&q&f=false>

[38] Munshi, M. Z. A., 1999, "Solid Polymer Electrolytes," U.S. WO2001017051A1.

[39] Raytheon Missile Systems Internal Document 15

[40] Raytheon Missile Systems Internal Document 16

[41] Thinky, "Planetary Centrifugal Vacuum Mixer "Thinky Mixer" ARV-310/ARV-310 LED," from <http://www.thinkyusa.com/products/item-all/vacuum-mixer/arv-310.html>

[42] American Society for Testing and Materials, 2000, "Standard Test Method for Rubber Property—Volume Resistivity of Electrically Conductive and Antistatic Products," D991-89.

[43] Cober Electronics, Inc., "Engineering Data, 31KW High Power Pulse Generator Model 606," from <http://public.hofstragroup.com/3057.pdf>

[44] resistorguide.com, 2018, "Wirewound resistor," from <http://www.resistorguide.com/wirewound-resistor/>

[45] Investopedia, 2018, "Trimmed Mean," from [https://www.investopedia.com/terms/t/trimmed\\_mean.asp](https://www.investopedia.com/terms/t/trimmed_mean.asp)

[46] Minitab Express™ Support, 2017, "Interpret All Statistics and Graphs for Normality Test," from <http://support.minitab.com/en-us/minitab-express/1/help-and-how-to/basic-statistics/summary-statistics/normality-test/interpret-the-results/all-statistics-and-graphs/>

[47] Minitab Express™ Support, 2017, "Analysis of Variance Table for Analyze Response Surface Design," from <https://support.minitab.com/en-us/minitab/18/help-and-how-to/modeling-statistics/doe/how-to/response-surface/analyze-response-surface-design/interpret-the-results/all-statistics-and-graphs/analysis-of-variance-table/>

[48] Minitab Express™ Support, 2017, "Interpret the Key Results for Analyze Factorial Design," from <https://support.minitab.com/en-us/minitab/18/help-and-how-to/modeling-statistics/doe/how-to/factorial/analyze-factorial-design/interpret-the-results/key-results/>

[49] Minitab Express™ Support, 2017, "Coded Coefficients Table for Analyze Variability," from <https://support.minitab.com/en-us/minitab/18/help-and-how-to/modeling-statistics/doe/how-to/factorial/analyze-variability/interpret-the-results/all-statistics-and-graphs/coded-coefficients-table/>

[50] Minitab Express™ Support, 2017, "What are Hierarchical Models?," from <https://support.minitab.com/en-us/minitab/18/help-and-how-to/modeling-statistics/anova/supporting-topics/anova-models/what-are-hierarchical-models/>

[51] Minitab Express™ Support, 2017, "Regression equation table for Analyze Variability," from <https://support.minitab.com/en-us/minitab/18/help-and-how-to/modeling-statistics/doe/how-to/factorial/analyze-variability/interpret-the-results/all-statistics-and-graphs/regression-equation/>

[52] Minitab Express™ Support, 2017, "Unusual Observations," from <http://support.minitab.com/en-us/minitab-express/1/help-and-how-to/modeling-statistics/regression/supporting-topics/model-assumptions/unusual-observations/>

[53] Minitab Express™ Support, 2017, "Interpret the Key Results for Interaction Plot," from <http://support.minitab.com/en-us/minitab-express/1/help-and-how-to/modeling-statistics/anova/how-to/interaction-plot/interpret-the-results/>

[54] Montgomery, D.C, and Runger, G. C., 2013, Applied Statistics and Probability for Engineers, 6th ed., Wiley.

[55] Libretexts, 2018, "Propagation of Error," Chemistry LibreTexts, from [https://chem.libretexts.org/Core/Analytical\\_Chemistry/Quantifying\\_Nature/Significant\\_Digits/Propagation\\_of\\_Error](https://chem.libretexts.org/Core/Analytical_Chemistry/Quantifying_Nature/Significant_Digits/Propagation_of_Error)

Approved for Public Release DOPSR 19-S-0112  
Placed in the Public Domain Per E18-9TPV

APPENDIX A

ADDITIVE BILL OF MATERIALS

<b>Additive Replacement Chemicals</b>	<b>CAS</b>	<b>Amount/Price</b>	<b>Order Amount</b>	<b>Vendor</b>
<b>TUNGSTEN</b>				
WP-102, Tungsten Metal Powder, 1-5 micron <a href="https://micronmetals.com/product/tungsten-metal-powder-3/">https://micronmetals.com/product/tungsten-metal-powder-3/</a>	7440-33-7	1-2lbm/\$109.47	1lbm	Micron Metals
WP-104, Tungsten Metal Powder, -325 mesh (44 micron) <a href="https://micronmetals.com/product/tungsten-metal-powder-5/">https://micronmetals.com/product/tungsten-metal-powder-5/</a>	7440-33-7	1-2lbm/\$90.06	1lbm	Micron Metals
WP-106, Tungsten Metal Powder, -100 mesh (149 micron) <a href="https://micronmetals.com/product/tungsten-metal-powder-7/">https://micronmetals.com/product/tungsten-metal-powder-7/</a>	7440-337	1-2lbm/\$104.76	1lbm	Micron Metals
<b>COPPER</b>				
CU-110, Spherical Copper Metal Powder, 1-5 micron <a href="https://micronmetals.com/product/copper-metal-powder/">https://micronmetals.com/product/copper-metal-powder/</a>	7440-50-8	1-2lbm/\$149.16	1lbm	Micron Metals
CU-112, Spherical Copper Metal Powder, -325 mesh (44 micron) <a href="https://micronmetals.com/product/cooper-metal-powder-2/">https://micronmetals.com/product/cooper-metal-powder-2/</a>	7440-50-8	1-2lbm/\$34.80	1lbm	Micron Metals
CU-115, Spherical Copper Metal Powder, -100 mesh (149 micron) <a href="https://micronmetals.com/product/cooper-metal-powder-3/">https://micronmetals.com/product/cooper-metal-powder-3/</a>	7440-50-8	1-2lbm/\$35.90	1lbm	Micron Metals
<b>CARBON BLACK</b>				
EQ-Lib-SuperP, TIMCAL Graphite & Carbon Super P Conductive Carbon Black <a href="http://www.mtixtl.com/TIMCALGraphiteandCarbonSuperPConductiveCarbonBlack100g/bag-EQ-U.aspx">http://www.mtixtl.com/TIMCALGraphiteandCarbonSuperPConductiveCarbonBlack100g/bag-EQ-U.aspx</a>	1333-86-4	80g/\$29.95	7* 80g = 560g	MTI Corporation